Woods Hole Oceanographic Institution

WHOI-94-18

Technical Report

August 1994

Meteorological and Oceanographic Data Collected during the ASREX 91 Field Experiment

by

Nancy R. Galbraith
Anand Gnanadesikan
George H. Tupper
Bryan S. Way

Upper Ocean Processes Group
Woods Hole Oceanographic Institution

Eugene A. Terray
Department of Applied Ocean Science and Engineering
Woods Hole Oceanographic Institution

Upper Ocean Processes Group
Woods Hole Oceanographic Institution
Woods Hole, Massachusetts 02543

UOP Technical Report 94-1

WHOI-94-18

Meteorological and Oceanographic Data Collected during the ASREX 91 Field Experiment

by

Nancy R. Galbraith
Anand Gnanadesikan
George H. Tupper
Bryan S. Way

Upper Ocean Processes Group
Woods Hole Oceanographic Institution

Eugene A. Terray
Department of Applied Ocean Science and Engineering
Woods Hole Oceanographic Institution

August 1994

Technical Report

Funding was provided by the Ocean Acoustics Program (Code 324OA) of the Office of Naval Research under contract N00014-91-J-1891.

Approved for Distribution:

Philip L. Richardson, Chair
Department of Physical Oceanography

Abstract

The 1991 Acoustic Surface Reverberation Experiment (ASREX 91) took place in November and December off the coast of British Columbia. As part of this experiment, three moorings were deployed to characterize the environmental background. The moorings consisted of a meteorological/oceanographic mooring designed to measure surface meteorology, current and temperature in the upper 120 meters, and nondirectional wave parameters and two wave moorings which were instrumented with pitch-roll buoys to characterize the directional wave spectrum. This report presents results from these three moorings. The conditions seen during the experiment were extremely rough, with wind speeds at 3.4m above the water surface reaching a maximum of 22 m/s and wave heights reaching a maximum of over 10 meters. The air-sea flux of heat was strongly cooling, and the mixed layer deepened over the course of the experiment from approximately 40 to approximately 70 meters. Spectra of the temperature showed a strong semidiurnal tidal signal associated with temperature excursions of several degrees C. The velocity signal showed strong inertial oscillations with amplitudes of 30-50 cm/s Weaker low-frequency and semidiurnal tidal signals were also seen. The waves were very strong with significant wave heights of 5-6 meters persisting for up to 2 weeks at a time. Waves were generally out of the south or the west.

Table of Contents

List of Figures

List of Tables

1. Introduction

The 1991 Acoustic Surface Reverberation Experiment (ASREX 91) was designed to study processes causing degraded acoustic transmission in high sea states. The experiment took place in late 1991 and early 1992 off the coast of British Columbia. In support of this experiment, a group from the Woods Hole Oceanographic Institution deployed three moorings designed to provide the environmental background for the acoustic measurements made by other investigators. These moorings measured the meteorology, temperature structure over the top 120 meters of the water column, current velocity over the top 20 meters, and the directional wave spectrum. The resulting data set provides an opportunity to examine the wintertime deepening of a mixed layer, and to evaluate the importance of surface gravity waves for this process.

2. Mooring Information

The mooring operations took place onboard the University of Washington's *R/V Thomas G. Thompson.* Deployment was on Voyage 4, sailing out of Seattle on 29 October 1991. Recovery was on Voyage 5, also sailing from Seattle, on 5 January 1992. The moorings were sited about 350 km west of Vancouver Island. Table 2.1 lists the location and duration of the three moorings. Figure 2.1 shows a bathymetric map of the area around the experiment site. A list of cruise participants appears in Appendix 1, and the chronology of the cruises is described in Appendix 2.

Table 2.1: Locations and durations of the three moorings

Buoy	Deployment	Recovery	Latitude	Longitude
Discus Buoy (WHOI-920)	911031 21:09	920107 14:18	49 13.45 N	131 51.88 W
Seatex (WHOI-921)	911101 05:50	Surface Buoy 911204 19:00 Mooring: 920107 23:11	49 09.10 N	131 53.30 W
Endeco (WHOI-923)	911102 04:50	920108 18:04	49 08.25 N	131 47.42 W

On 1 December 1991, telemetry data from System Argos revealed that the Seatex buoy had gone adrift. The buoy was recovered on 4 December by the Canadian destroyer *HMCS Huron*. Upon recovery it was found that the Seatex buoy appeared to have been intentionally detached from the mooring and the surface tether had been cut. Information about this incident is given in more detail in Appendix 4.

The WHOI moorings were designed by and set by members of the Upper Ocean Processes Group (UOP) and the Ocean Acoustics Lab (OAL) at Woods Hole. Mooring diagrams are in figures 2.2 through 2.4. A summary of the instrumentation on the discus mooring is given in table 2.2.

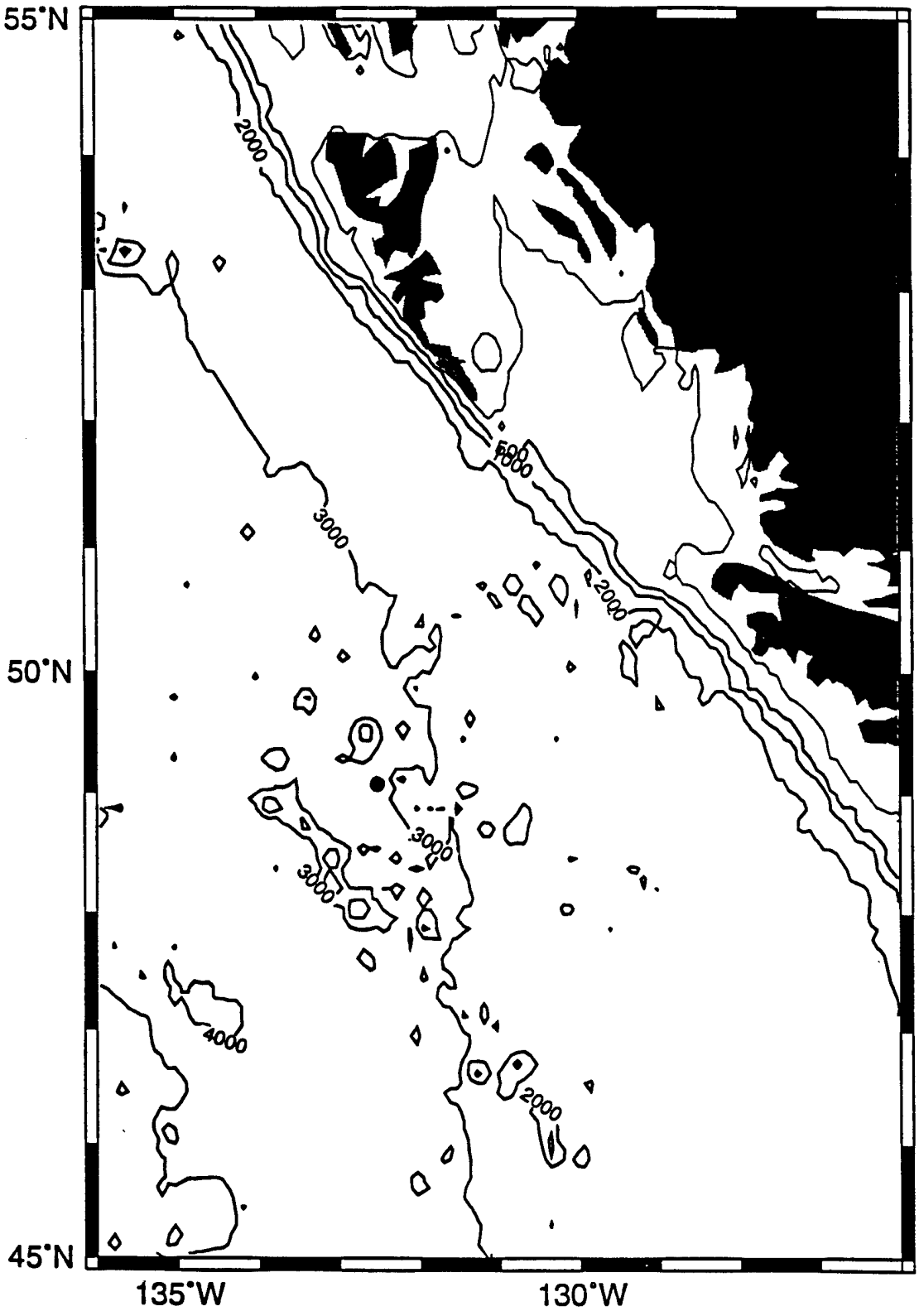

Figure 2.1: Map of ASREX 91 Experiment Site

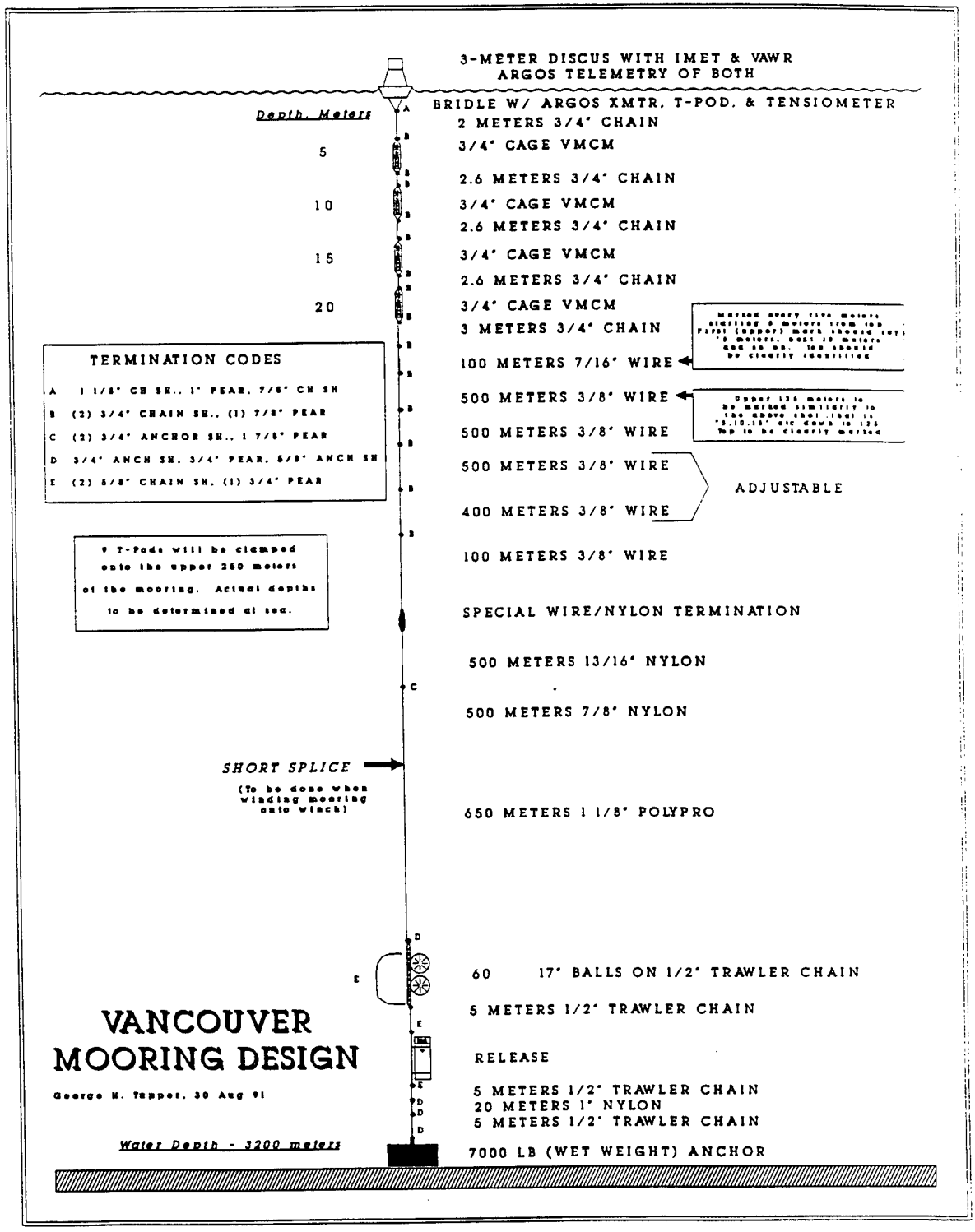

Figure 2.2: Mooring Diagram. Discus Mooring.

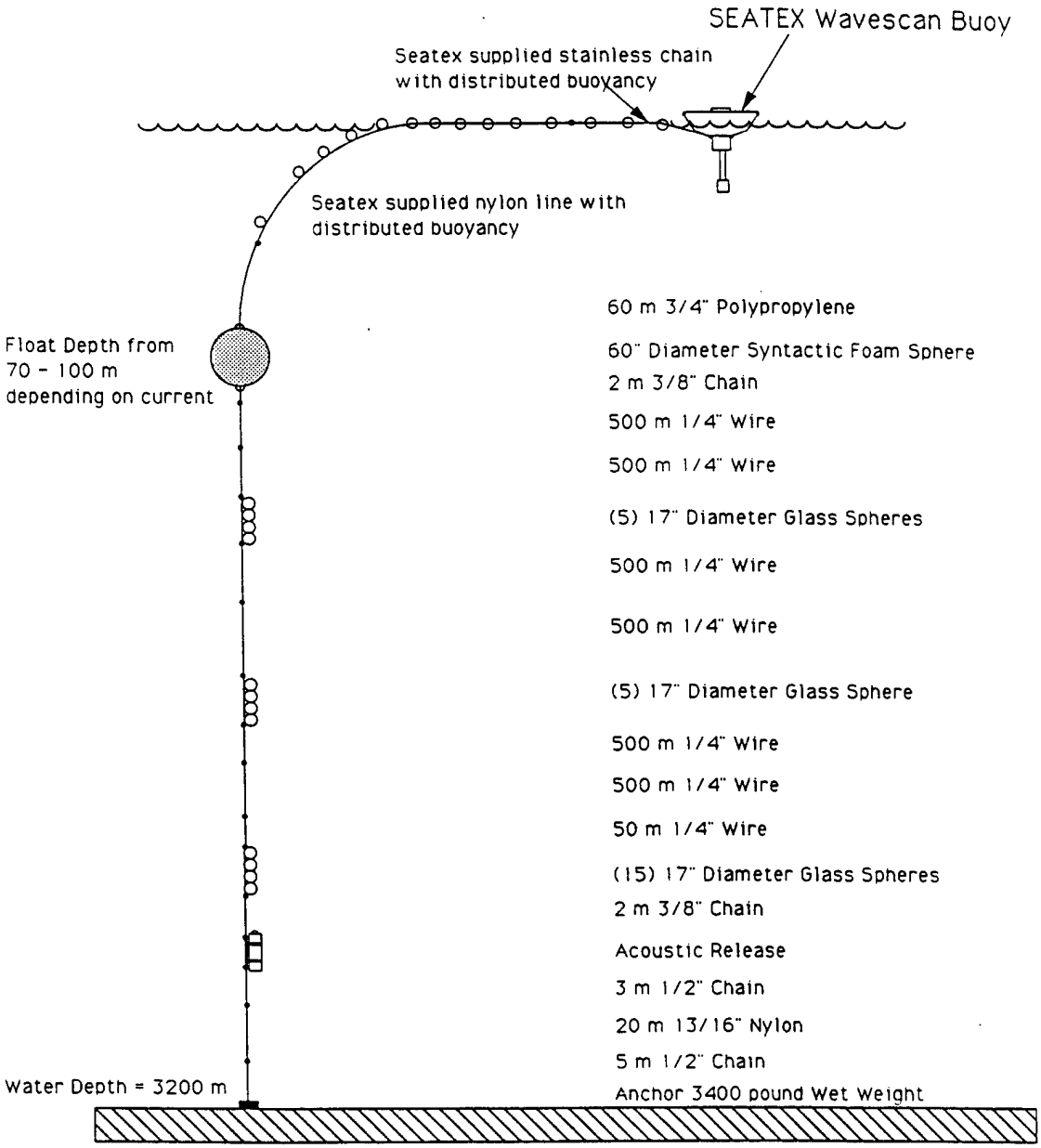

Figure 2.3: Mooring Diagram. Seatex Mooring.

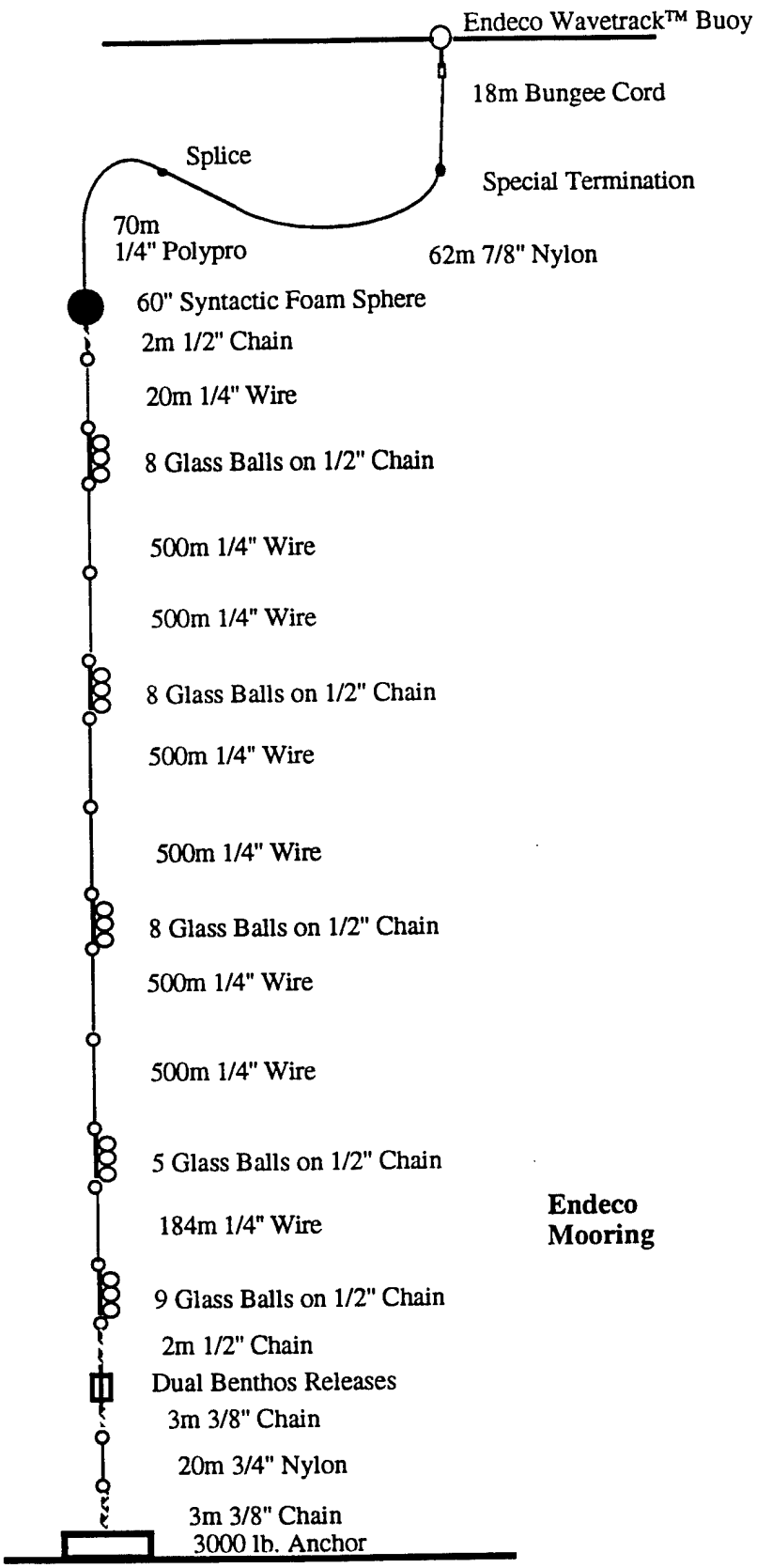

Figure 2.4: Mooring Diagram. Endeco Mooring.

Table 2.2: Instrumentation on the Discus mooring

Instrument Type	Serial Number	Sample Rate(sec)	Depth (meters)
VAWR	0723	900	Surface
IMET		60	Surface
TPOD	3699	450	2
VMCM	1405	112.5	5
VMCM	0201	1125	10
VMCM	0773	112.5	15
VMCM	0873	1125	20
TPOD	3702	450	40
TPOD	3662	450	60
TPOD	3700	450	80
TPOD	3667	450	100
TPOD	3705	450	120

3. Data Presentation

3.1 Meteorology during ASREX 91

Meteorological Observations

Meteorological data was recorded using a Vector-Averaging Wind Recorder (VAWR) with a 15 minute record rate. A second meteorological instrument package, an Improved Meteorological (IMET) system, also recorded data for a period of about one month, but its battery power, normally recharged by solar panels, failed as a result of too little sunlight on 5 December 1991 at midnight. The IMET system had a one minute record rate.

Tables 3.1.1-3.1.2 summarize the sensors, their accuracy, and the sampling strategy for each of the packages. Table 3.1.3 shows a schematic of how the VAWR sampled each sensor during the 15 minute recording interval. Note that while the wind and radiation sensors recorded over the entire interval, the relative humidity and barometric pressure are sampled for a very short period of time in the middle of the recording interval.

A check of the time base for the VAWR found 392 missing or incorrect clock counts. The data was interpolated over these gaps. The final processed data file had a total of 6455 records at 15 minute intervals between 91-11-01 00:07:30 UTC and 92-01-07 08:07:30 UTC. Figure 3.1.1 through 3.1.5 show time-series of meteorological data recorded by the VAWR and IMET. Displayed are wind velocity north and east, sea temperature, air temperature, barometric pressure, relative humidity, short wave and long wave radiation. IMET data is represented with a dashed line, and VAWR data with a solid line. A magnetic variation of 21.4° was applied to the data from both instruments.

The IMET data were found to agree very well with the VAWR data in general, although several small, systematic differences were found. The VAWR recorded wind speeds about 9% higher than the IMET. The IMET relative humidity was found to be about 1% higher than the VAWR with rms differences of order 1-2%. The barometric pressure also showed a systematic offset, with the VAWR being about 0.8 MB lower than the IMET. Except for the wind sensors, these differences were within the sensor specifications. Comparison of these differences with meteorological observations taken aboard the *Thompson* was made, but the differences were not resolvable. For purposes of the flux calculations reported here, the VAWR data will be taken as correct.

Air-Sea Fluxes

Fluxes of momentum, sensible heat, and latent heat for the Vancouver data site were computed from the meteorological variables using the stability-dependent bulk aerodynamic formulae of Large and Pond (1981; 1982). The net shortwave radiation is computed using an albedo of 0.06. The net longwave radiation is estimated using sea surface temperature. air temperature and the mixing ratio from Clark et al., 1974. This formula also includes a cloud-correction function which depends on the cloud cover. The cloud cover n was estimated from the incoming shortwave radiation. by comparing the observed radiation to clear-sky radiation predicted from astronomical theory (List,1984) assuming some atmospheric transmission coefficient. An atmospheric transmission coefficient of 0.7 was used, and compared well with observed short wave radiation from the VAWR during the few clear-sky days over the course of the deployment. Night-

time values of cloud cover were estimated by linear interpolation between the nearest two daytime values.

Time series of the heat fluxes computed from the VAWR are shown in Figures 3.1.6 through 3.1.10. From top to bottom, the sensible, latent, net shortwave, net long wave and total heat flux in W/m^2 are shown. Figures 3.1.11 through 3.1.15 show the wind stress time series computed from the VAWR. From top to bottom, the eastward wind stress, northward wind stress, wind stress magnitude, wind stress direction (towards), and the nondimensional stability parameter z/L . L is the Monin-Obhukhov length $-c_pTu_*^3/\kappa gQ$, (where c_p is the specific heat, T is the temperature , u* the friction velocity, g is gravity, κ is the Von Karman constant, and Q is the heat gained by the atmosphere from the ocean) are shown. Large negative values of L mean that the atmospheric boundary layer is convectively unstable, so that the shear of the velocity is reduced from a logarithmic profile.

Figure 3.1.16 shows the rotary spectrum of the wind stress (solid represents clockwise rotation, dashed counterclockwise rotation), and the spectrum of the sea-surface temperature, air temperature, shortwave radiation, barometric pressure and relative humidity. Other than the shortwave radiation, which shows a distinct set of peaks at the first, second, and third harmonics of the diurnal frequency, there are no significant peaks.

Figure 3.1.17 shows the precipitation measured by the IMET system. The sensor used was an R.M Young self siphoning rain gauge, which emptied itself upon reaching a level of 5 cm. Over the course of the deployment, the gauge emptied itself 2 times, on 3 November and 16 November.

Parameter	Sensor Type	Accuracy	Record Time
Wind Speed	R.M. Young 3-cup Anemometer	+/- 2% above 0.7 m/s	Vector Averaged
Wind Direction	Integral Vane w/vane follower WHOI/EG&G	+/- 1 bit 5.6 degrees	Vector Averaged
Insolation	Pyranometer Eppley 8-48	+/- 3% of reading	Averaged over record interval
Long Wave Radiation	Pyrgeometer Eppley PIR	+/- 10%	Averaged over record interval
Relative Humidity	Vaisala Humicap 0062HMP	+/- 2% RH	3.515 Seconds Average Note 1
Barometric Pressure	Paroscientific Model 216-B-101	+/- 0.2 mbars wind < 20 m/s	2.636 Seconds Average Note 1
Sea Temperature	Thermistor Thermometrics 4K @ 25 degrees C	+/- 0.005 degrees C	Averaged over 1/2 record time Note 2
Air Temperature	Thermistor Yellow Springs #44034 5K @ 25 degrees C	+/- 0.2 degrees C wind > 5 m/s	Averaged over 1/2 record time Note 3

Notes:

1. Relative Humidity and Barometric Pressure are averaged in the middle of the recording interval for the time noted.
2. Sea temperature is measured during the first half of the recording interval.
3. Air temperature is measured during the second half of the recording interval.

Table 3.1.1: Meteorological Sensor Specifications. Vector Averaging Wind Recorder (VAWR) Deployed on Discus Buoy.

IMET (Improved Meteorological Record) (60 second record interval)

Parameter	Sensor Type	Accuracy	Record Time
Wind Speed	R. M. Young propeller Anemometer	± 2% above 0.7 m/s	Scalar average over 1 min
Wind Direction	9 bit encoder KVH compass	± 1 bit 0.7 degrees	Scalar average over 1 min
Insolation	Pyranometer Eppley PSP	± 3% of reading	Averaged over record interval
Long Wave Radiation	Pyrgeometer Eppley PIR	± 10%	Averaged over record interval
Relative Humidity	Rotronics MP-100F	± 2% RH	Averaged over record interval
Barometric Pressure	Air DB1-A	± 0.2 mbars wind < 20 m/s	Averaged over record interval
Sea Temperature	PRT 1k	± 0.005 degrees C	Averaged over record interval
Air Temperature	PRT 1k	± .005 degrees C wind > 5 m/s	Averaged over record interval

Table 3.1.2: Meteorological Sensor Specifications. Improved Meteorological system (IMET) Deployed on Discus Buoy.

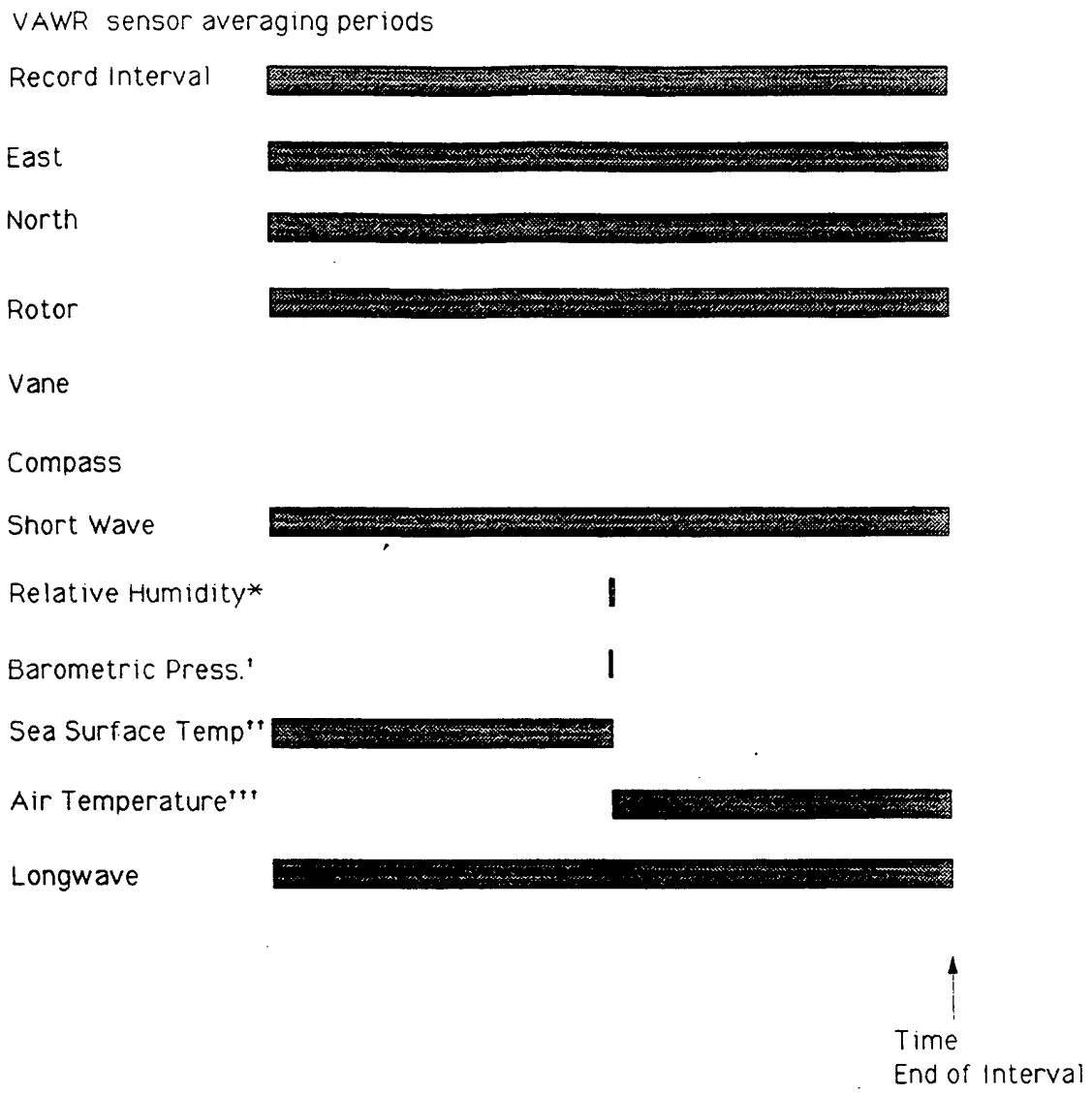

* Relative humidity sensor is on for 7 seconds and counted for 3.515 seconds

' Barometric Pressure sensor is on for 4.39 seconds and counts for 2.636 seconds

'' Sea surface temperature is averaged during the first half of the record rate. Actual averaging interval is half the record rate minus 1.7578125 seconds (delay and settle time from SST to AT)

''' Air temperature is counted for the second half of the averaging interval. The air temp average interval is half the record rate minus 1.7578125.

Recorded compass and vane information is the last sample taken in the record interval.

Table 3.1.3: Schematic of VAWR Sensor Averaging Periods.

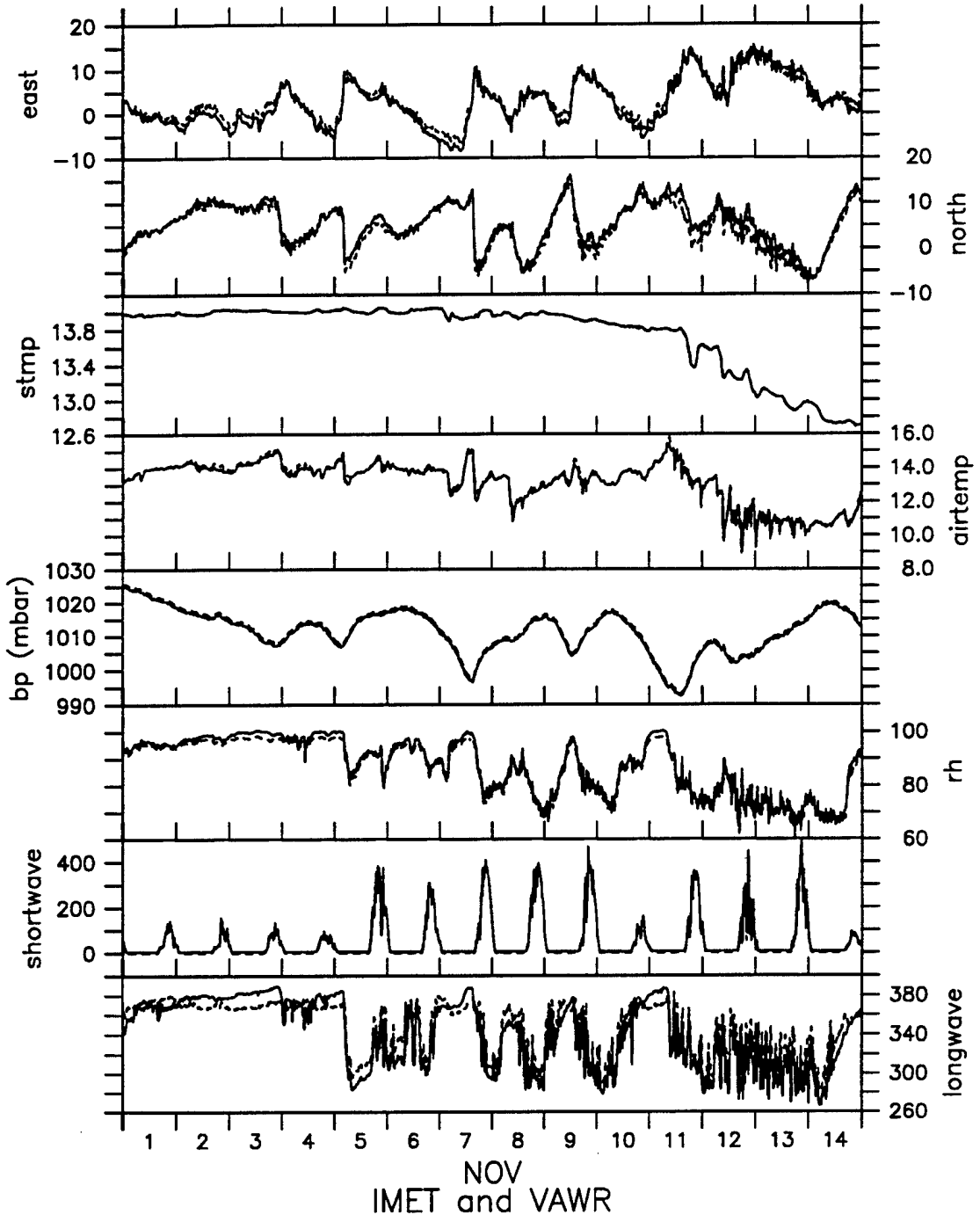

Figure 3.1.1 VAWR and IMET Meteorological Time Series. IMET data is dashed, VAWR data is solid line.

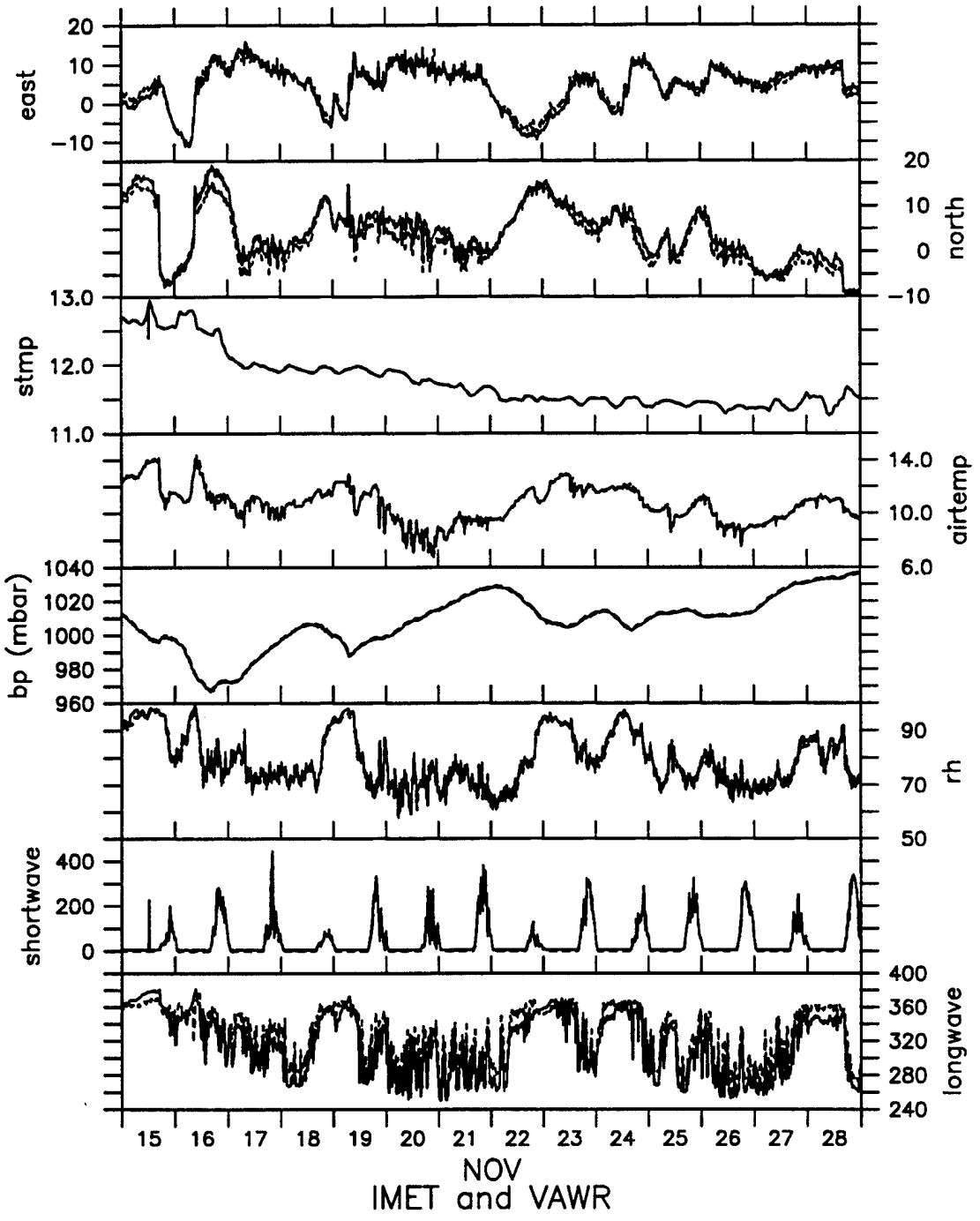

Figure 3.1.2 VAWR and IMET Meteorological Time Series. IMET data is dashed, VAWR data is solid line.

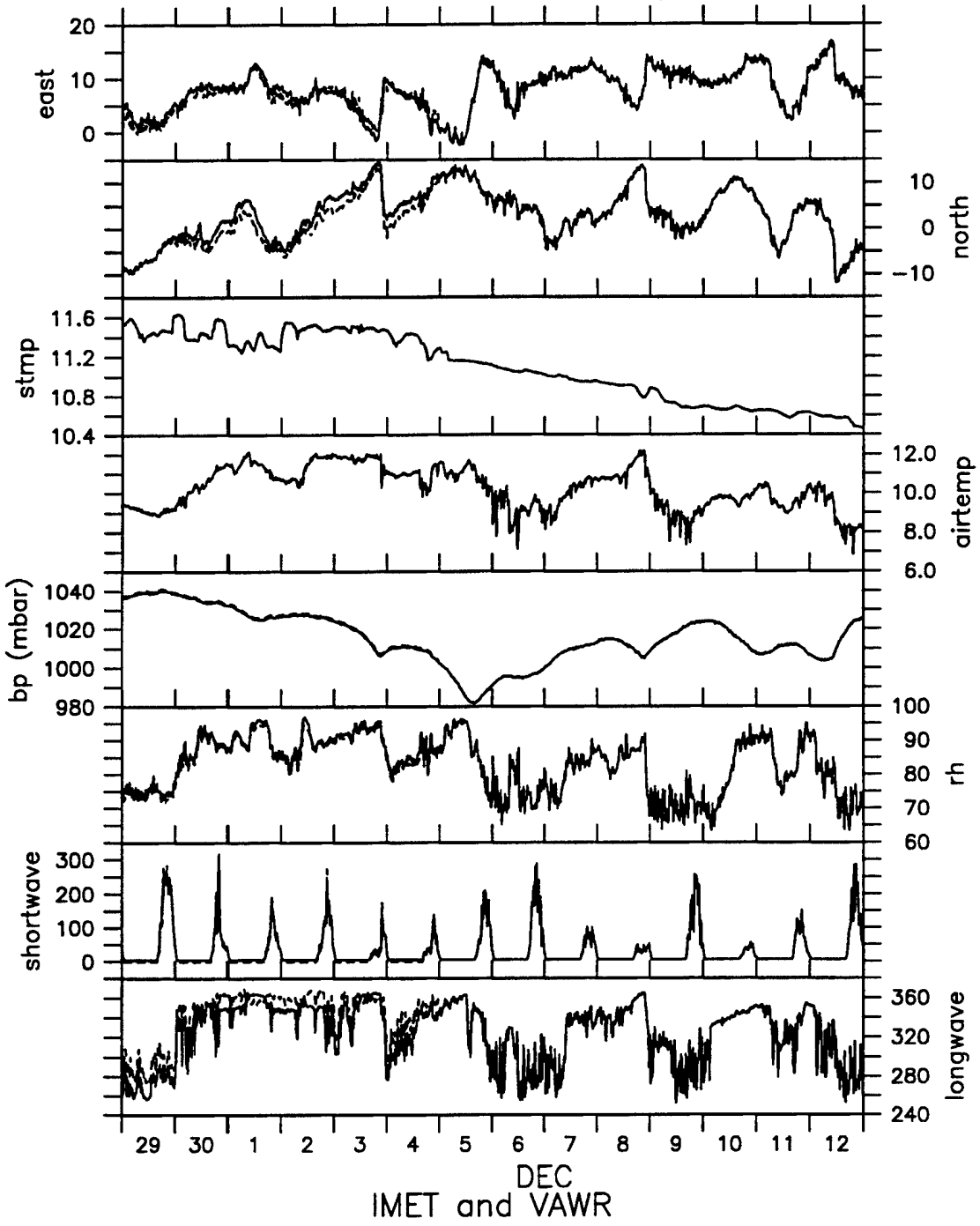

Figure 3.1.3 VAWR and IMET Meteorological Time Series. IMET data is dashed, VAWR data is solid line. IMET failed on December 4 at 2359 UTC.

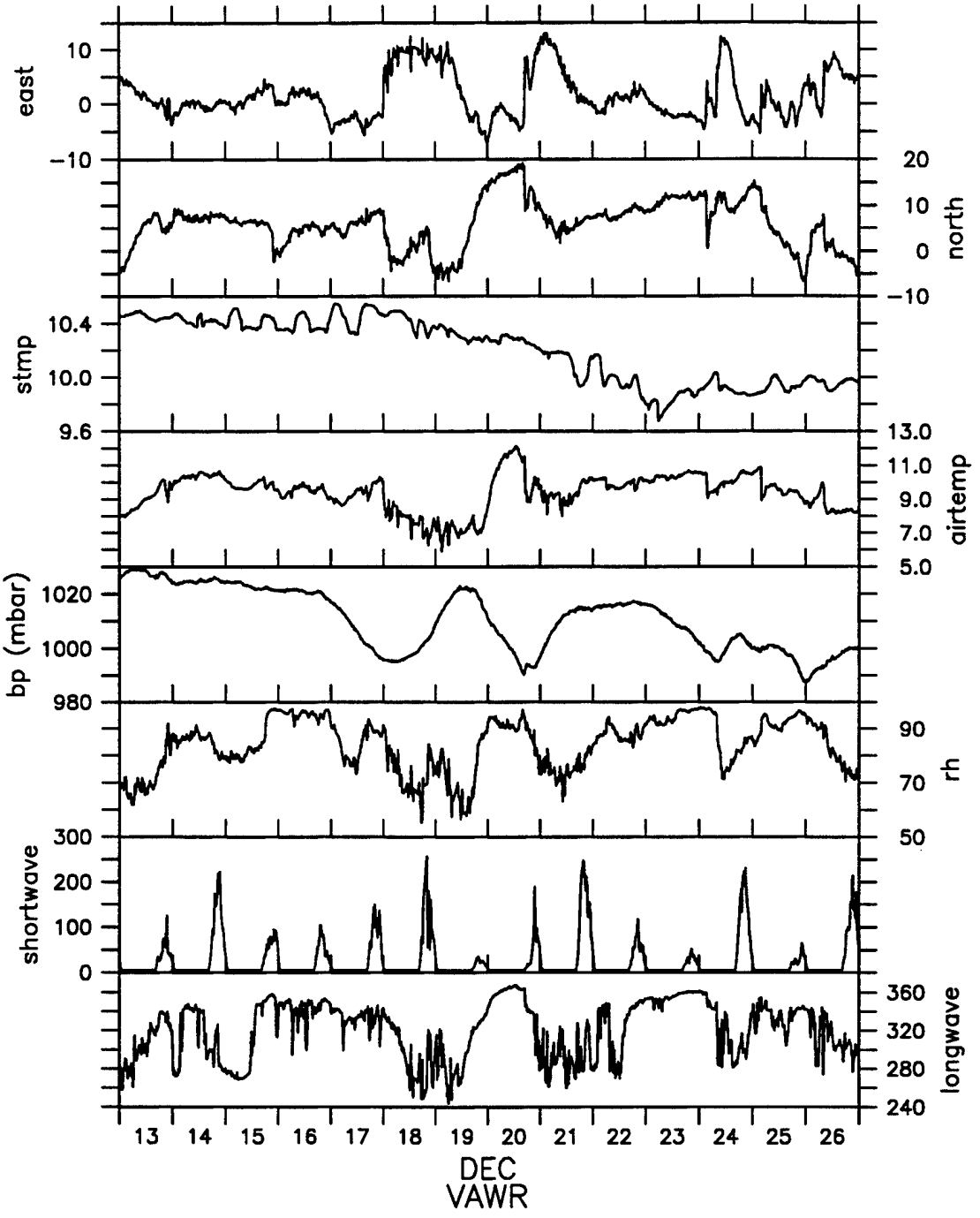

Figure 3.1.4 VAWR Meteorological Time Series.

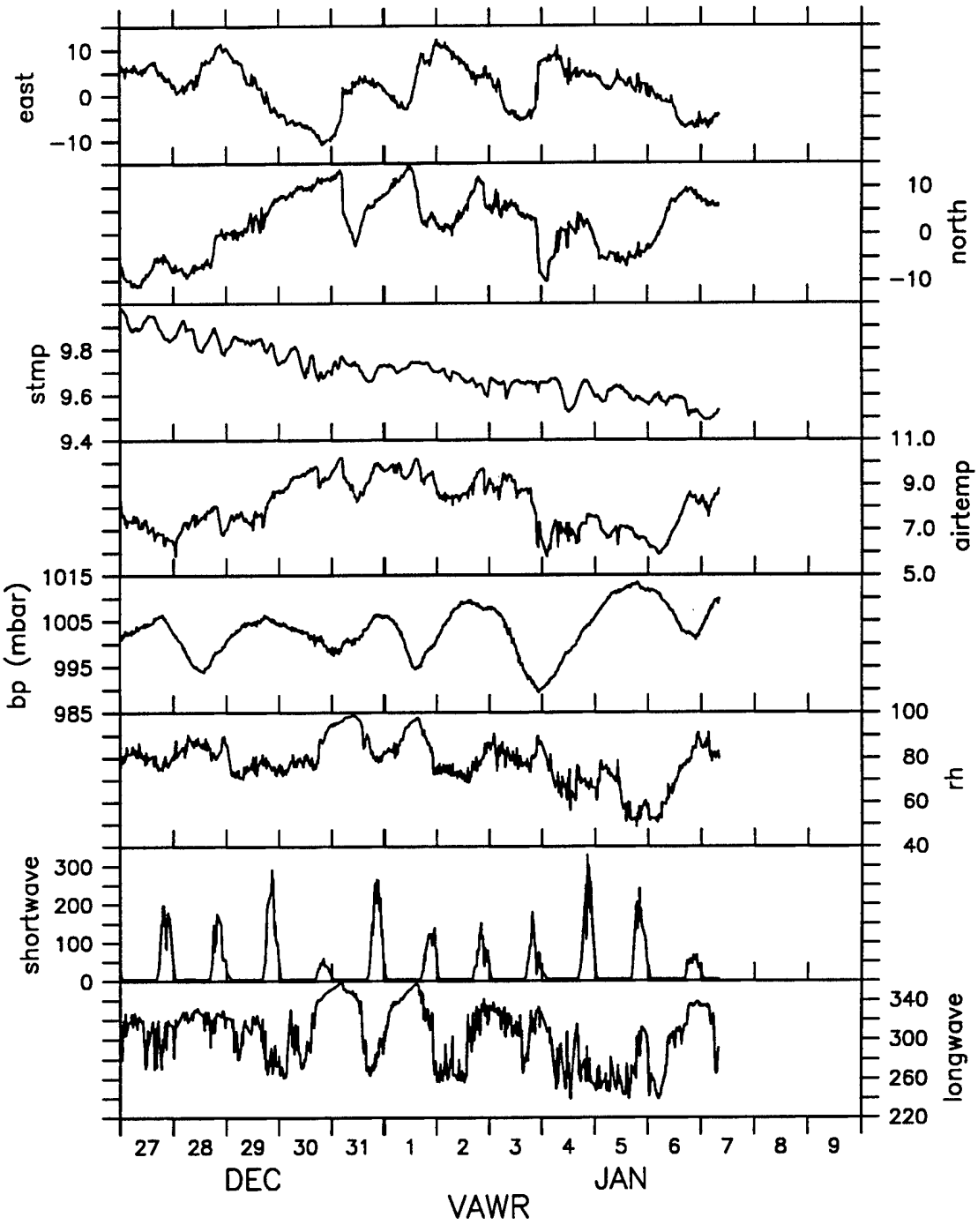

Figure 3.1.5 VAWR Meteorological Time Series.

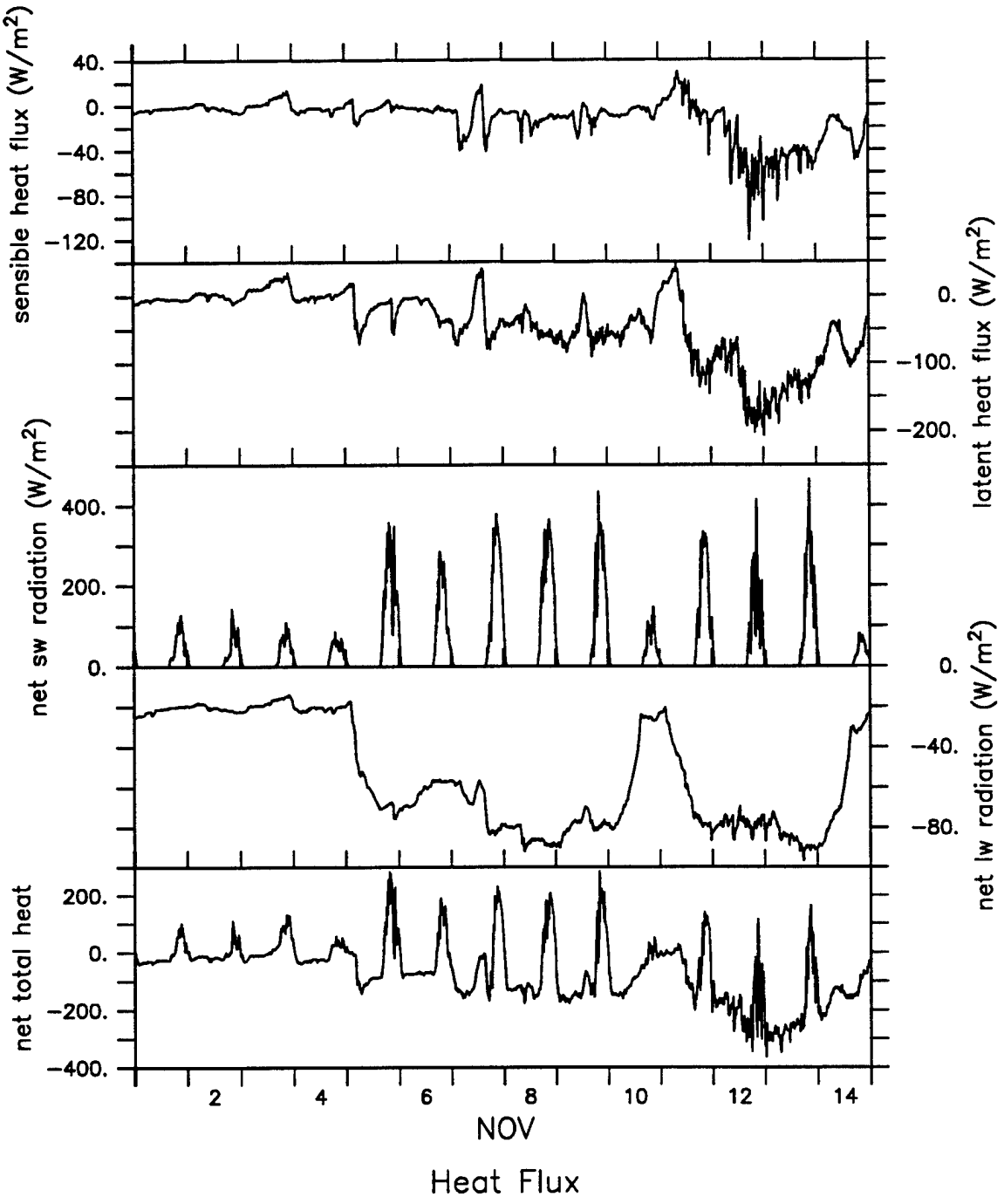

Figure 3.1.6 Heat Flux Time Series from VAWR.

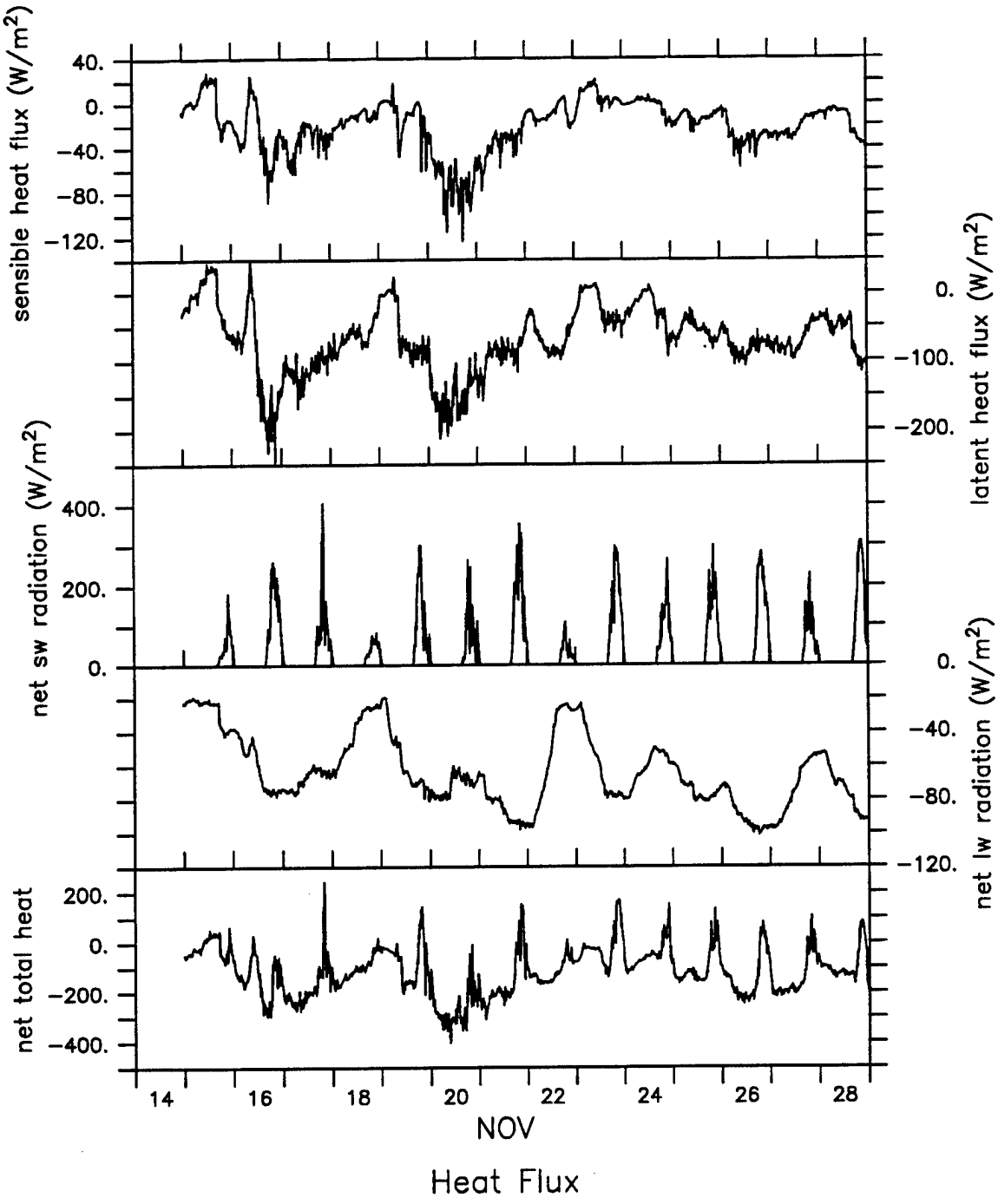

Figure 3.1.7 Heat Flux Time Series from VAWR.

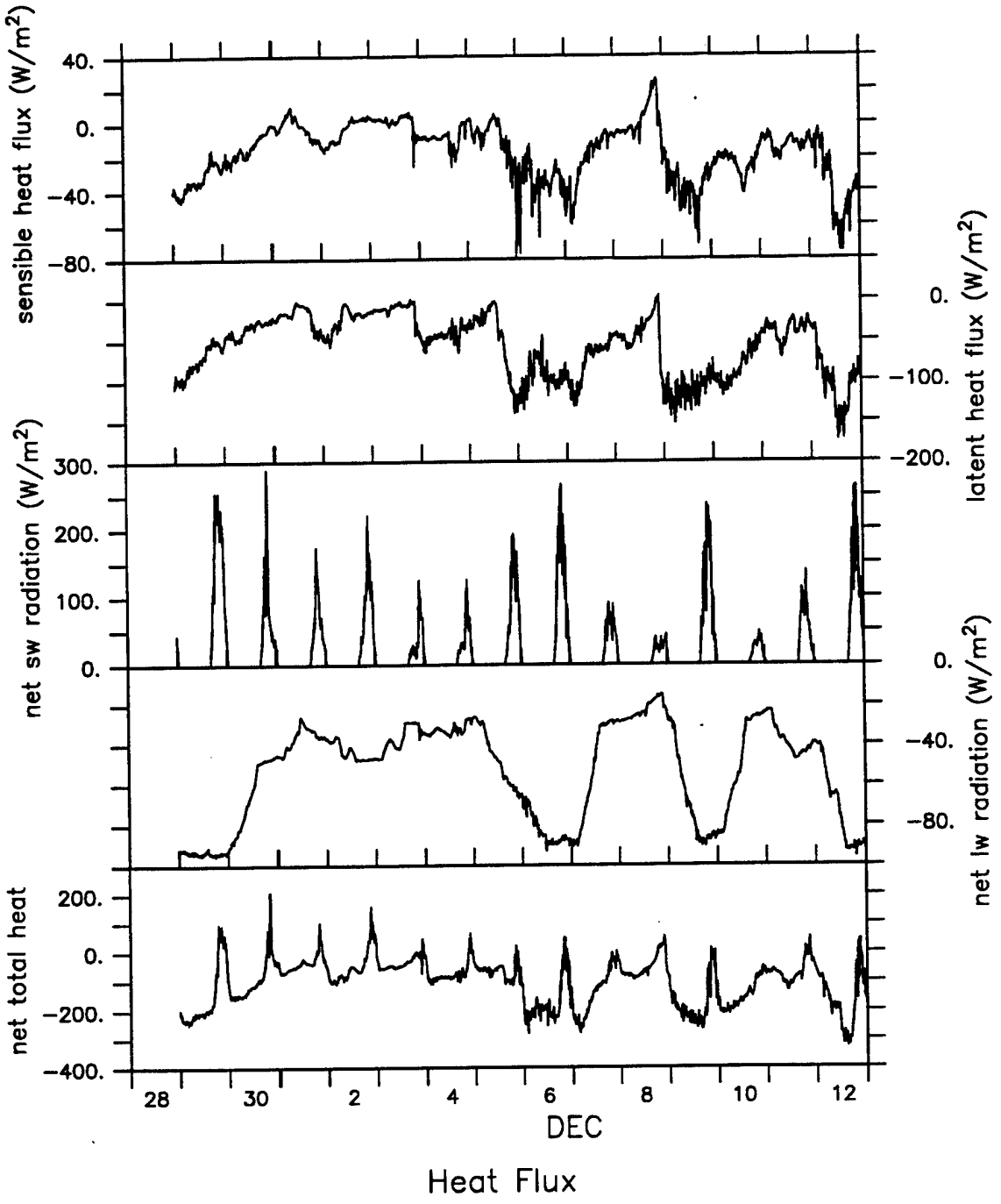

Figure 3.1.8 Heat Flux Time Series from VAWR.

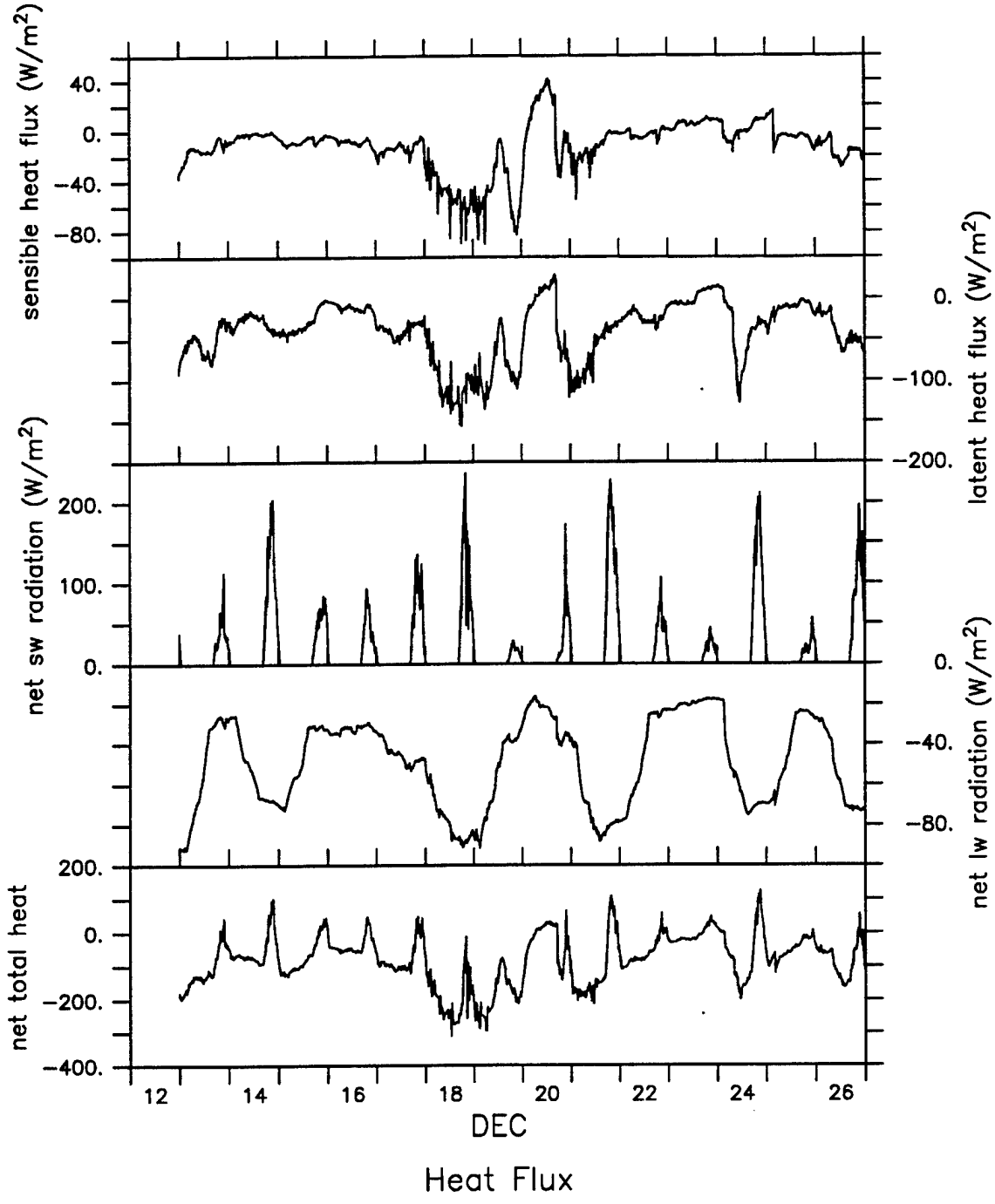

Figure 3.1.9 Heat Flux Time Series from VAWR.

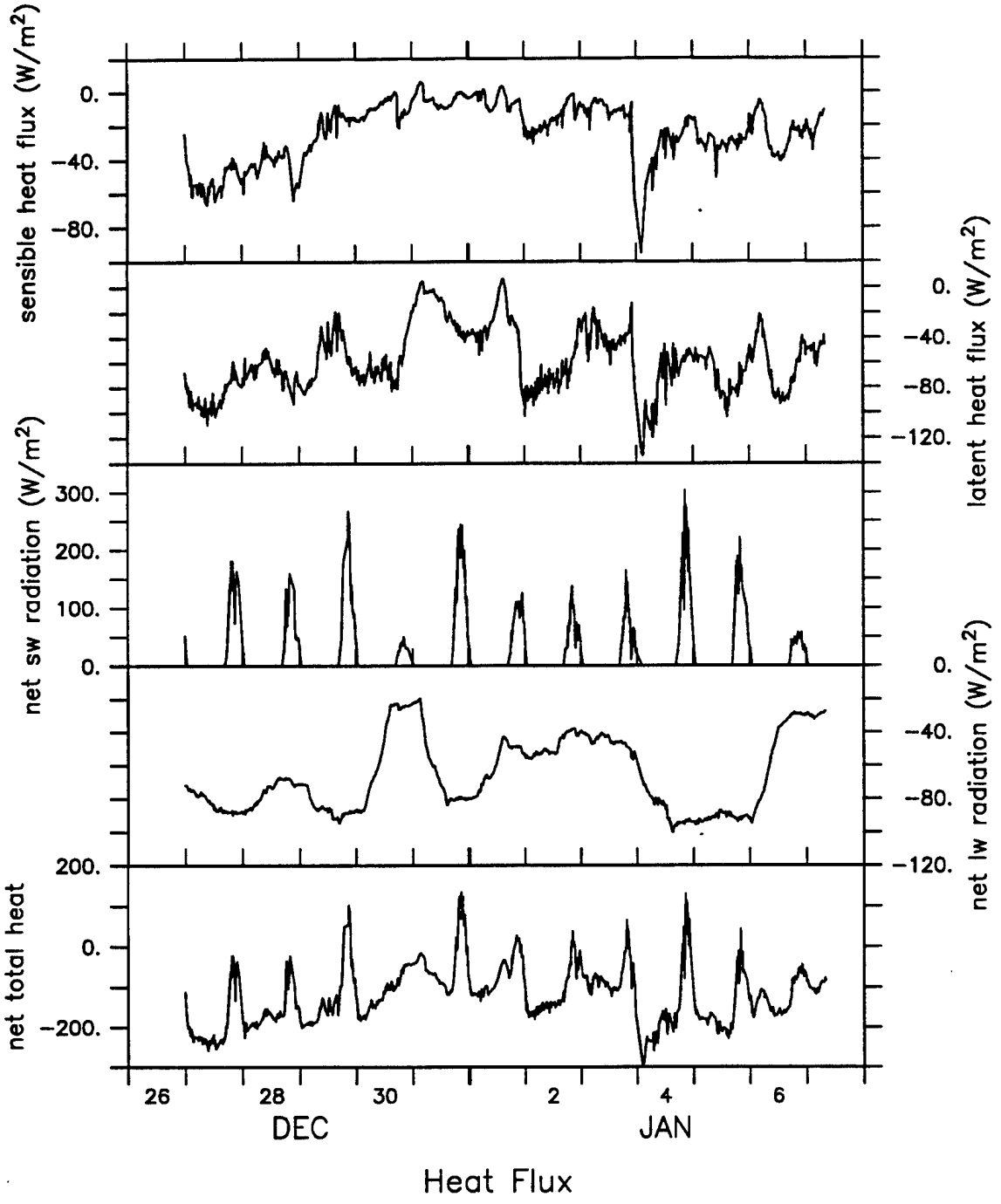

Figure 3.1.10 Heat Flux Time Series from VAWR.

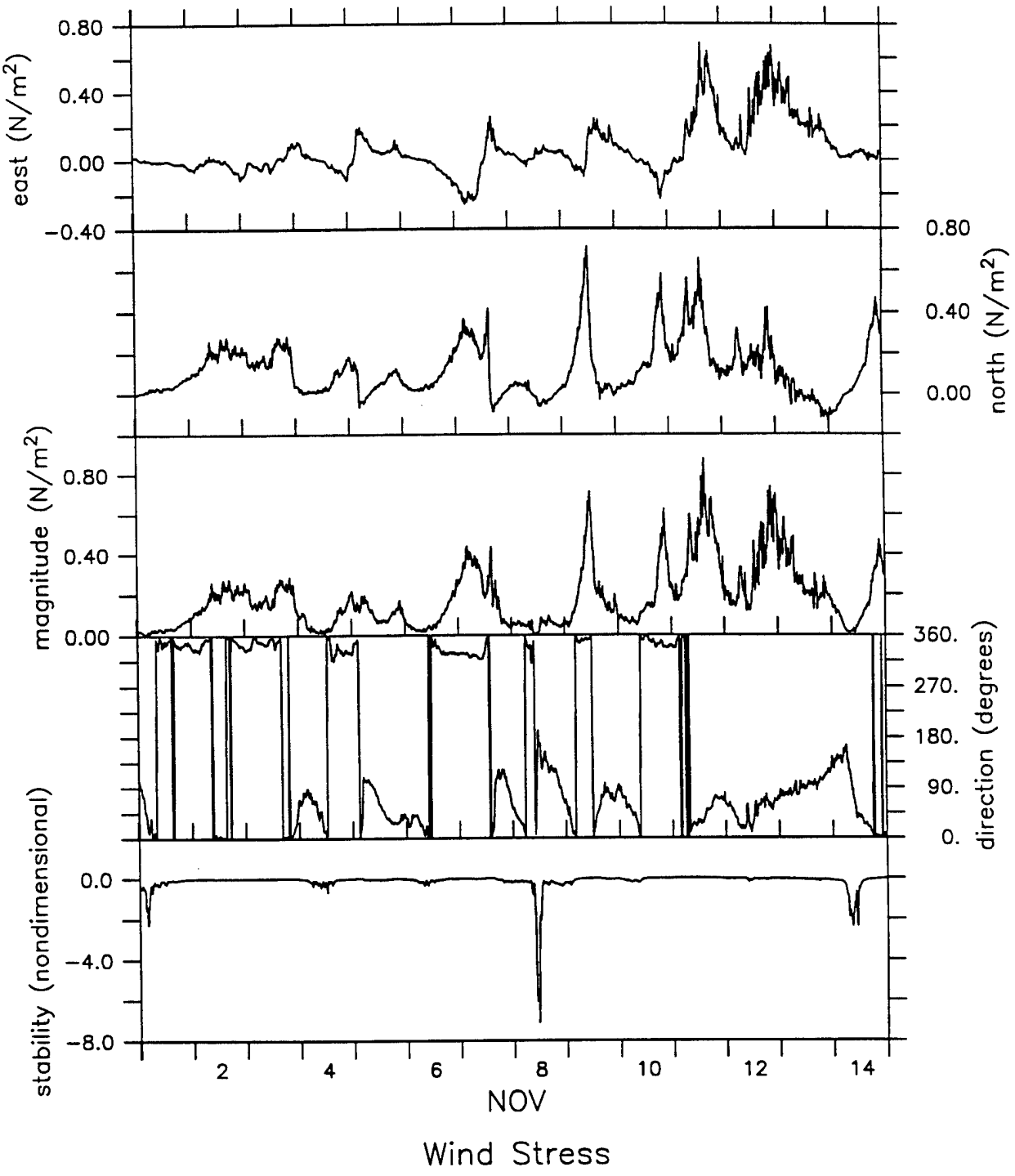

Figure 3.1.11 Wind StressTime Series from VAWR.

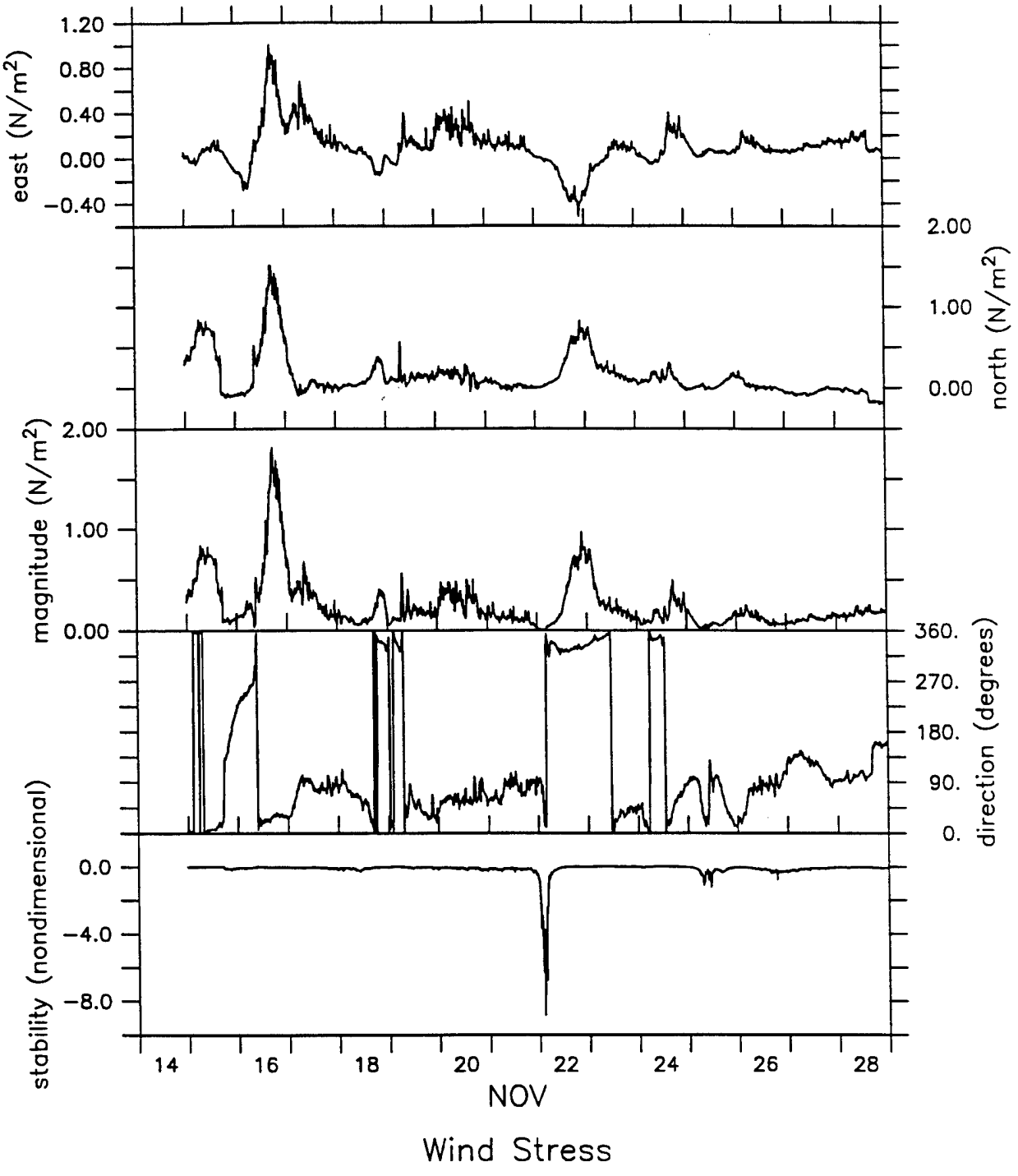

Figure 3.1.12 Wind Stress Time Series from VAWR.

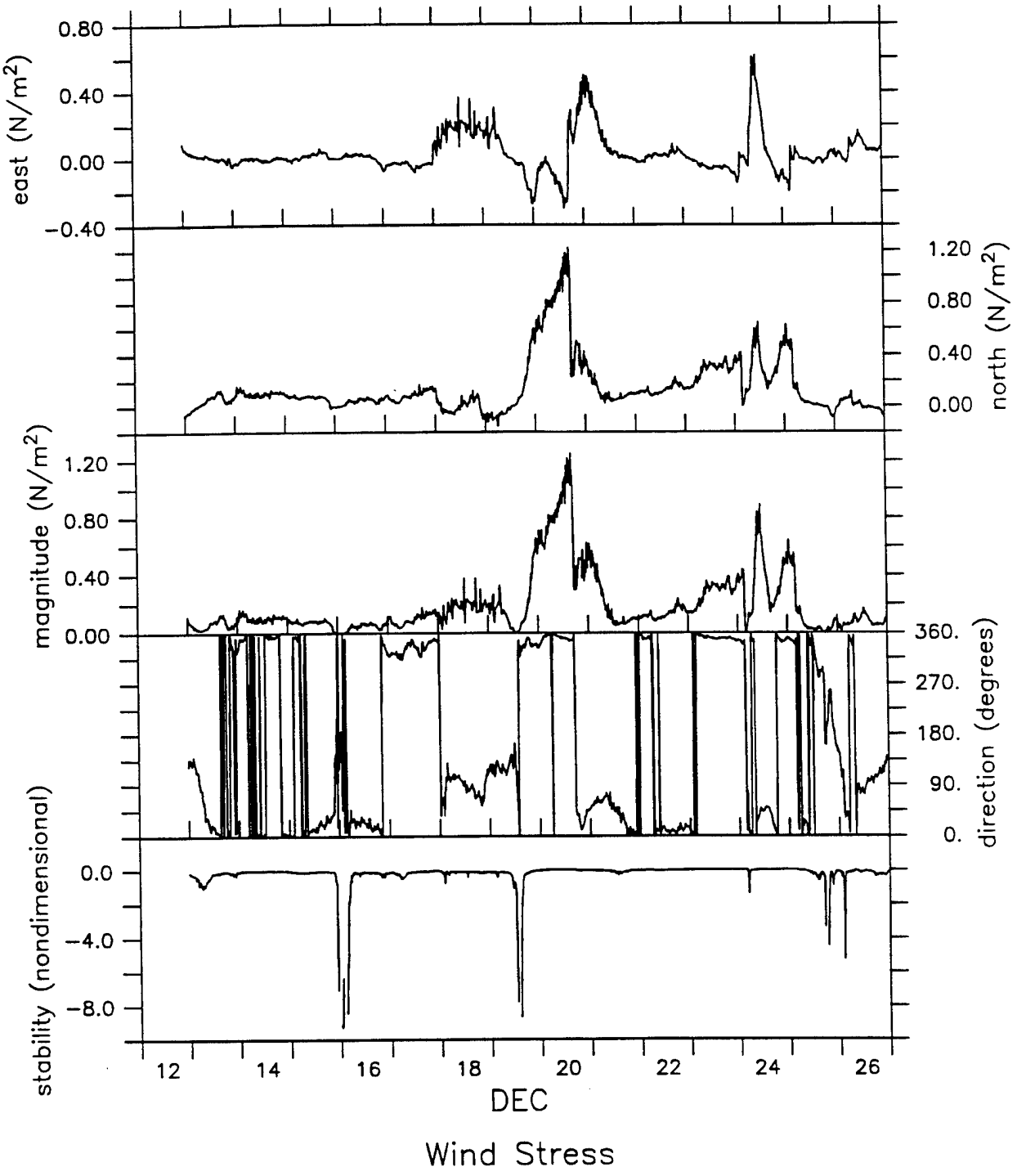

Figure 3.1.13 Wind Stress Time Series from VAWR.

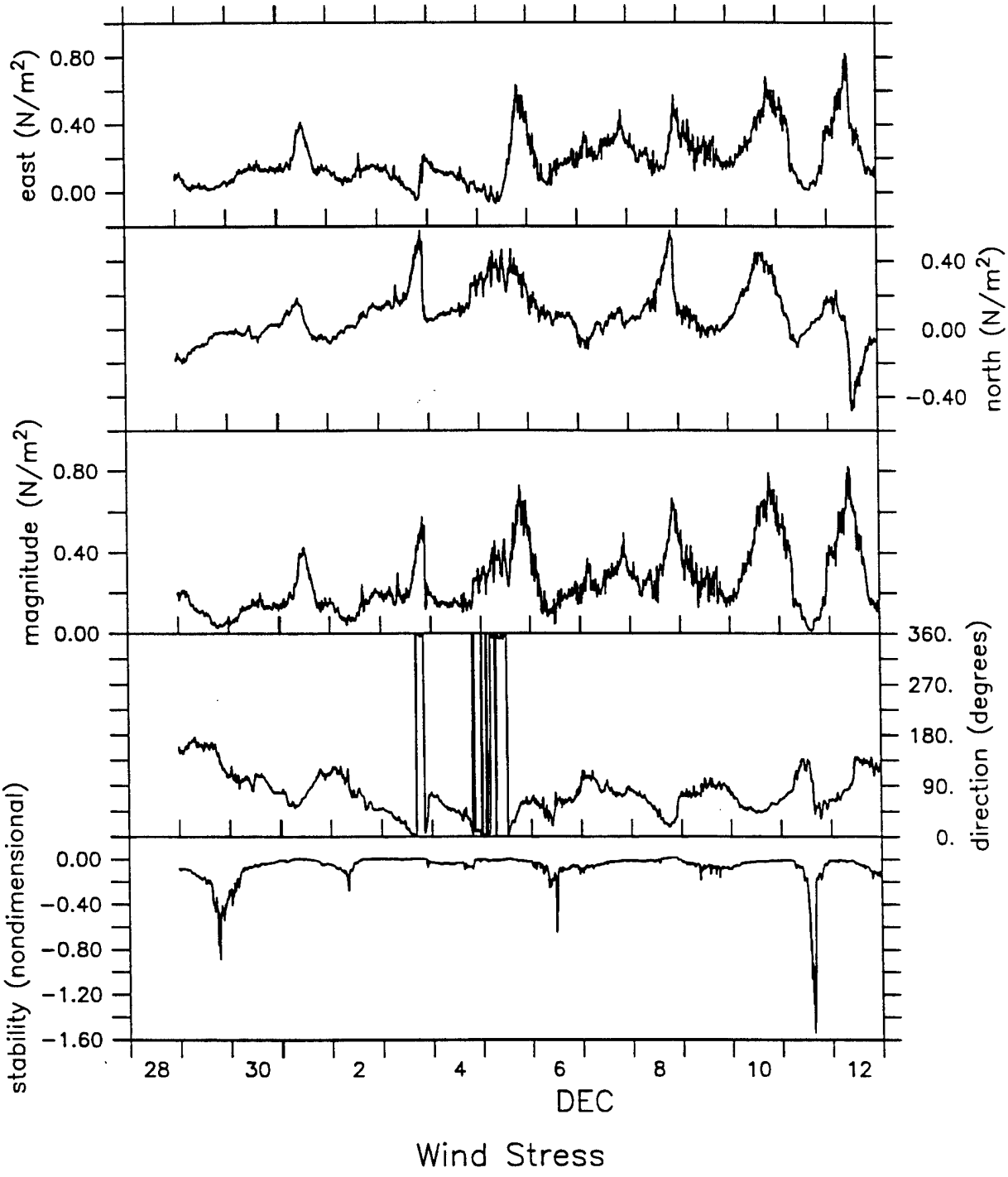

Figure 3.1.14 Wind Stress Time Series from VAWR.

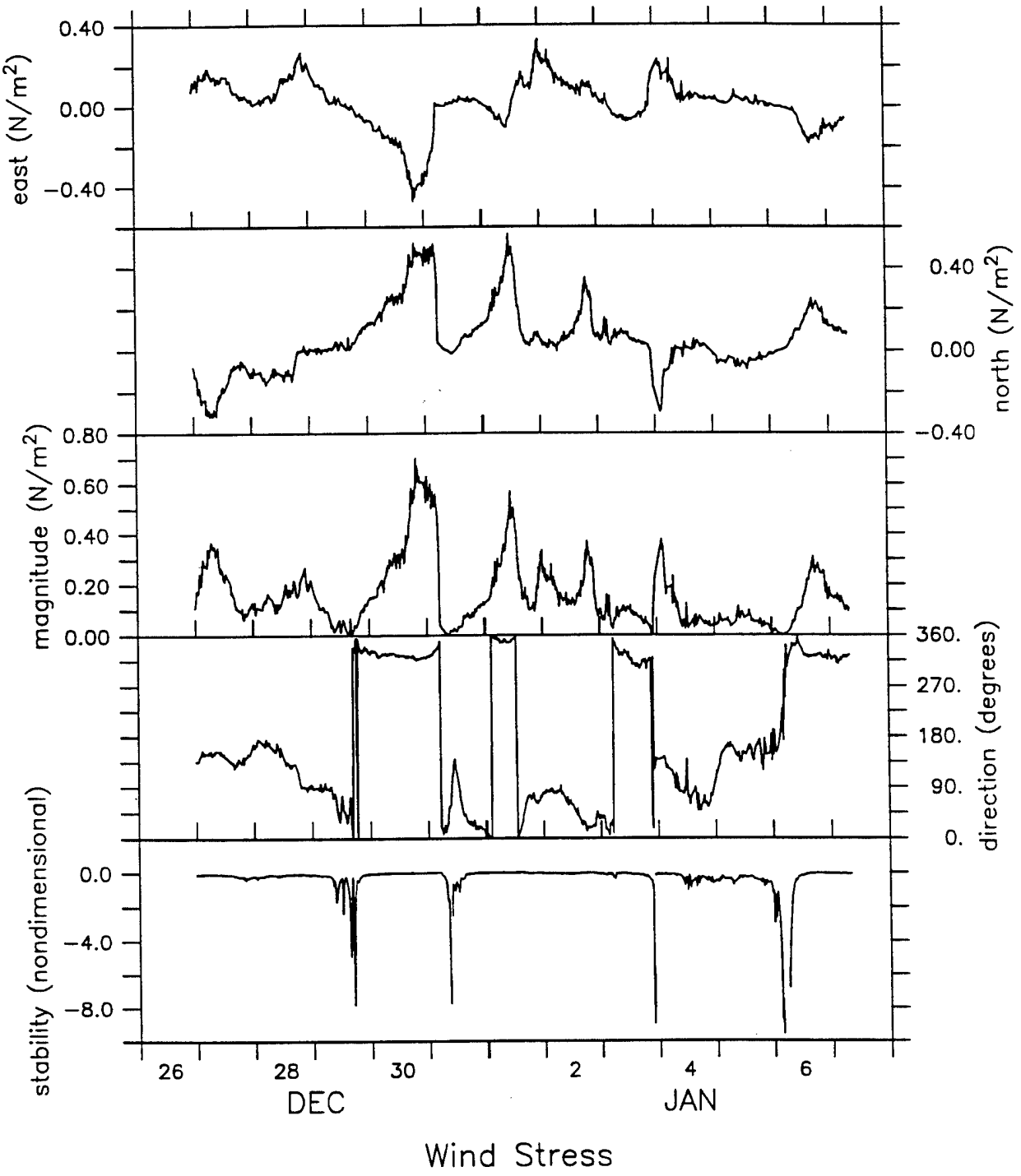

Figure 3.1.15 Wind Stress Time Series from VAWR.

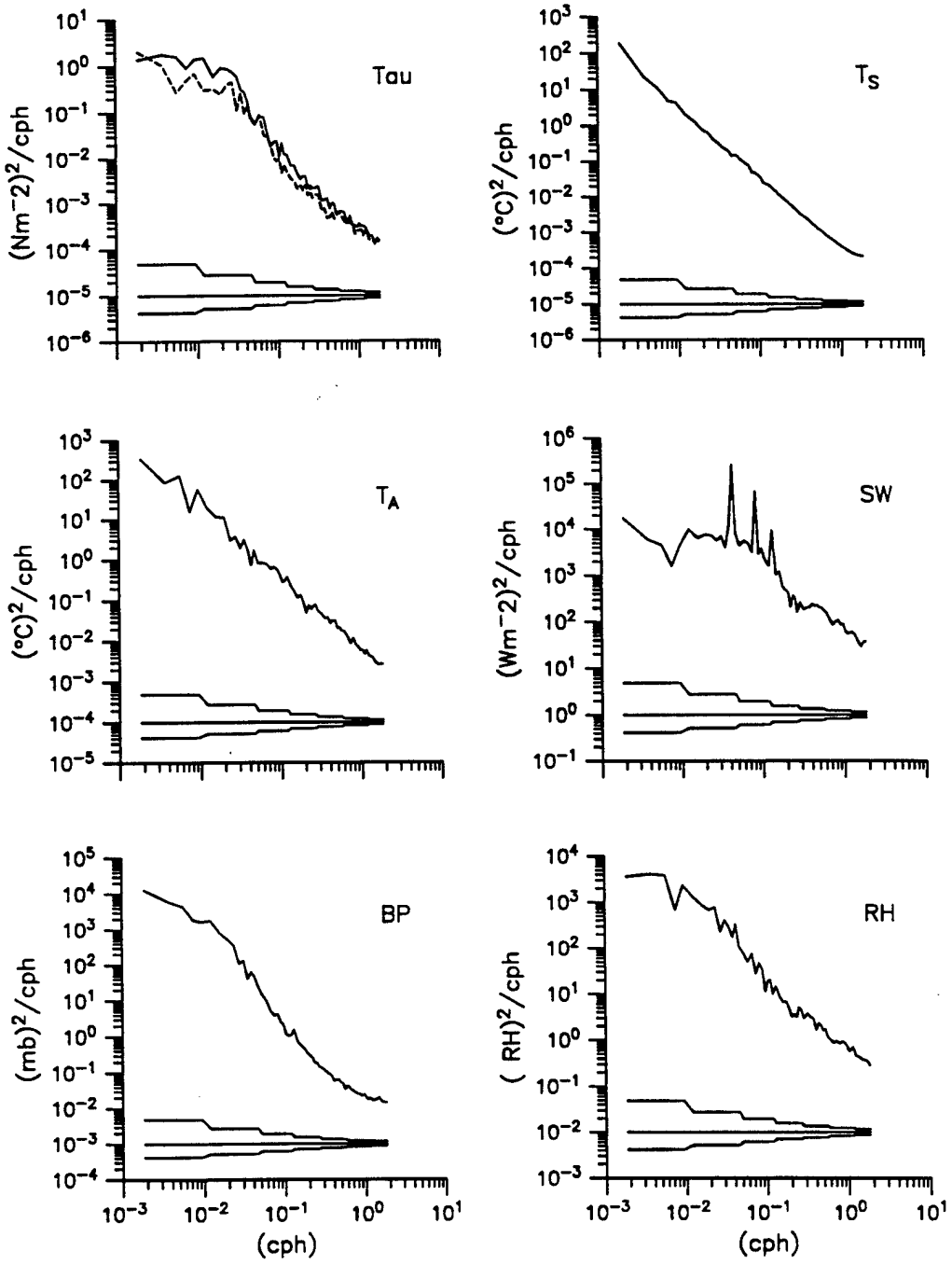

Figure 3.1.16 Autospectra of wind stress, air temperature, barometric pressure, sea surface temperature, insolation, and relative humidity . Rotary autospectra are shown for wind stress; solid curves show the clockwise component, and dashed curves show the counter-clockwise component.

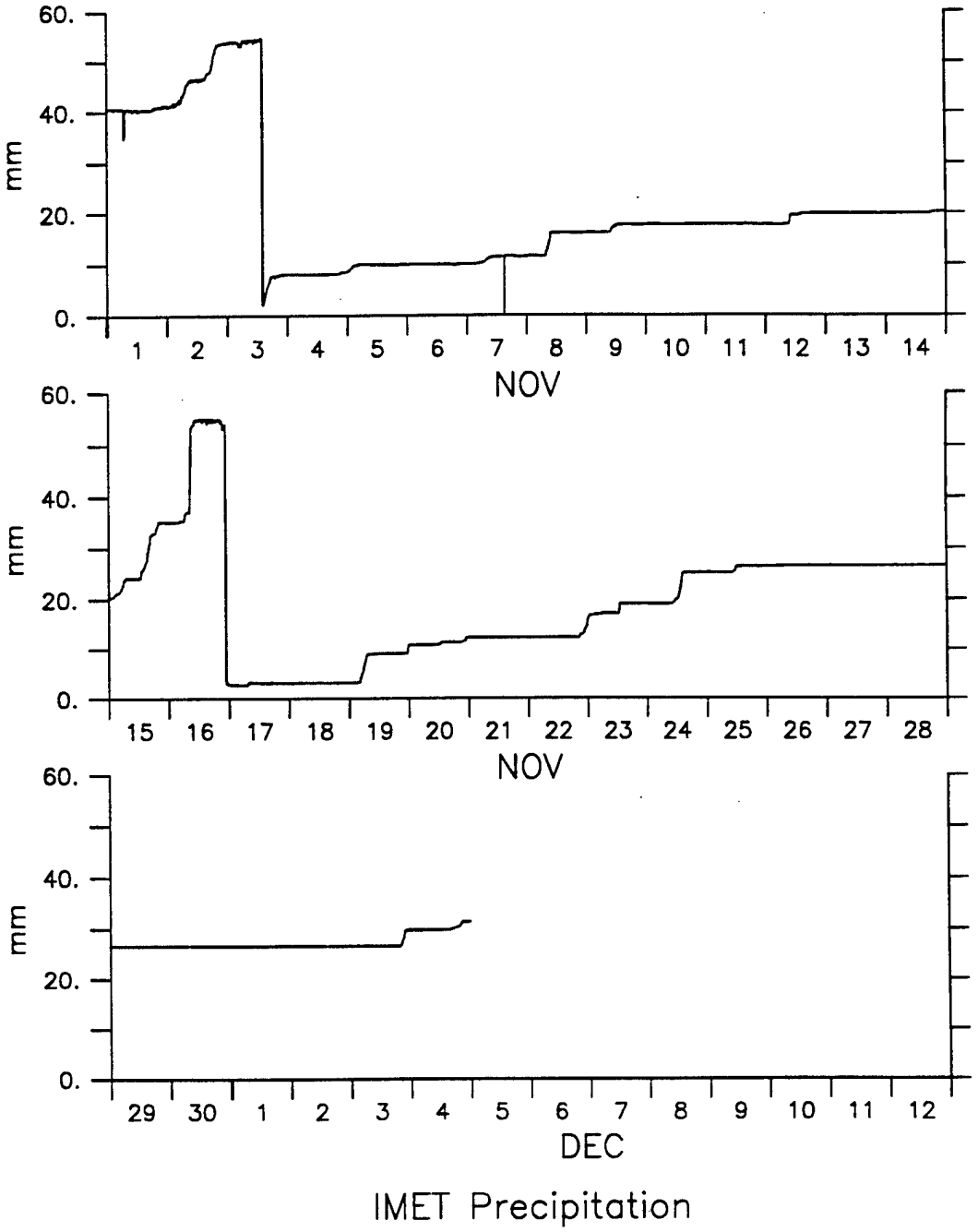

Figure 3.1.17 Cumulative Precipitation in mm measured by IMET system using an R.M. Young self siphoning rain gauge. Rain gauge drains when level reaches a critical value.

3. 2 Temperature and Density Structure during ASREX 91

Sea temperatures were measured by the VAWR, by six Brancker temperature recorders (TPODs) at depths of 2, 40, 60, 80, 100, and 120 meters, and by four Vector Measuring Current Meters (VMCMs) at 5, 10, 15, and 20 meters. VMCMs recorded data every 112.5 seconds, and TPODs recorded every 450 seconds.

Each temperature sensor was calibrated in the lab before and after the experiment, with the exception of TPOD 3700, which did not recieve a post-cruise calibration. Because data comparisons for the shallow instruments looked good using pre-cruise calibrations, all but Brancker 3662, at 60m, were processed with pre-cruise calibrations.

Figure 3.2.1 is a contour plot of all the temperature data from the moored array instruments. Data was filtered using a 24-hour running mean to remove the semidiurnal tide signal, and subsampled at 900 second intervals to produce a uniform time-series for the contour plot.

Time-series and spectra of temperature at each depth are presented in figures 3.2.2 through 3.2.11. In the upper frame of each of these plots, temperature is represented along the y axis and time (UTC) along the x axis. The lower frame contains the spectra. The long arrows on the lower frames indicate the frequency of the semidiurnal tidal peak and the short arrows show the frequency of the Coriolis peak. Confidence limits are displayed at the bottom of the frame. Captions indicate instrument type and depth. Unlike the previous plot,

the data here is not smoothed, so that the strong signals associated with the semidiurnal tides are readily visible.

CTD casts were taken to a depth of about 375 meters. Five casts were taken before deployment of the moored array, and two casts were taken after recovery. Information on CTD cast dates and locations is contained in Appendix 3. Profiles of CTD temperature, salinity, and density are shown in figures 3.2.12 through 3.2.17. These plots show that over the course of the deployment, the mixed layer depth increased from about 40 meters to about 80 meters as indicated by the temperature data alone.

The temperature records in the upper 40 meters of the water column show relatively little short-time variability. The temperature records at 60, 80, 100 and 120 meters show strong peaks at the frequency of the semidiurnal tide. The tidal signal appears to be strongest near the top of the main thermocline.

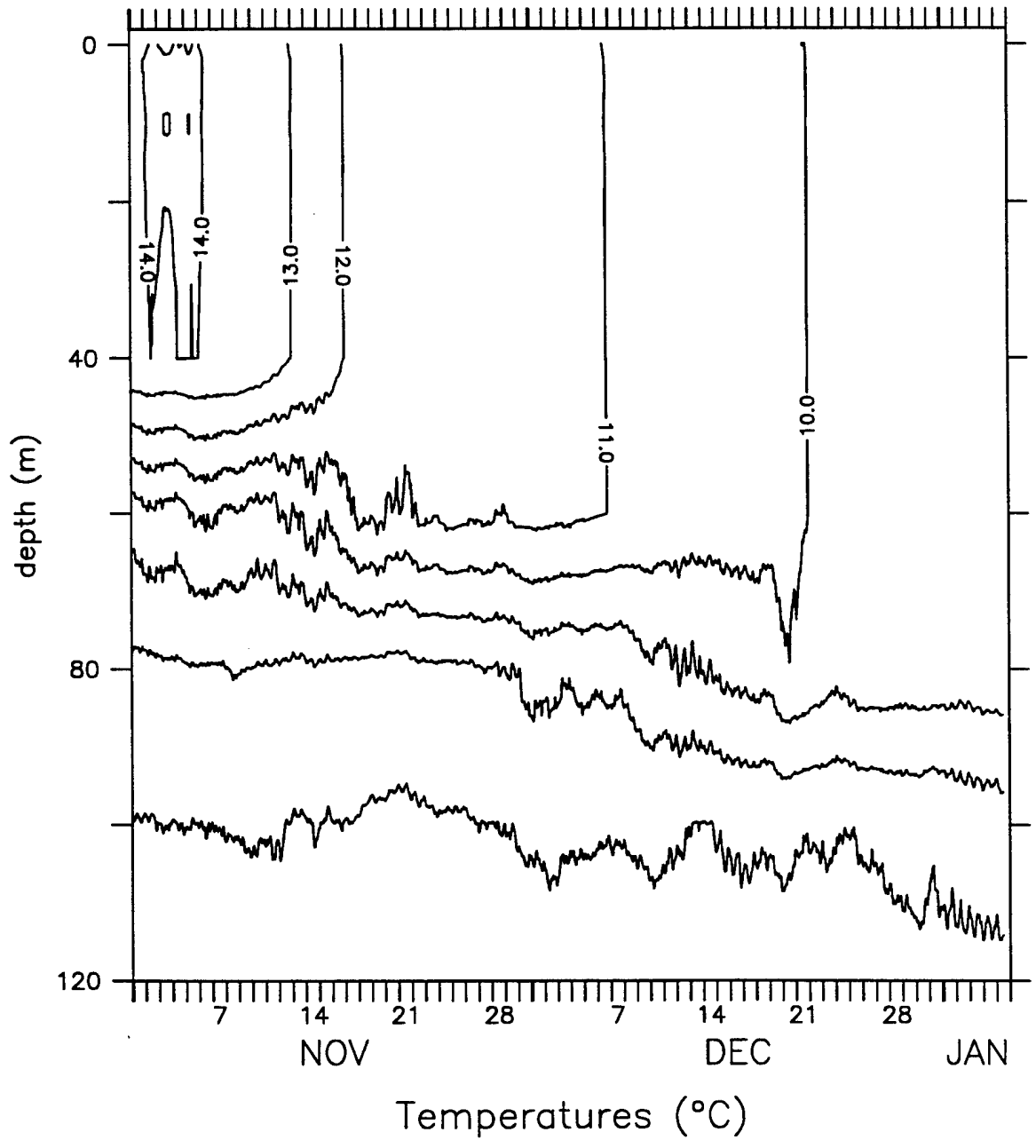

Figure 3.2.1 Temperature Contours from data at 0, 2, 5, 10, 15, 20, 40, 60, 80, 100, and120 meters. Data is filtered over 24 hours and decimated to 15 minutes per record before plotting.

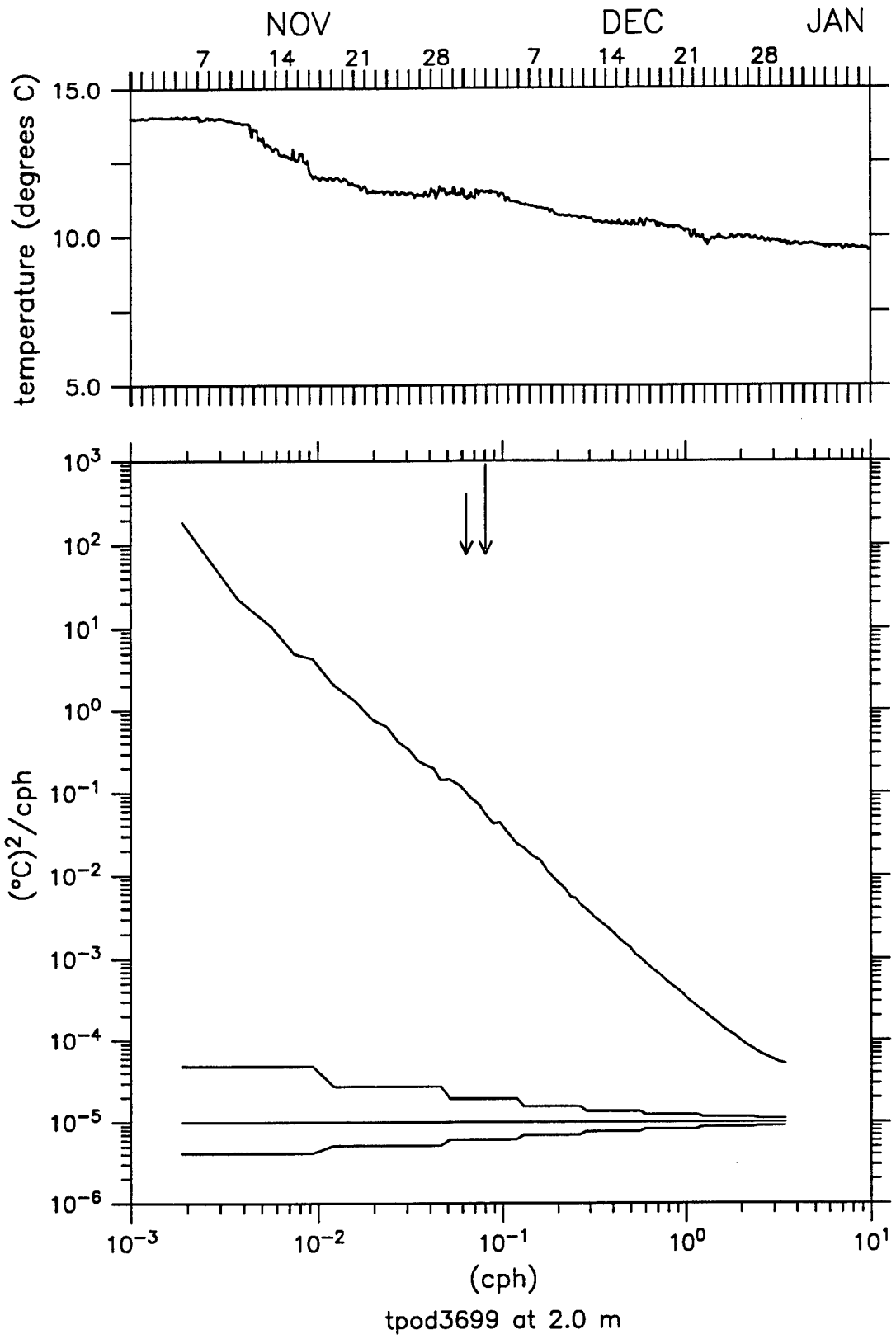

Figure 3.2.2 Temperature Time Series and Spectra at 2 m. Long arrow indicates semi-diurnal tidal frequency, short arrow indicates coriolis frequency.

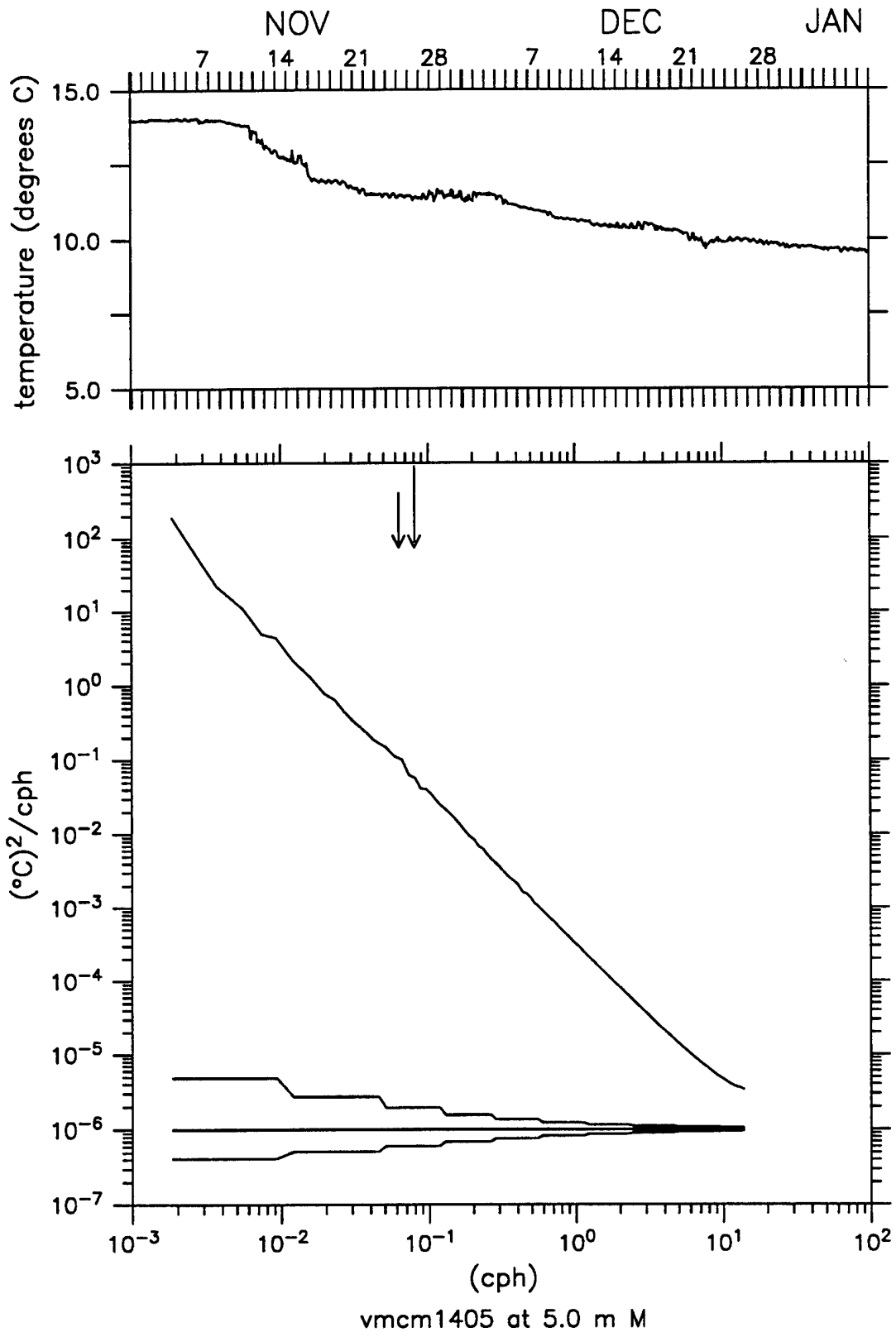

Figure 3.2.3 Temperature Time Series and Spectra at 5 m. Long arrow indicates semi-diurnal tidal frequency, short arrow indicates coriolis frequency.

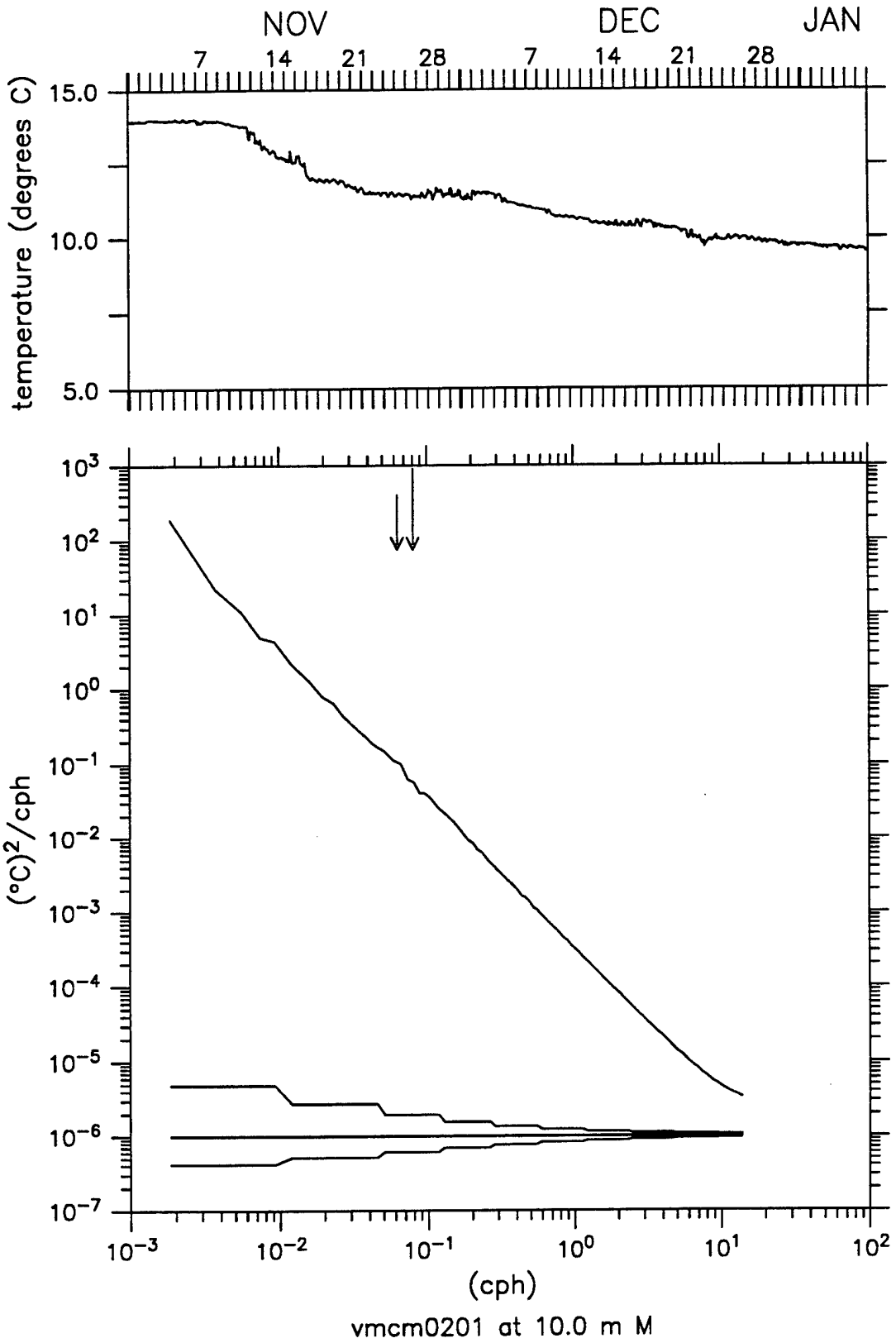

Figure 3.2.4 Temperature Time Series and Spectra at 10m. Long arrow indicates semi-diurnal tidal frequency, short arrow indicates coriolis frequency.

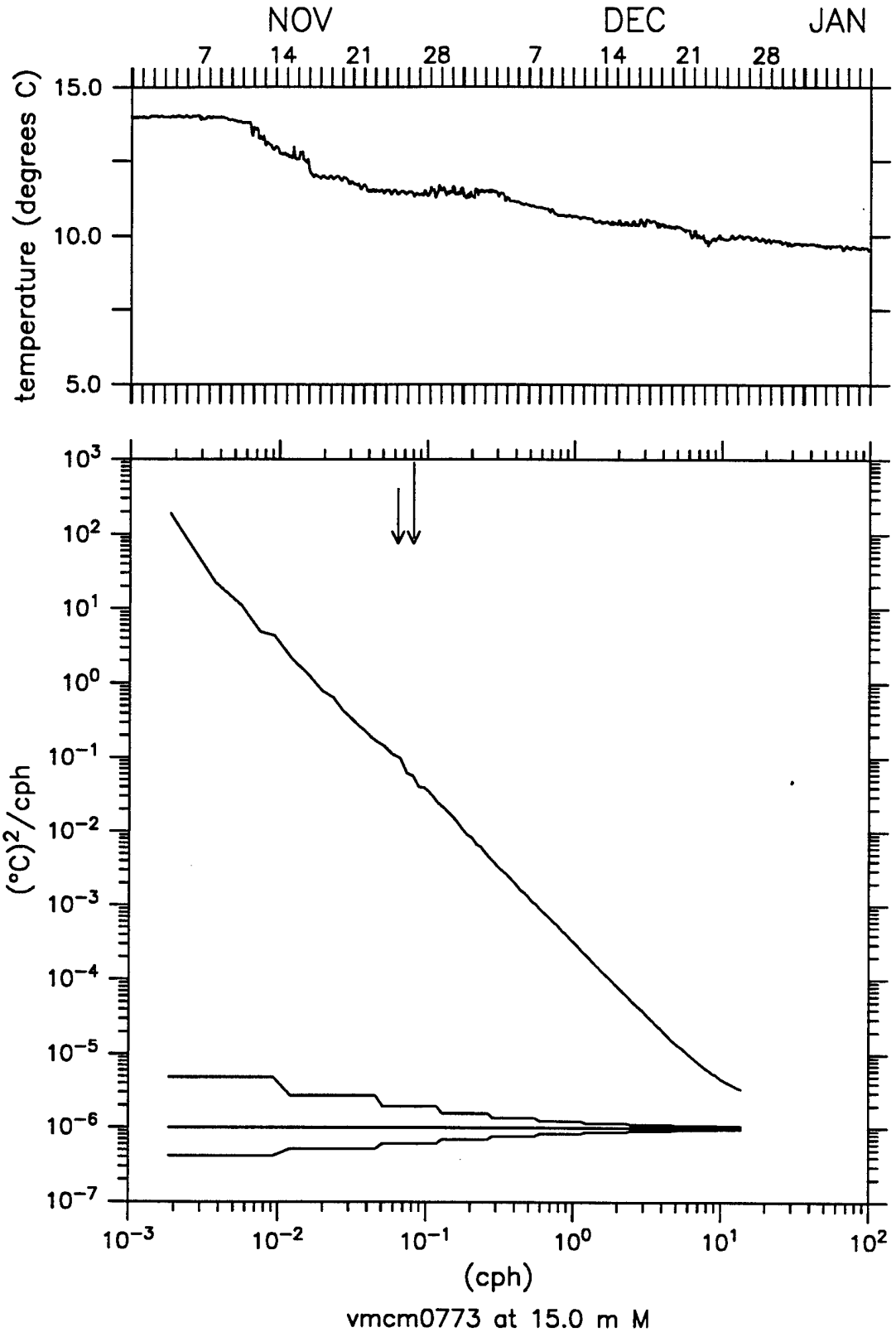

Figure 3.2.5 Temperature Time Series and Spectra at 15m. Long arrow indicates semi-diurnal tidal frequency, short arrow indicates coriolis frequency.

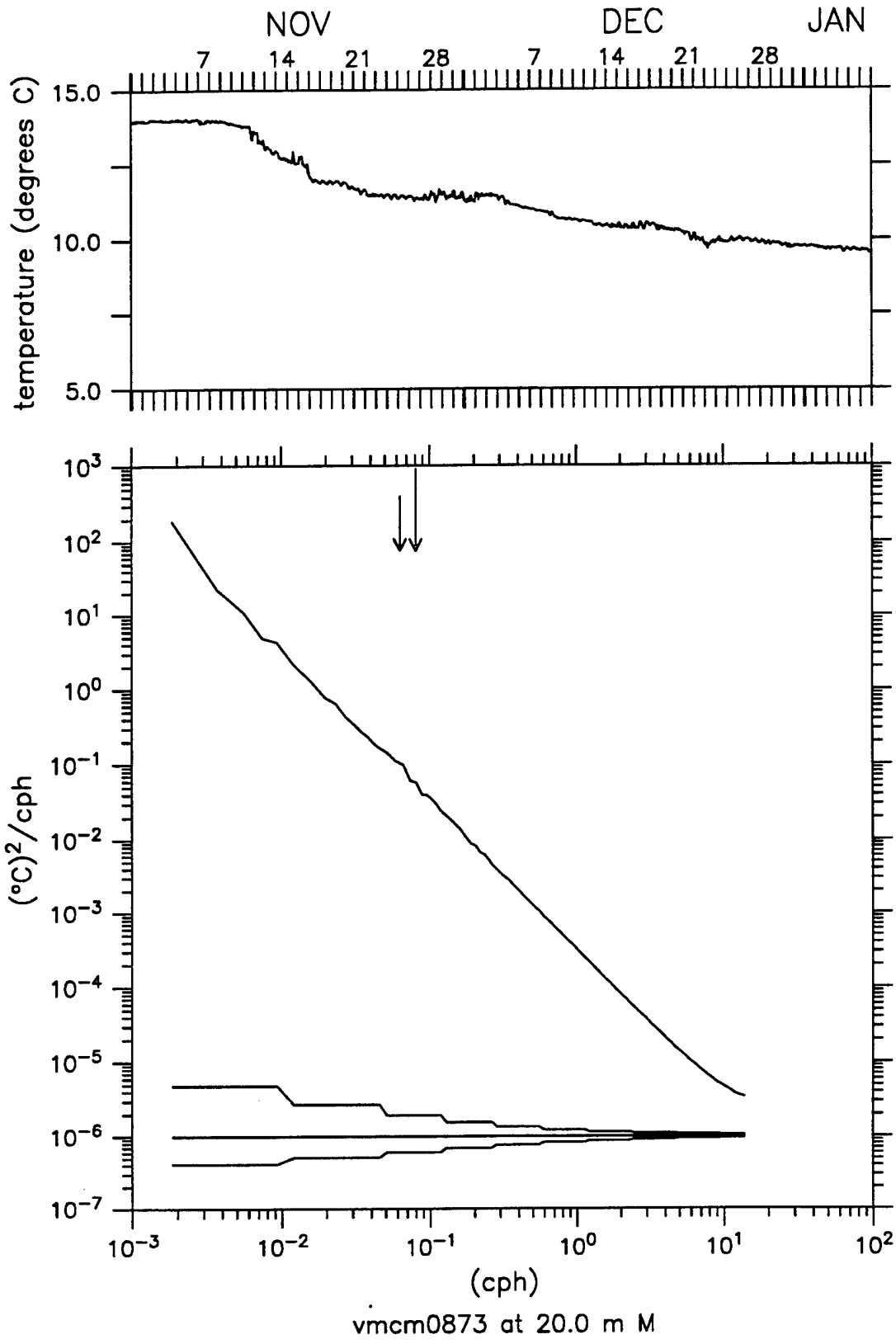

Figure 3.2.6 Temperature Time Series and Spectra at 20m. Long arrow indicates semi-diurnal tidal frequency, short arrow indicates coriolis frequency.

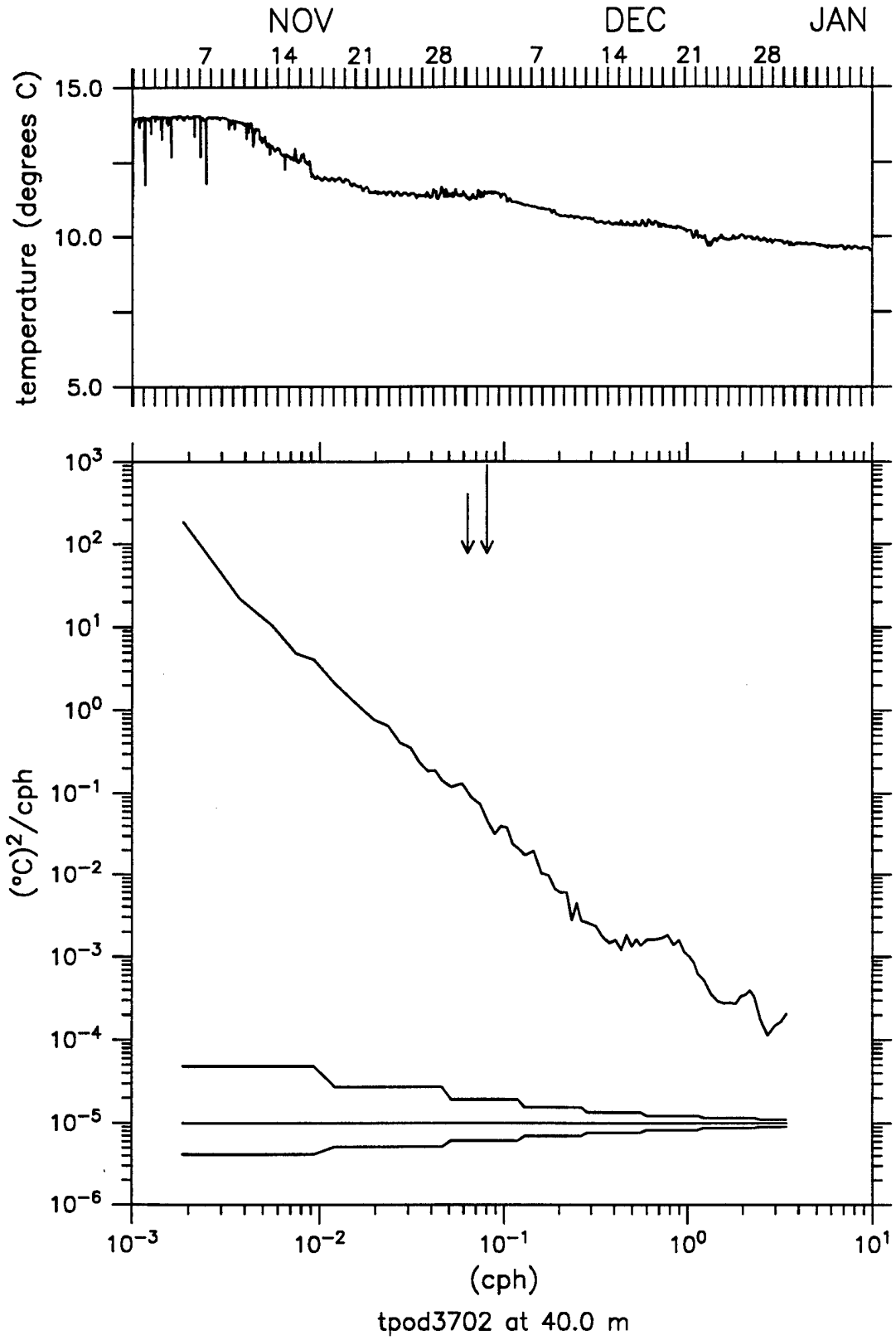

Figure 3.2.7 Temperature Time Series and Spectra at 40m. Long arrow indicates semi-diurnal tidal frequency, short arrow indicates coriolis frequency.

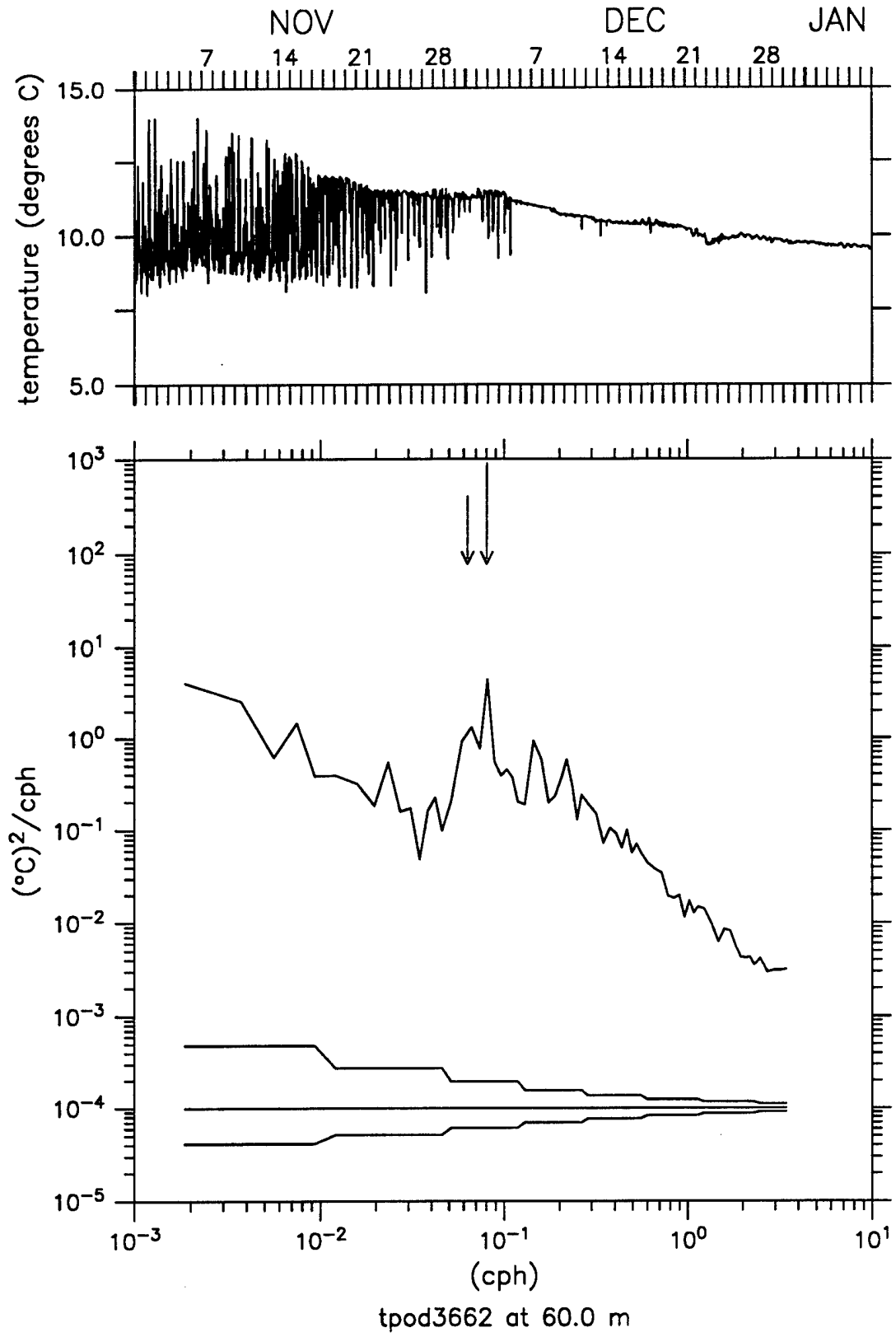

Figure 3.2.8 Temperature Time Series and Spectra at 60m. Long arrow indicates semi-diurnal tidal frequency, short arrow indicates coriolis frequency.

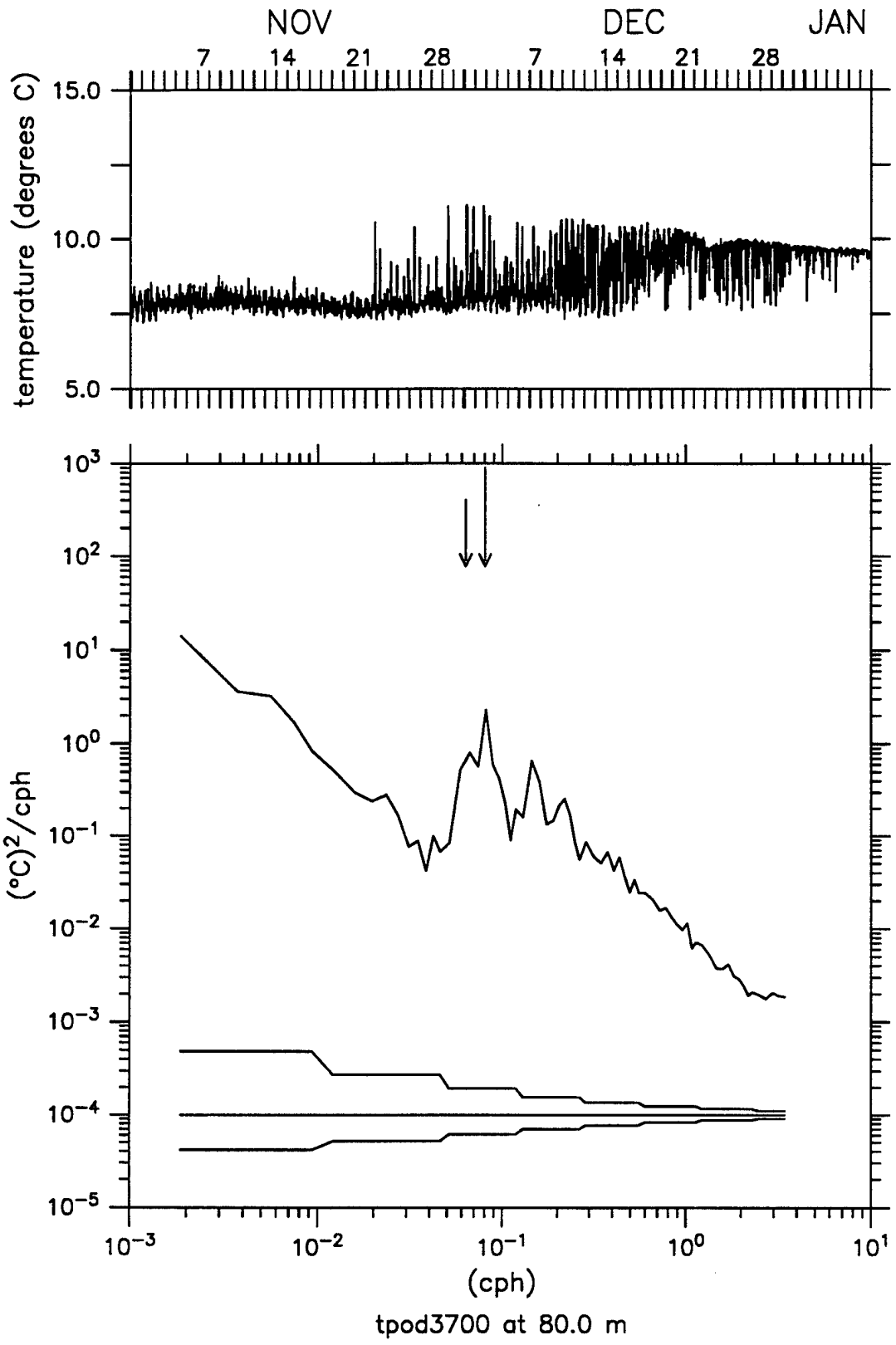

Figure 3.2.9 Temperature Time Series and Spectra at 80m. Long arrow indicates semi-diurnal tidal frequency, short arrow indicates coriolis frequency.

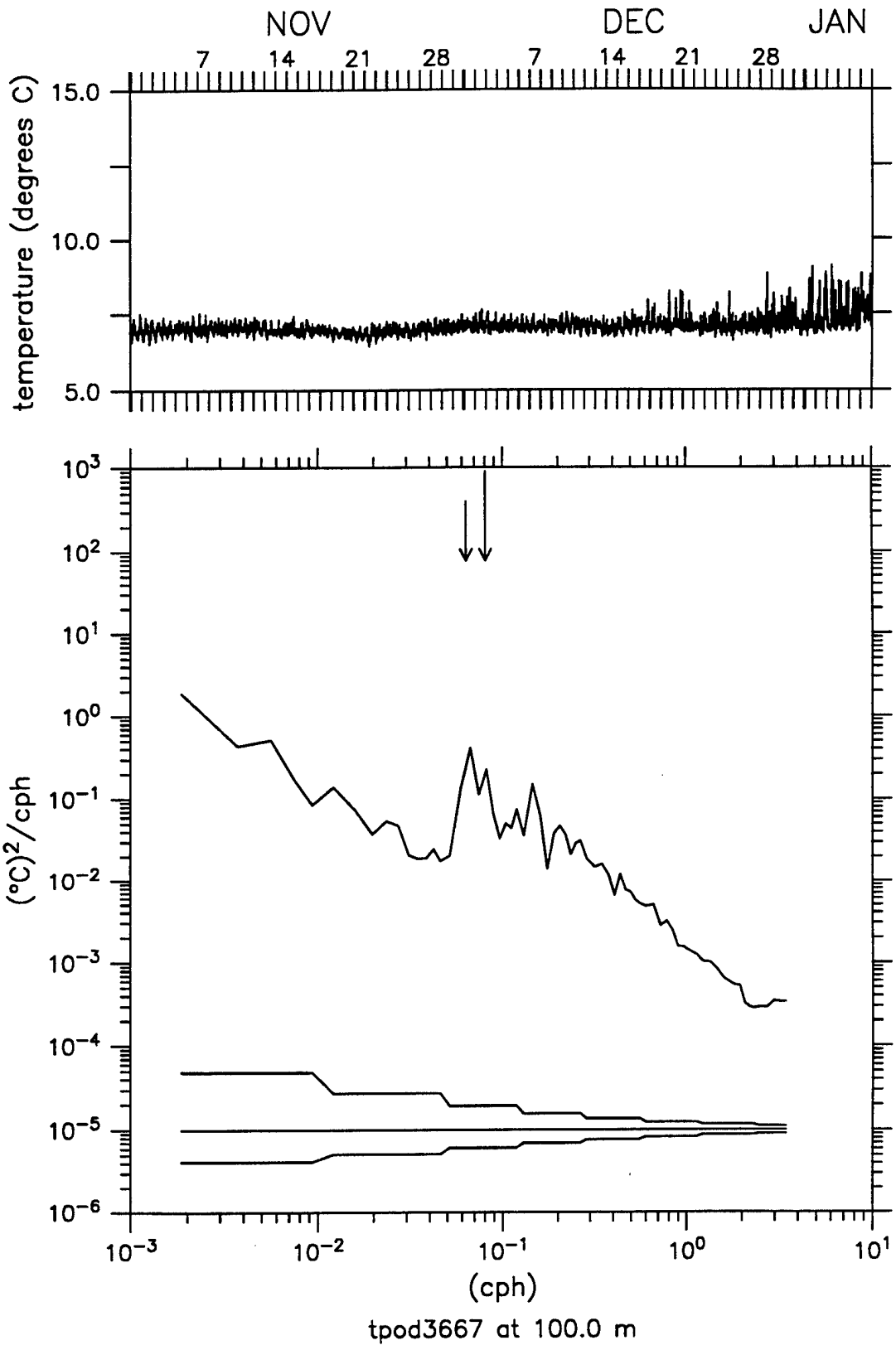

Figure 3.2.10 Temperature Time Series and Spectra at 100m. Long arrow indicates semi-diurnal tidal frequency, short arrow indicates coriolis frequency.

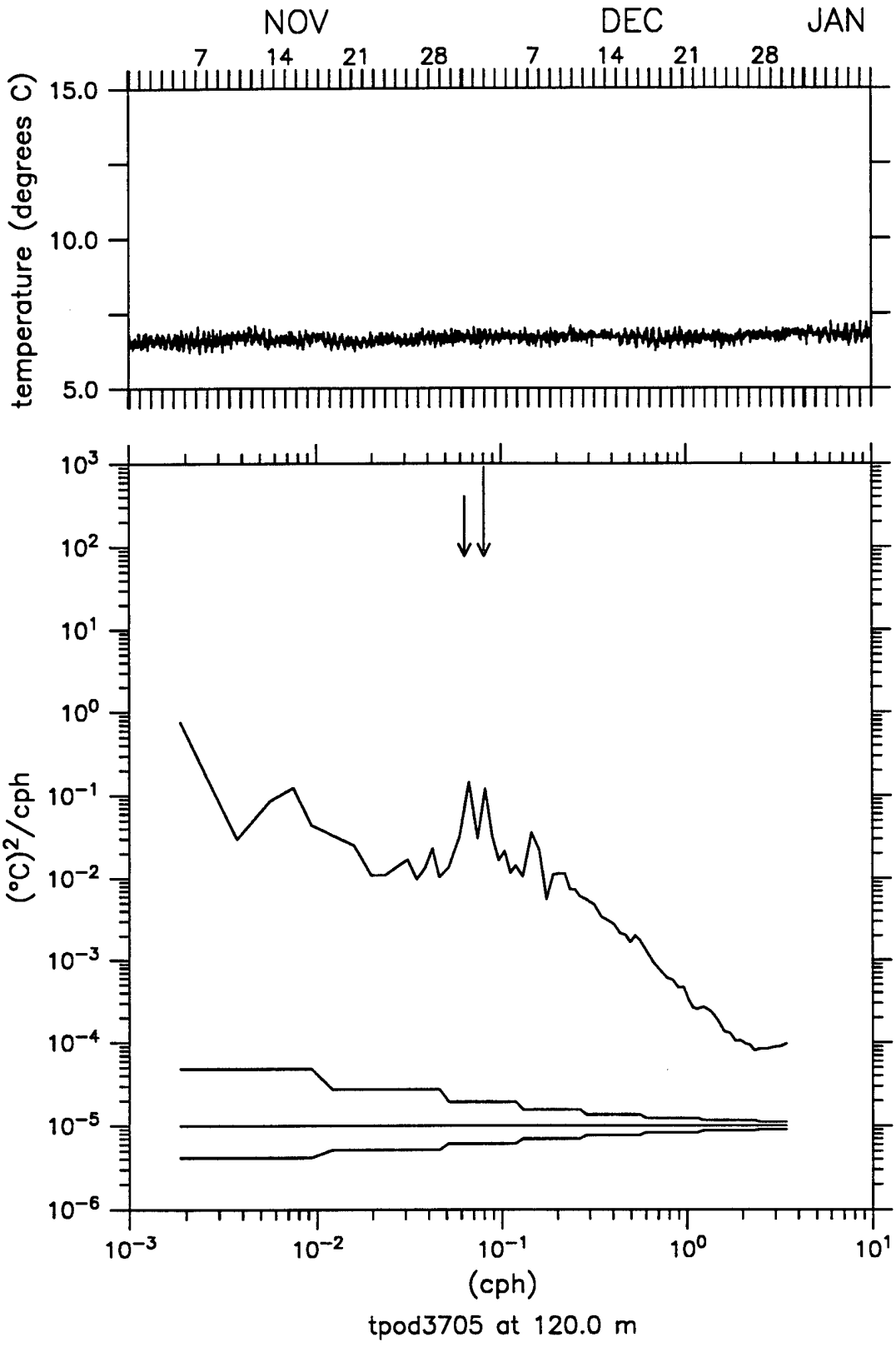

Figure 3.2.11 Temperature Time Series and Spectra at 120m. Long arrow indicates semi-diurnal tidal frequency, short arrow indicates coriolis frequency.

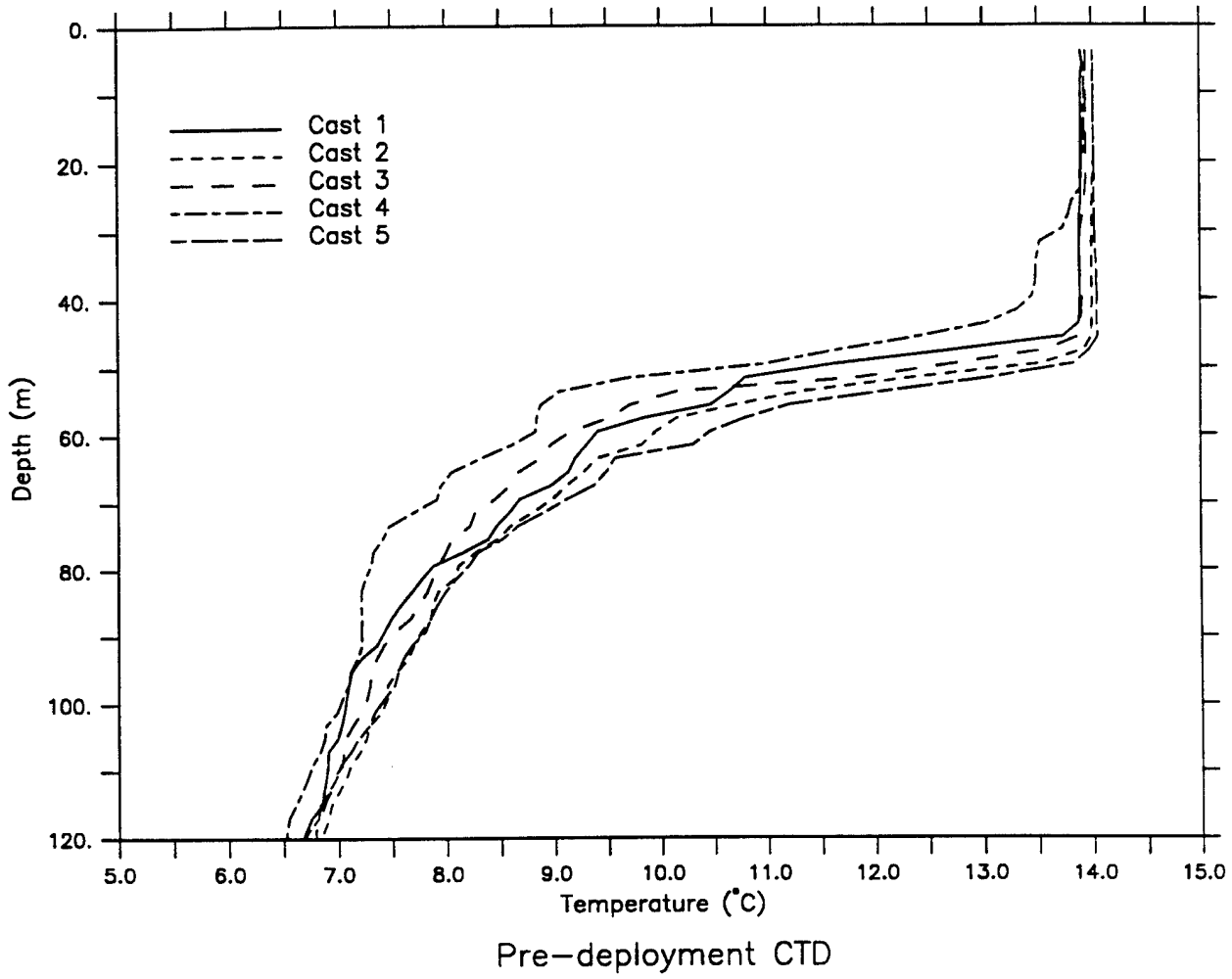

Figure 3.2.12 Temperature profiles from pre-deployment CTD casts taken on Thompson Cruise 4, leg 1. Cast 1 is solid, cast 2 is short dash, cast 3 is long dash, cast 4 is a short chain, cast 5 is a long chain.

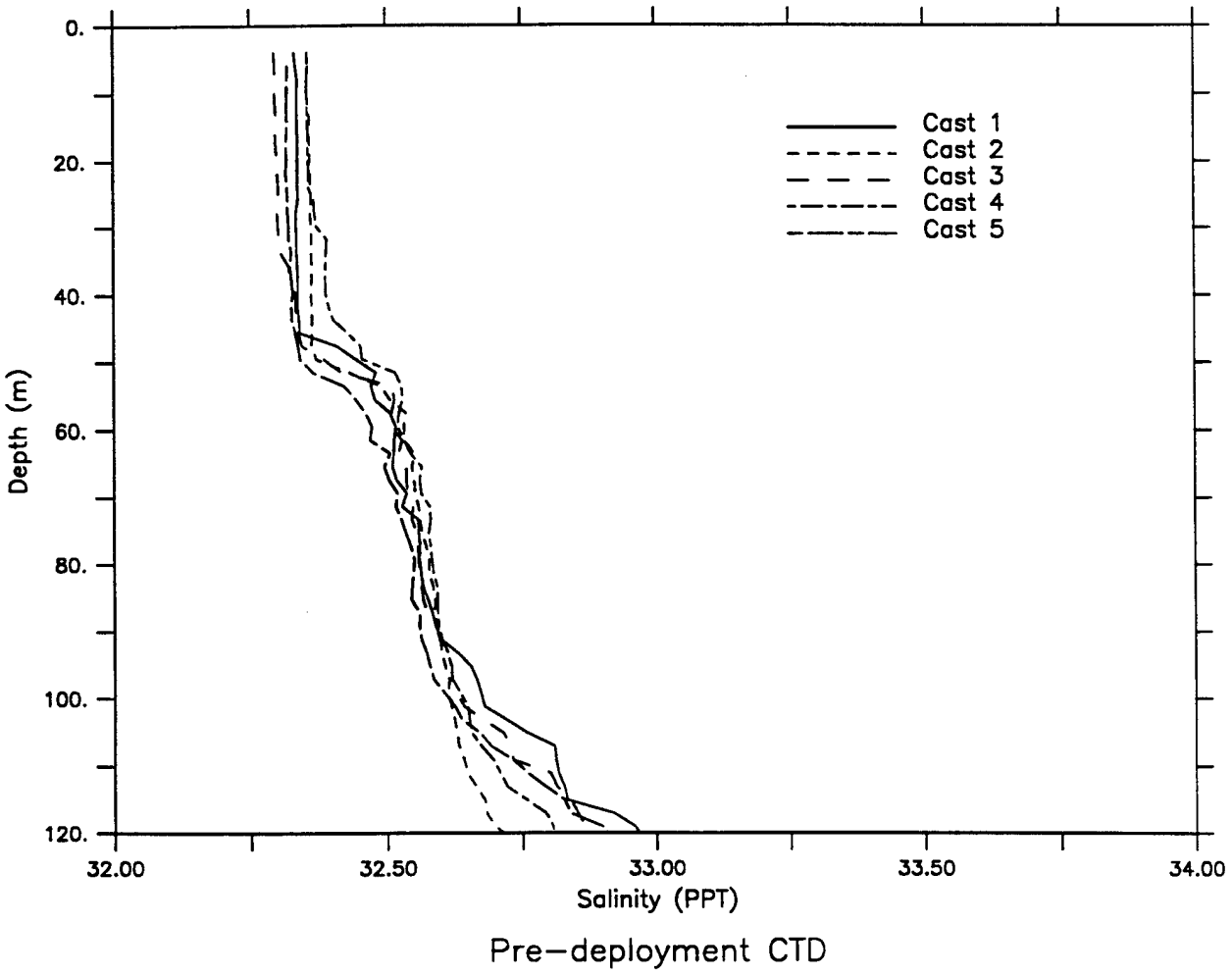

Figure 3.2.13 Salinity profiles from pre-deployment CTD casts taken on Thompson Cruise 4, leg 1. Cast 1 is solid, cast 2 is short dash, cast 3 is long dash, cast 4 is a short chain, cast 5 is a long chain.

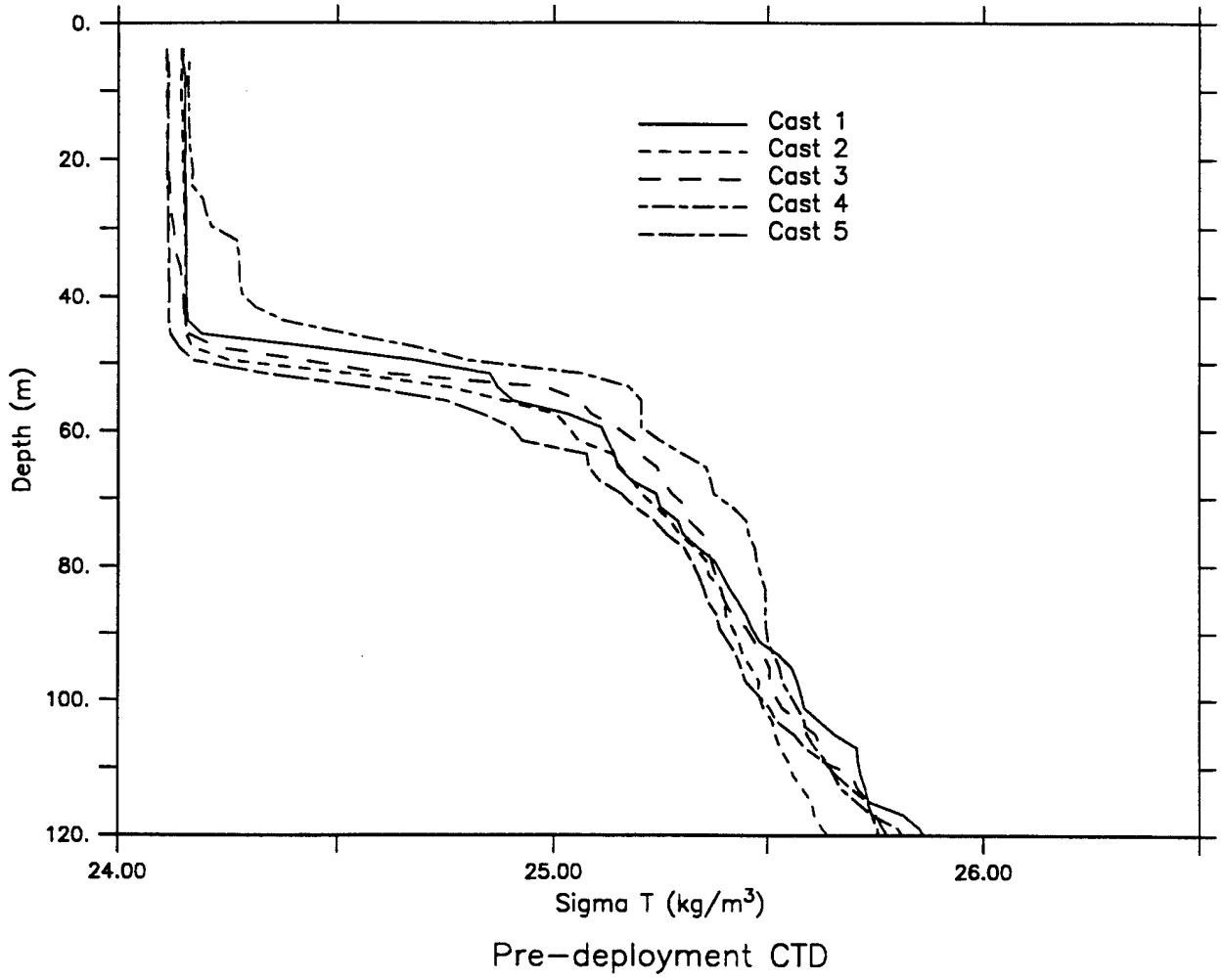

Figure 3.2.14 Density profiles from pre-deployment CTD casts taken on Thompson Cruise 4, leg 1. Cast 1 is solid, cast 2 is short dash, cast 3 is long dash, cast 4 is a short chain, cast 5 is a long chain.

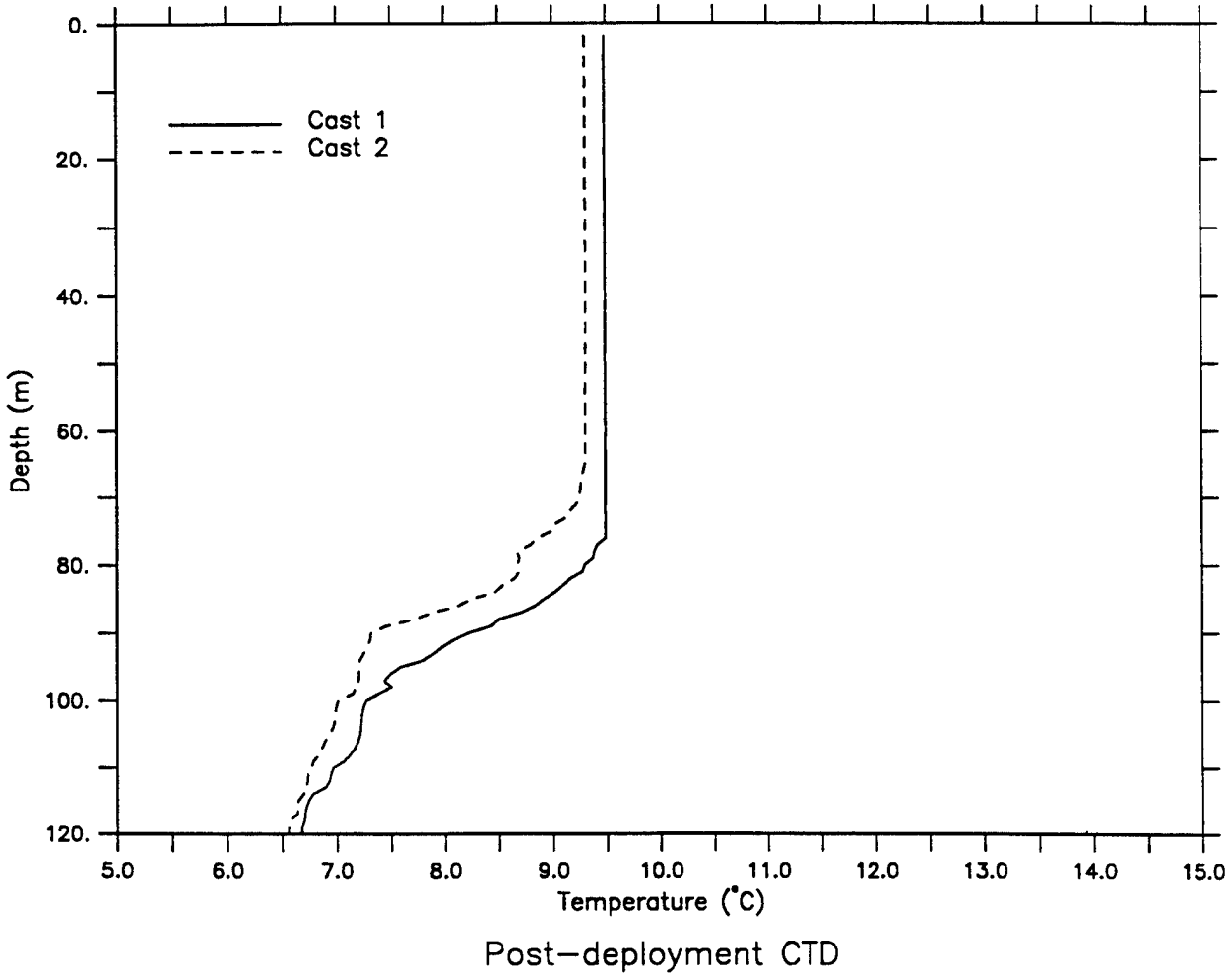

Figure 3.2.15 Temperature profiles from post-deployment CTD casts taken on Thompson Cruise 4, leg 2. Cast 1 is solid, cast 2 is dashed.

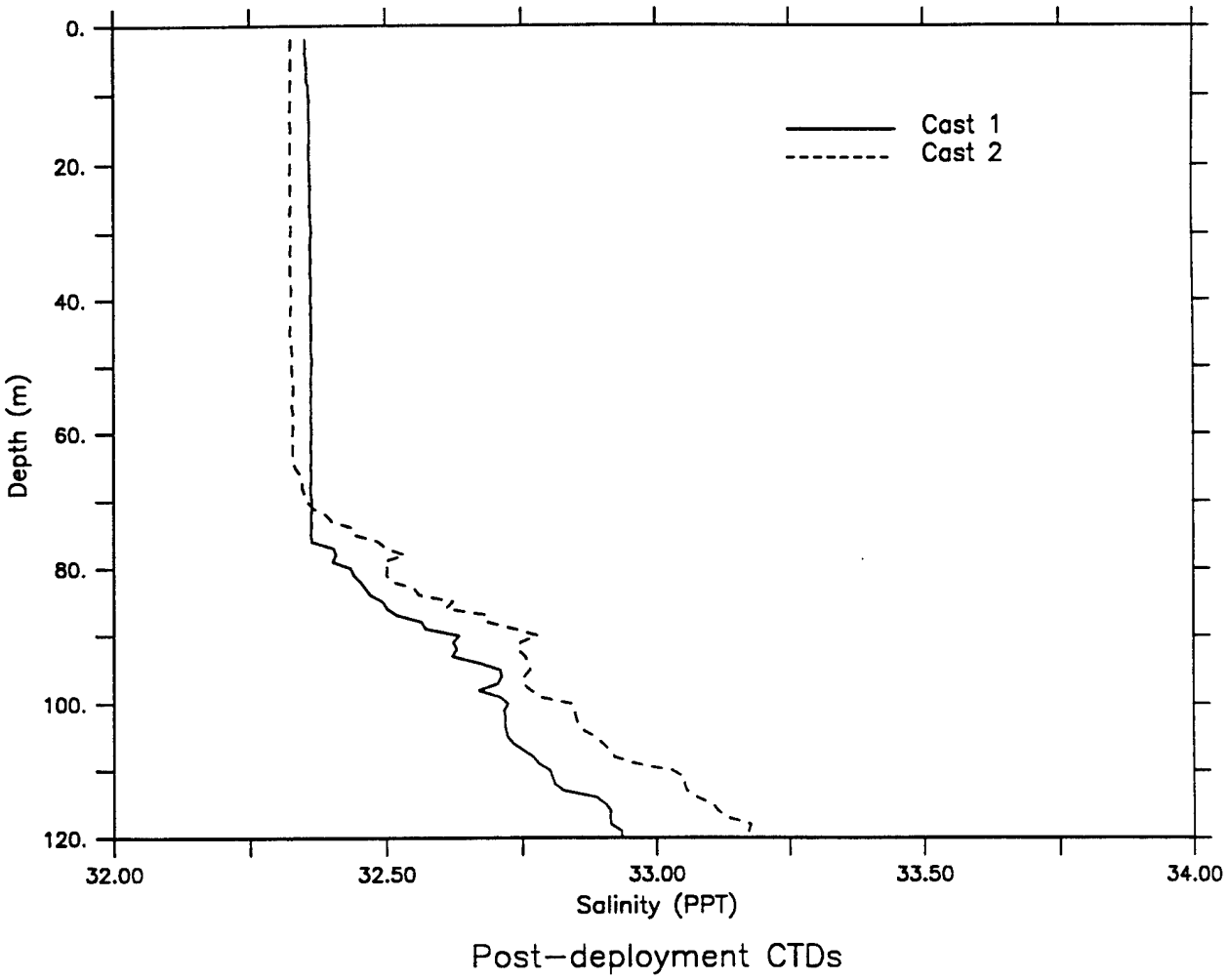

Figure 3.2.16 Salinity profiles from post-deployment CTD casts taken on Thompson Cruise 4, leg 2. Cast 1 is solid, cast 2 is dashed.

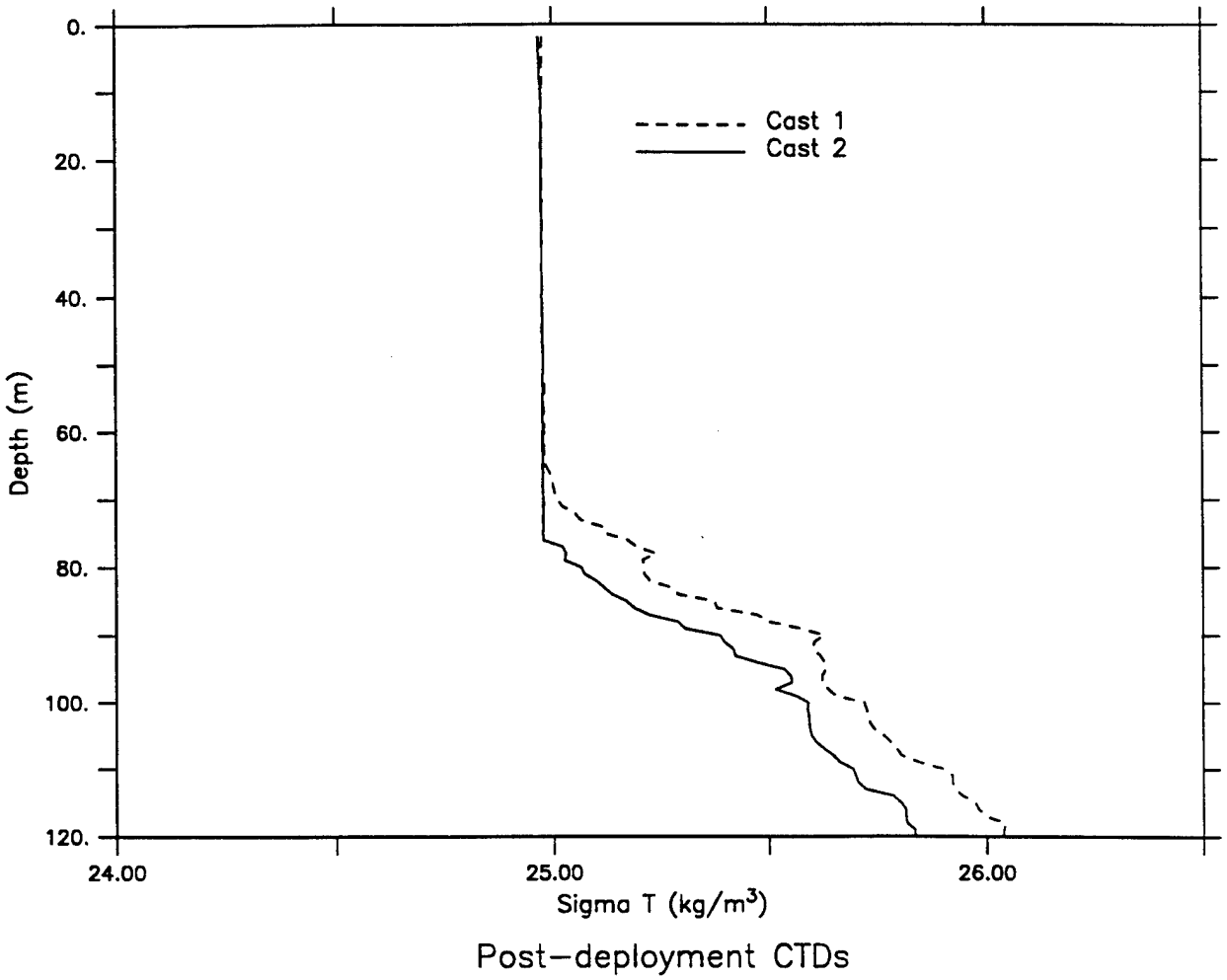

Figure 3.2.17 Density profiles from post-deployment CTD casts taken on Thompson Cruise 4, leg 2. Cast 1 is solid, cast 2 is dashed.

3.3. Current Velocities during ASREX 91

Currents were measured by VMCMs at 5, 10, 15, and 20 meters. The current meters recorded at a rate of once every 112.5 seconds. A time-base checking program was used to correct missing data and data with invalid time-words before any further processing was carried out. The final data set consists of 51713 reconds beginning at 0000Z 1 November, 1991 and concluding at 0801Z on 7 January, 1992.

Time series stick-plots of the water vectors at each depth are in figures 3.3.1 through 3.3.5. Data was filtered over a 48 hour period and decimated to 2 hours for the vector plots. Northerly velocities are represented by vectors pointing toward the top of the page.

Progressive vector plots for all four VMCMs are in figure 3.3.6. Velocity data was filtered over 8 hours and decimated to 4 hour values before plotting.

Figures 3.3.7 through 3.3.10 are combined time-series and spectra for currents at each depth. These plots show unfiltered data. The upper frame for each plot represents the north and east velocities along the vertical axes and time (UTC) along the horizontal axis. The lower frame contains the spectra, with a solid line indicating the clockwise component and a dashed line indicating the counter-clockwise component. As for temperature plots, the frequency of the Coriolis parameter and the semidiurnal tide are shown on the plots, and confidence limits are displayed. There are significant peaks associated with both the tide and Coriolis frequency.

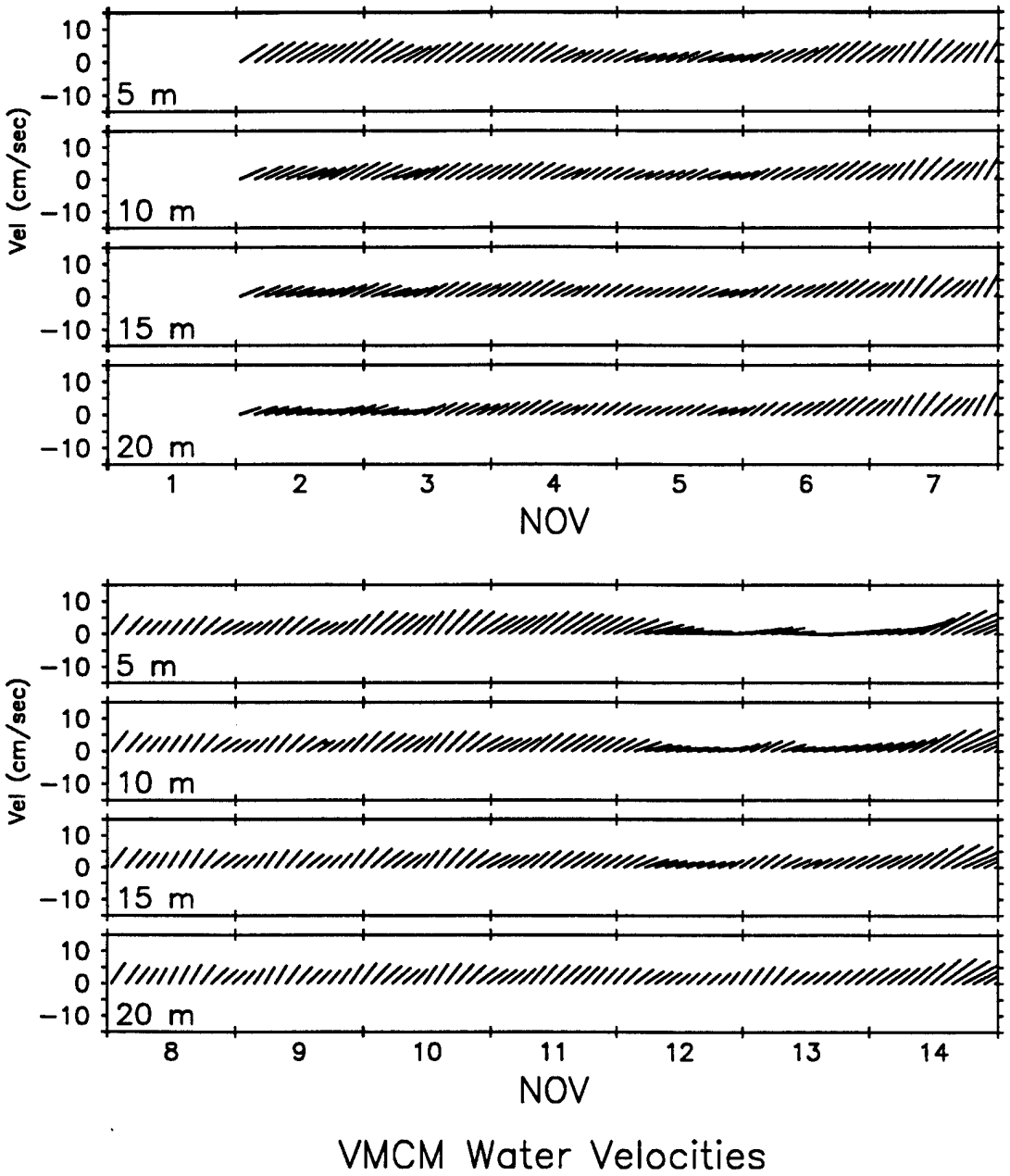

Figure 3.3.1 Sub-surface velocity vectors at 4 depths. Northerly component is toward top of page. Data is averaged over 48 hours and subsampled to 2 hours before plotting.

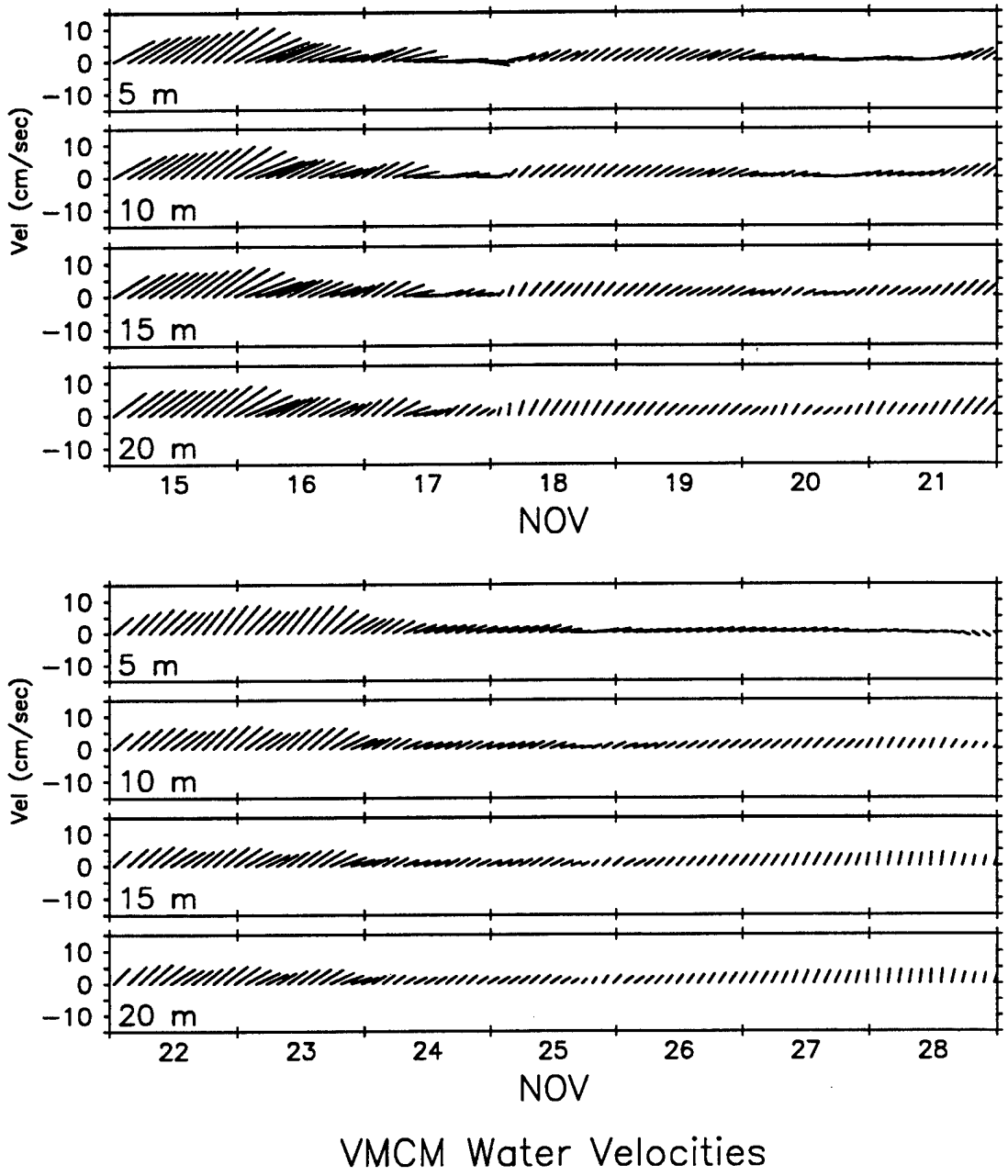

Figure 3.3.2 Sub-surface velocity vectors at 4 depths. Northerly component is toward top of page. Data is averaged over 48 hours and subsampled to 2 hours before plotting.

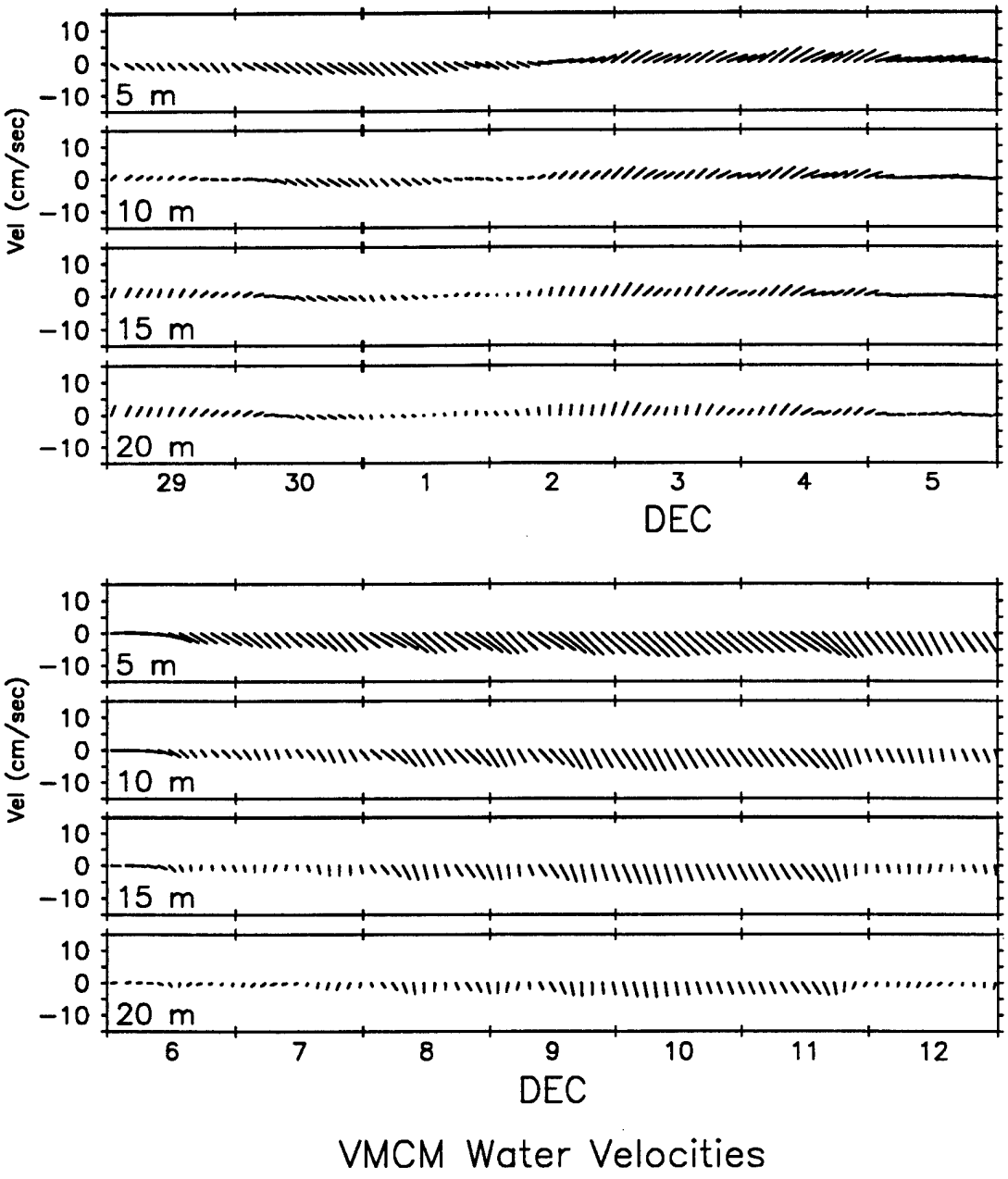

Figure 3.3.3 Sub-surface velocity vectors at 4 depths. Northerly component is toward top of page. Data is averaged over 48 hours and subsampled to 2 hours before plotting.

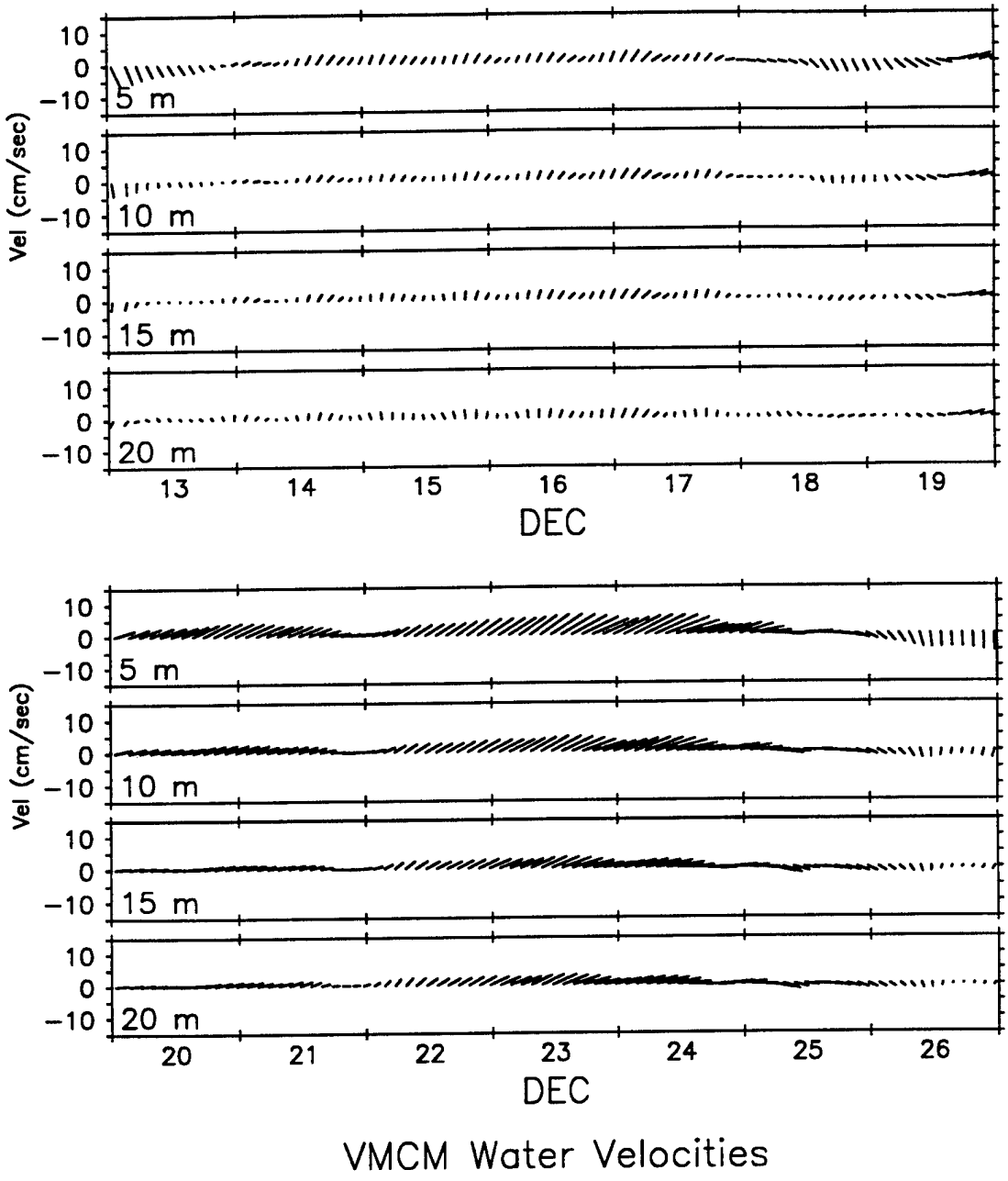

Figure 3.3.4 Sub-surface velocity vectors at 4 depths. Northerly component is toward top of page. Data is averaged over 48 hours and subsampled to 2 hours before plotting.

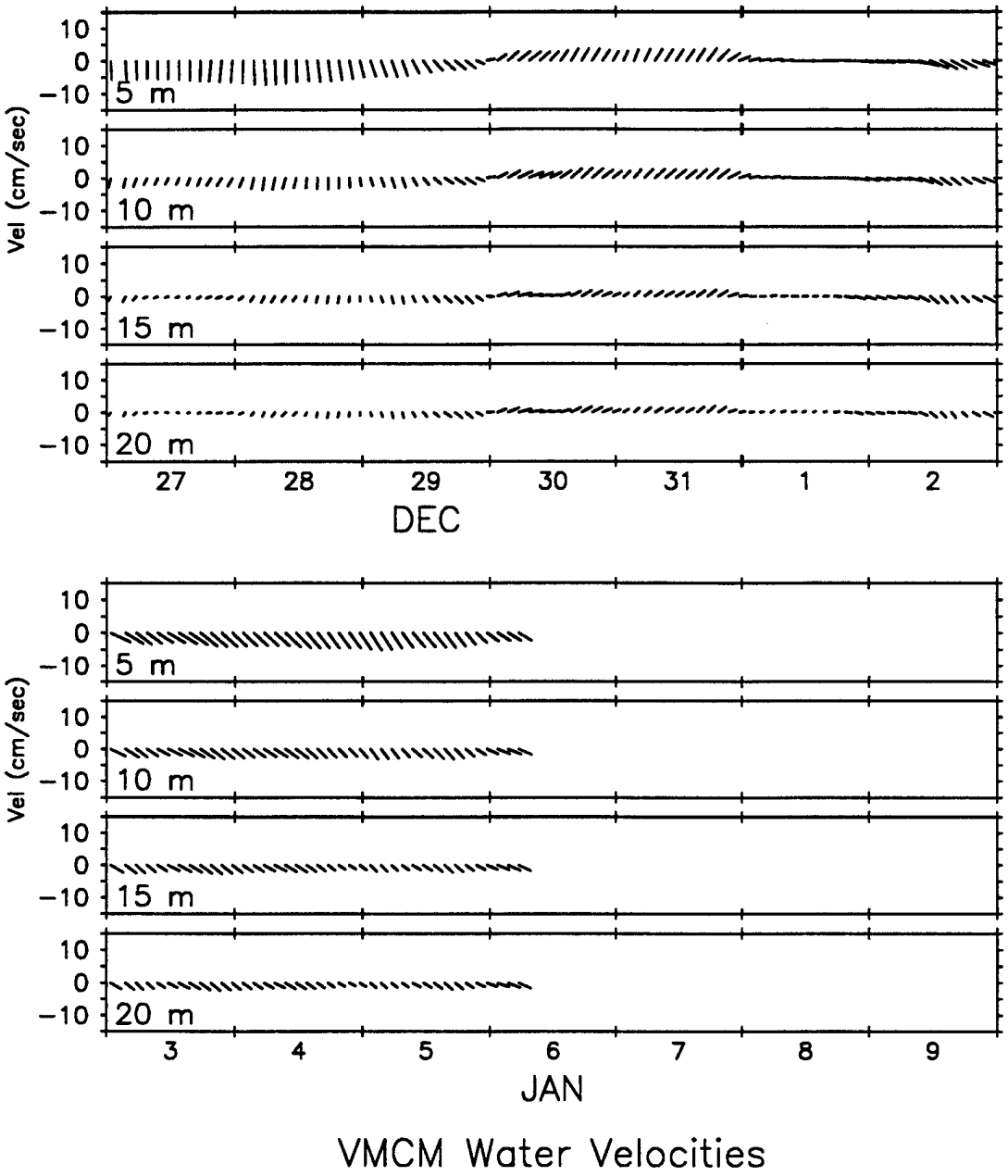

Figure 3.3.5 Sub-surface velocity vectors at 4 depths. Northerly component is toward top of page. Data is averaged over 48 hours and subsampled to 2 hours before plotting.

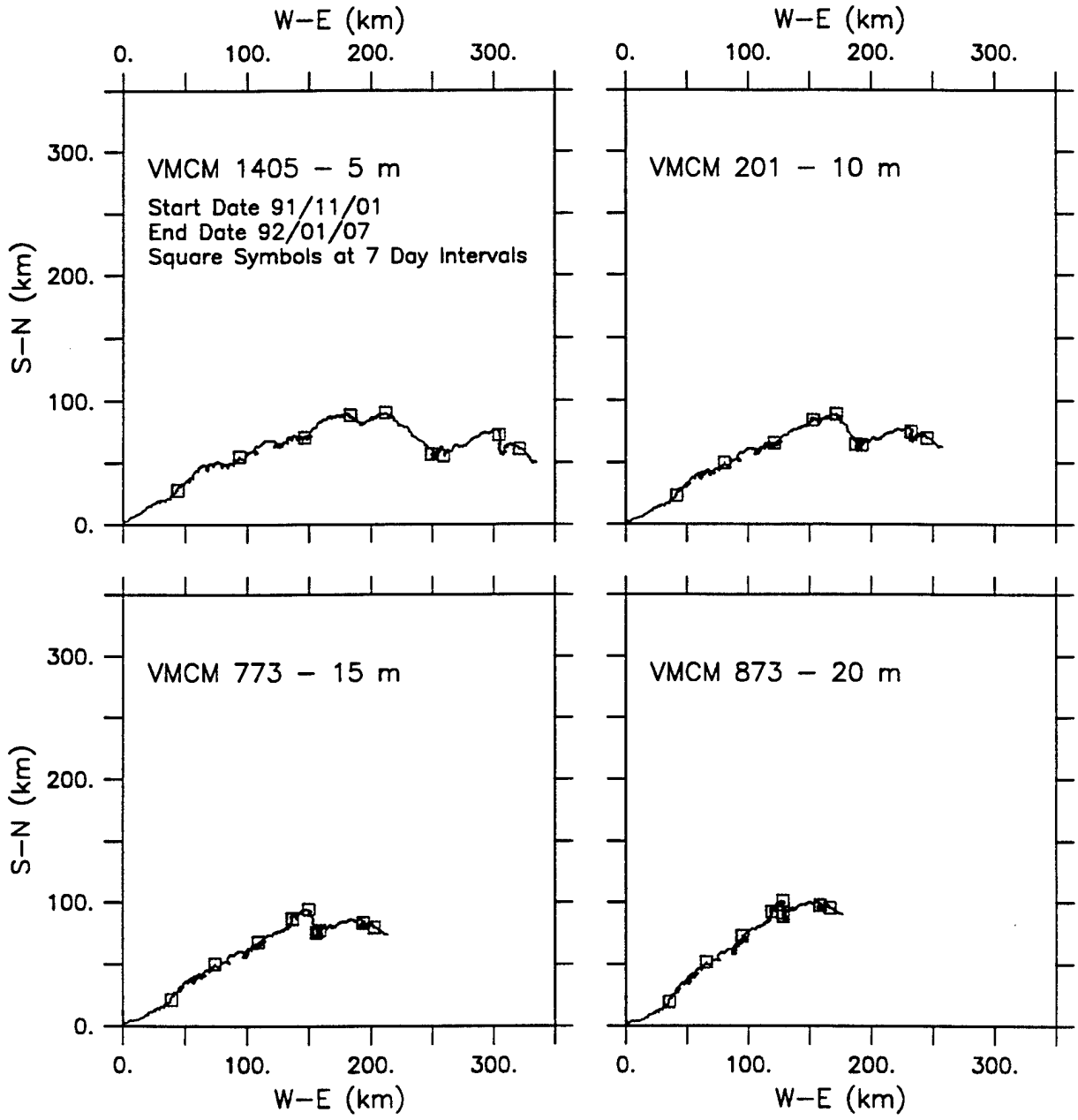

Figure 3.3.6 Progressive water velocity vectors, constructed from velocities averaged over 4 hours.

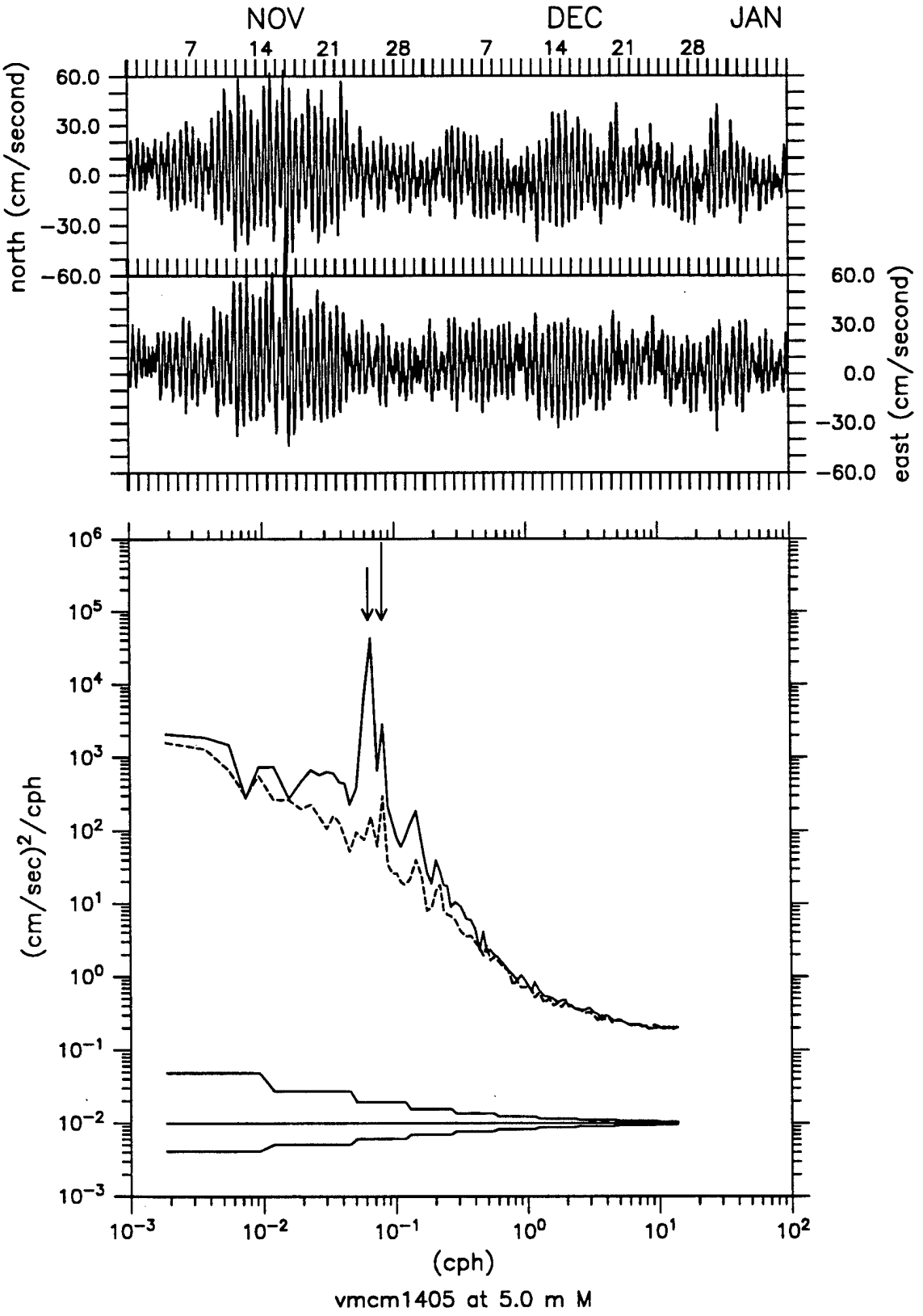

Figure 3.3.7 Water Velocity Time Series and Spectra at 5 m. Solid curves show the clockwise component, and dashed curves show the counter-clockwise component. Long arrow indicates semi-diurnal tidal frequency, short arrow indicates coriolis frequency.

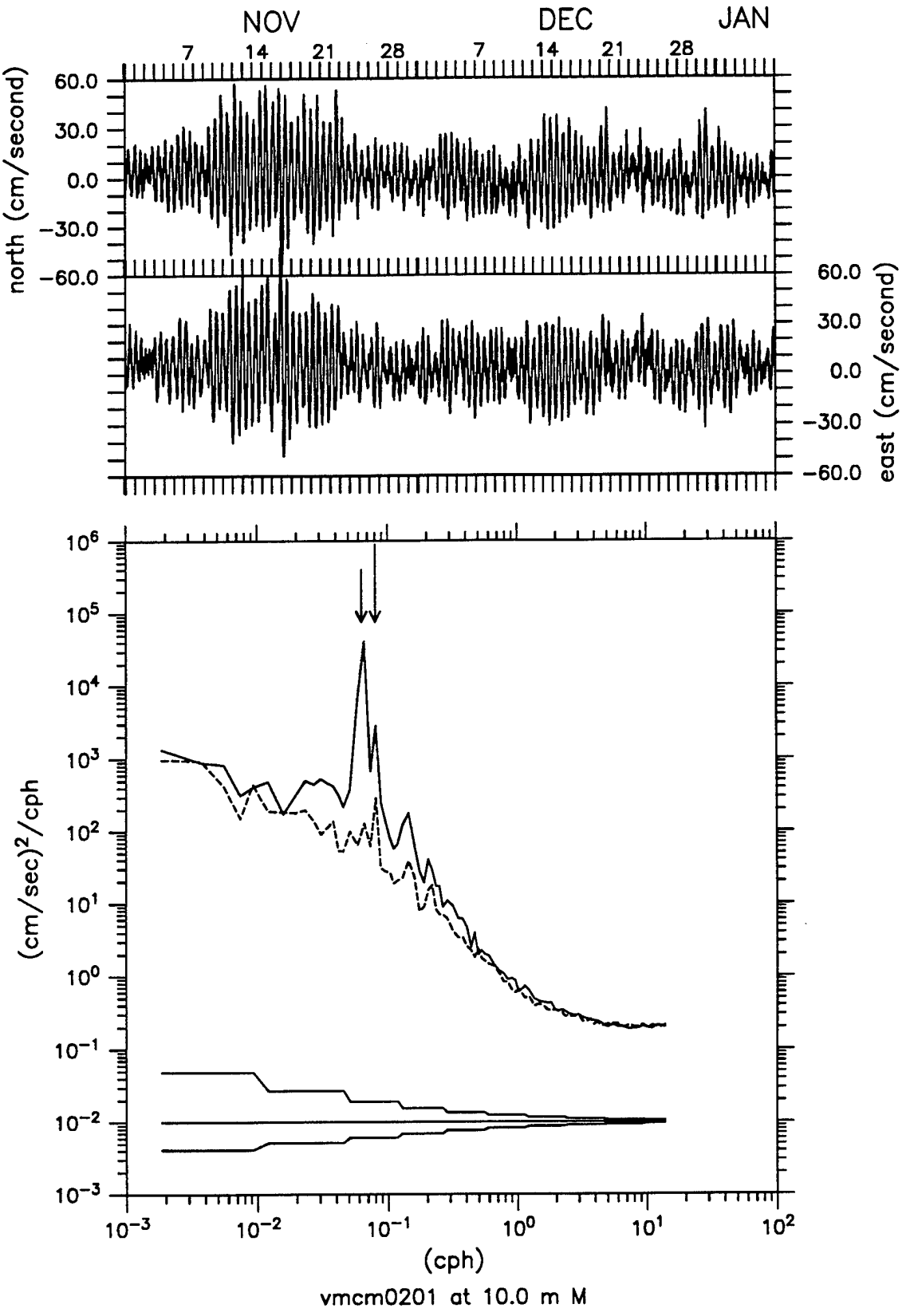

Figure 3.3.8 Water Velocity Time Series and Spectra at 10m. Solid curves show the clockwise component, and dashed curves show the counter-clockwise component.Long arrow indicates semi-diurnal tidal frequency, short arrow indicates coriolis frequency.

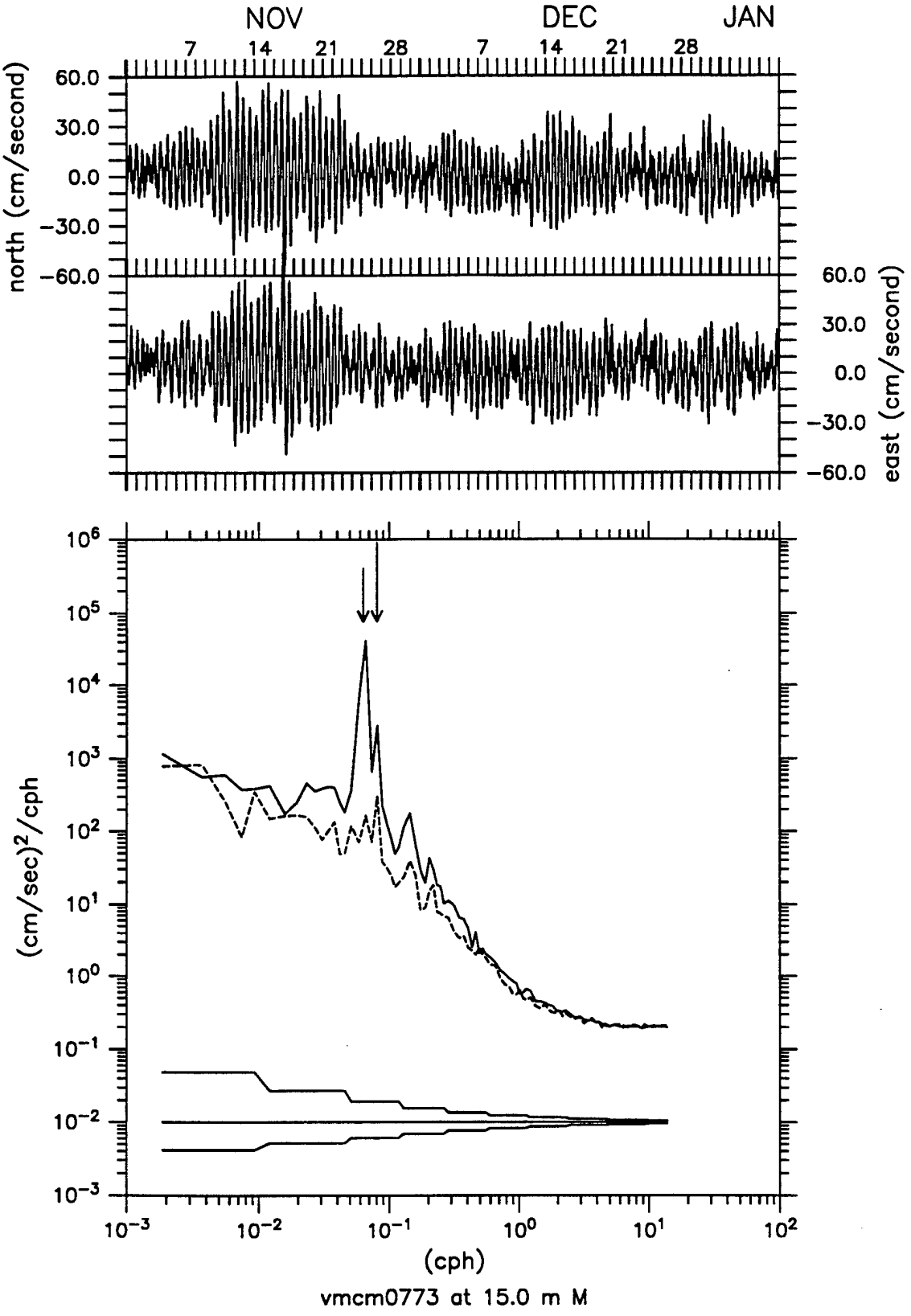

Figure 3.3.9 Water Velocity Time Series and Spectra at 15 m. Solid curves show the clockwise component, and dashed curves show the counter-clockwise component. Long arrow indicates semi-diurnal tidal frequency, short arrow indicates coriolis frequency.

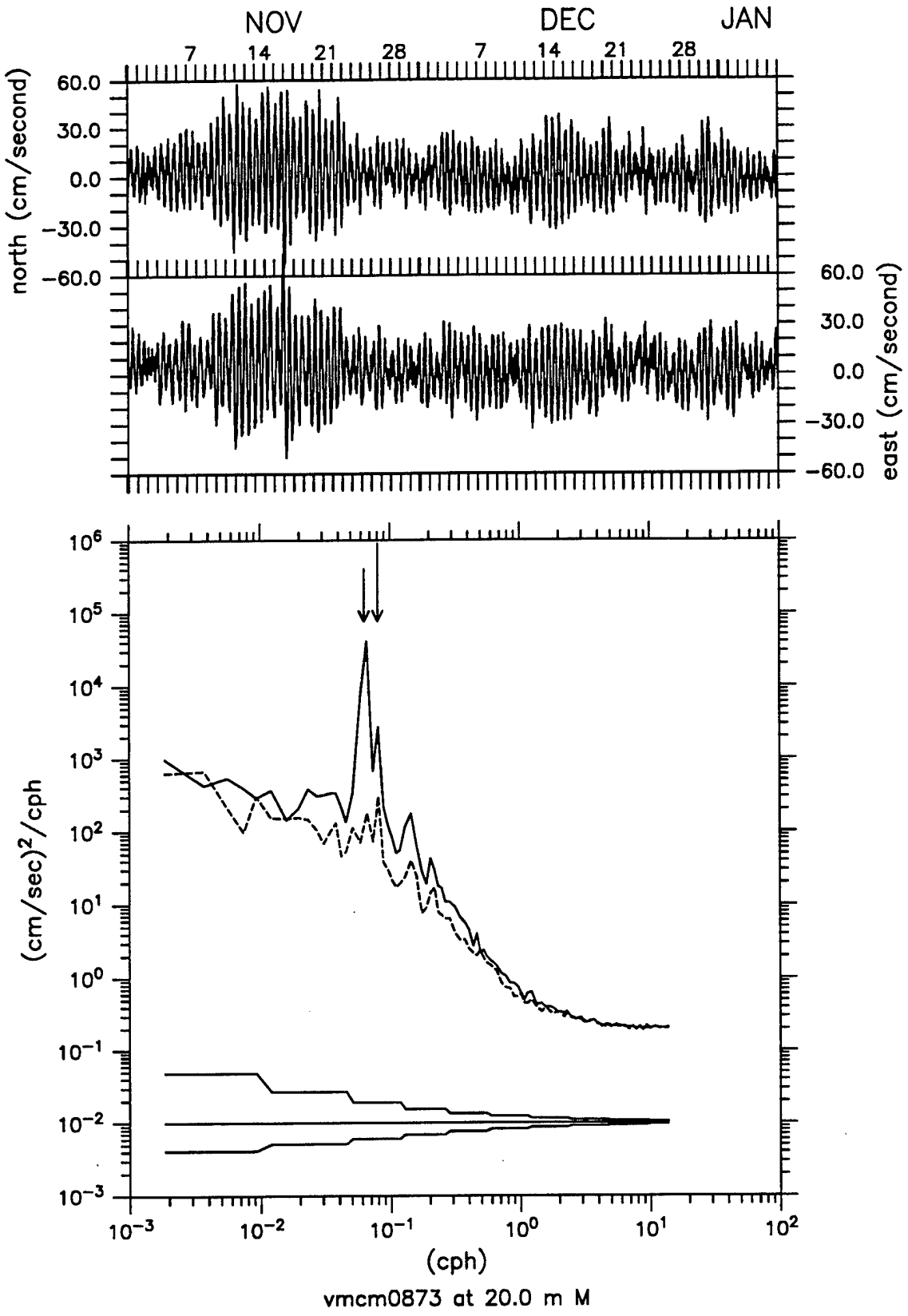

Figure 3.3.10 Water Velocity Time Series and Spectra at 20 m. Solid curves show the clockwise component, and dashed curves show the counter-clockwise component. Long arrow indicates semi-diurnal tidal frequency, short arrow indicates coriolis frequency.

3.4. Measurement of Ocean Surface Gravity Waves During ASREX 91

During the experiment, wave-measuring sensors were deployed on three buoys by the Upper Ocean Processes Group. The discus buoy from which the meteorological measurements were made was also outfitted with a Datawell Hippy 40 in the well, measuring heave, pitch, and roll. The buoy recorded 900 seconds of data at 4 Hz every 6 hours, and wrote the data to the IMET system. Data was acquired beginning on 31 October every 6 hours until the IMET system went down due to low battery on 5 December 1991. The directional response of this buoy is still being studied. Although an initial characterization of the response is presented in Gnanadesikan and Terray (1994), there are still major gaps in our understanding of the transfer function at low frequencies. Directional spectra from this buoy will therefore not be presented in this report.

Two dedicated pitch-roll buoys were also deployed during ASREX. The first of these buoys to be deployed was a Wavescan™ made by Seatex A/S of Trondheim, Norway. A Datawell Hippy 120 sensor on this buoy 2048 samples heave, pitch and roll at a rate of 1 Hz every 3 hours. Buoy heading was recorded simultaneously from a two-axis fluxgate compass. The time series of good data from this buoy begins at 0600Z on November 1 November, 1991 and continues until 1800Z on 4 December 1991 when it was recovered by the *HMCS Huron.* The Wavescan buoy is described in more detail in Barstow et al., 1991. As noted in Gnanadesikan and Terray (1994) the response of the Seatex buoy to surface gravity waves is the best studied and may be easily corrected by modelling the buoy as a damped harmonic oscillator. The Seatex was thus taken as the standard against which other buoys were compared.

The second pitch/roll buoy was a Wavetrack™ manufactured by Endeco/YSI of Marion MA. This buoy measured vertical acceleration using a gimballed accelerometer and two electrolytic tilt sensors. The buoy recorded 2048 samples of heave, north tilt, and east tilt at a rate of 2 Hz every 12 hours. The time series of good nondirectional data from this buoy begins at 0000Z on 3 November 1991 and continues until 1200 Z on 8 January. The directional response of this buoy has been studied by Gnanadesikan and Terray (1994), who found that it is not as simple as that of the Seatex buoy. This report will present some directional results from the Endeco buoy, but will not present an exhaustive listing of the spectra.

Figure 3.4.1 shows time series of wave parameters measured from the Seatex buoy. Figure 3.4.1a and 3.4.1b show time series of the significant wave height and period, computed as follows. The period between successive zero-up crossings of the sea-surface height was defined as corresponding to a single wave. The height of this wave was defined as the difference between the maximum and minimum surface heights. The period of the wave was defined as the time interval between the sucessive zero-up-crossings. The significant wave is defined as the height of the highest 1/3 of the waves. The significant wave period is the mean period of the highest 1/3 of the waves. The height of the largest wave seen during the 2048 second observing period is shown in Figure 3.4.1c. During the deployment we see that the waves were in general quite large, with a peak significant height of 10.03 meters at 1800Z on 16 November 1991. The largest wave seen during the entire deployment (15.97 meters in height) was seen at this time.

Figure 3.4.2 shows the evolution of the energy in the surface wave field as a function of frequency over the course of the ASREX 91 experiment. Contours are $\log_{10}$ spectral density, The heavy dashed lines show some of the clearly identifiable events corresponding to locally generated windsea for which the frequency of the peak of the spectrum increases with time. The straight heavy solid lines show identifiable swell propagation events for which the frequency of the peak of the spectrum decreases with time.

Directional wave spectra were calculated using the Maximum Entropy Method of Lygre and Krogstad (1986). Corrections to the measured direction of orientation due to buoy tilt were calculated and applied. The tilts were then rotated into geographic coordinates. The spectra and cross-spectra of the heave and tilt were calculated with corrections being made for sensor response and buoy transfer function. The resulting heave and tilt spectra, quadrature spectrum of heave and north and east tilt, and cospectrum of north and east tilt were input to the Maximum Entropy routine of Lygre and Krogstad, and directional spectra were produced. The MATLAB code used to produce these spectra is given in Appendix 5. If the resulting spectra are integrated over frequency, one may get a sense of how the wave energy depends on direction. Figure 3.4.3a shows a contour plot of the wave energy as a function of direction measured from the Seatex buoy over 1 November- 21 November. The plot shows the direction from which the waves were propagating. 3.4.3b shows the wind direction during this time period. Figures 3.4.3c and d repeat 3.4.3a and b for 21 November to 5 December. During the deployment, the winds were generally from the west and the south, and the wave climate seems to mirror this fact. The directional distribution wave energy in general reflects the wind direction, but there are some clear cases where there are differences.

Figure 3.4.4 shows comparisons of wave parameters measured from the the Seatex, Endeco and Discus buoys during the month of November, 1991. In all plots the data from the Seatex buoy is shown as a solid line, that from the Endeco as open circles and that from the discus as an x. Figure 3.4.4a shows the significant wave height measured from the three buoys and 3.4.4b shows the frequency at the peak of the spectrum. The agreement between the three buoys is excellent with the standard deviation of the difference between the Seatex and Endeco buoys being 0.25 m and the standard deviation of the difference between the Seatex and discus buoys being 0.34m.

Wave directions were computed from the Seatex and Endeco buoys at various frequencies. Figure 3.4.4c and 3.4.4d. Figure 3.4.4c shows the direction associated with the spectral peak from the Seatex and Endeco buoys. The two buoys agree most of the time, but show occasional differences. Gnanadesikan and Terray (1994) argued that these differences were most likely due to uncertainties in the buoy transfer function. Figure 3.4.4d shows the wave direction in a frequency band from 0.25-0.33 Hz. The dashed line shows the wind direction. Clearly in this band, the waves track the wind very closely.

Figures 3.4.7–3.4.38 show a subset of the Seatex directional wave spectra. Four spectra are shown on each day (eight were taken) at 00,06,12, and 18Z.

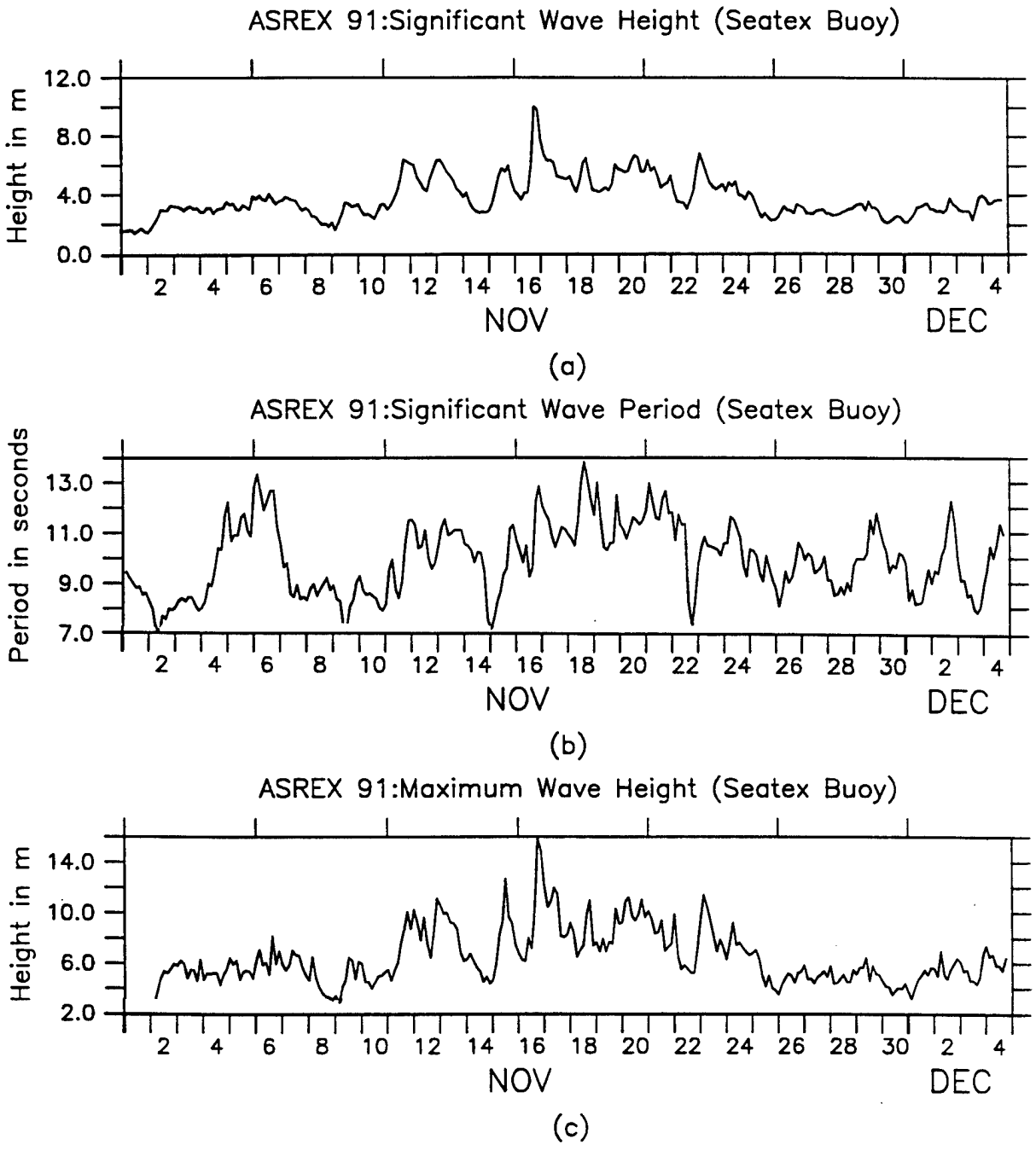

Figure 3.4.1: Wave parameter time series from Seatex Buoy.

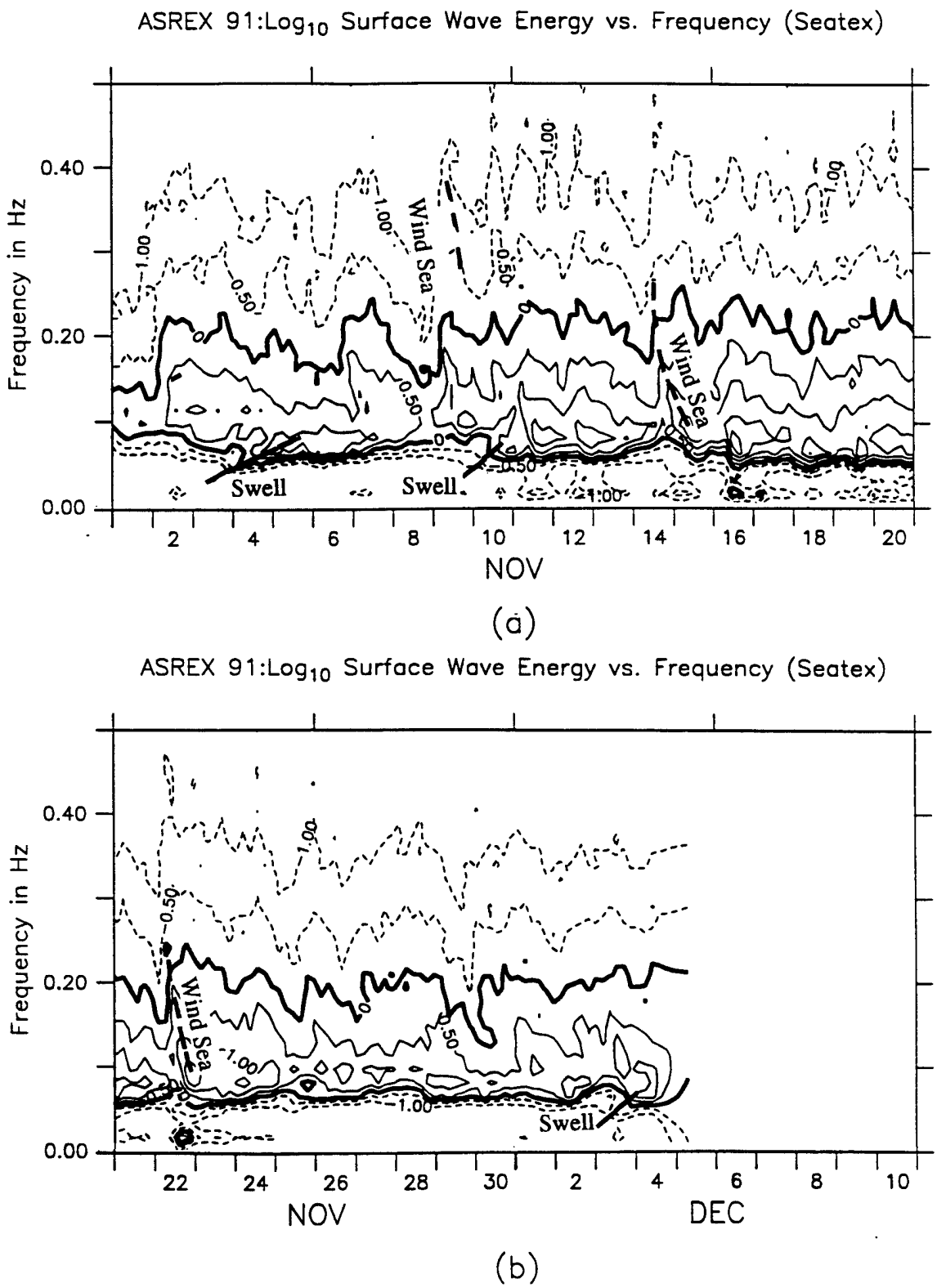

Figure 3.4.2: Evolution of wave field vs frequency during ASREX 91. Data are taken from the Seatex buoy and run from 0300Z 1 November 1991 through 1800Z 4 December 1991. (a) Contours of $\log_{10}$ spectral density 1–21 November. (a) Contours of $\log_{10}$ spectral density 21 November – 5 December.

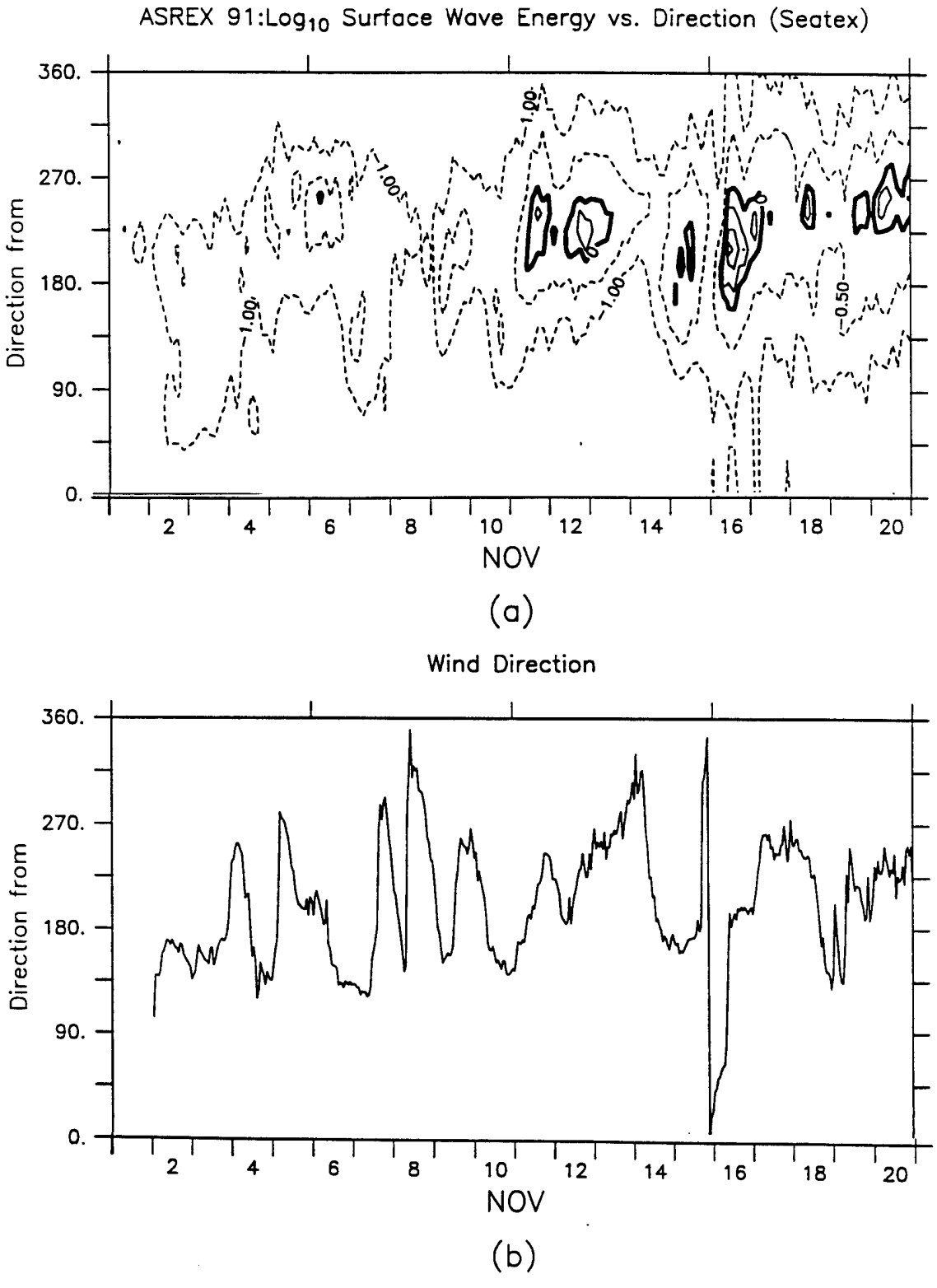

Figure 3.4.3: Directional Wave Evolution during ASREX 91 from Seatex buoy. (a) Log_{10} wave energy vs. direction 1 - 21 November. (b) Wind direction 1 - 21 November. (c) Log_{10} wave energy vs. direction 21 November - 5 December. (c) Wind direction 21 November - 5 December.

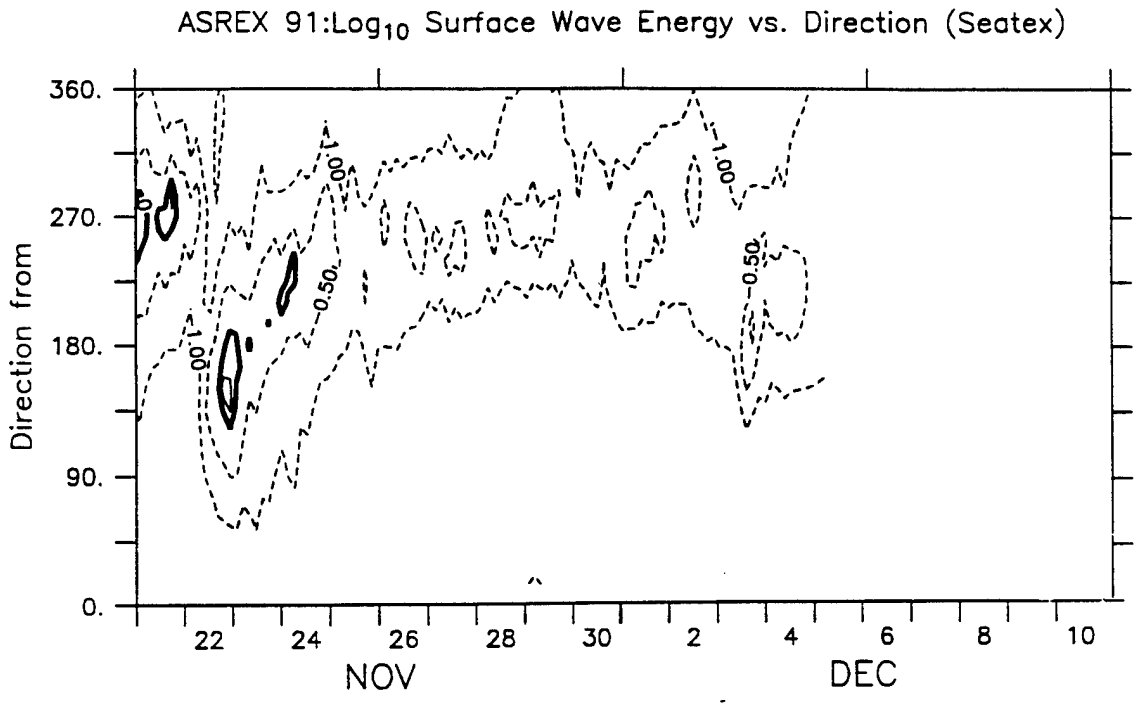

(c)

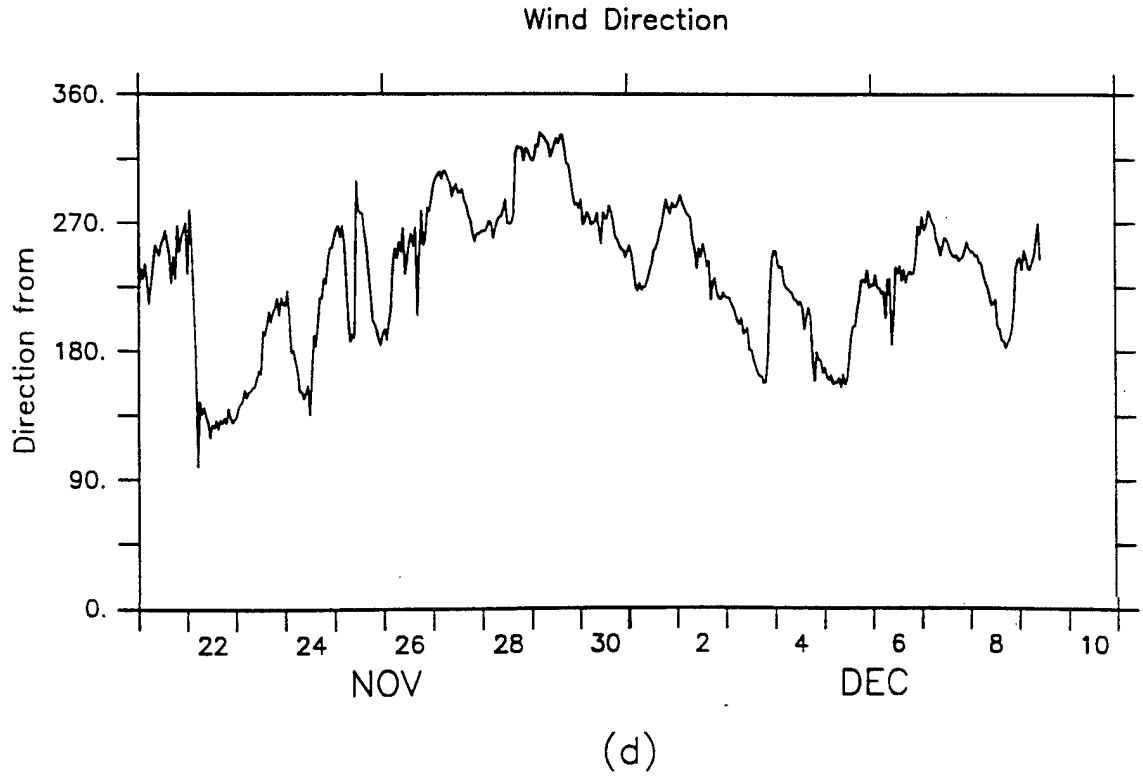

(d)

Figure 3.4.3 (continued)

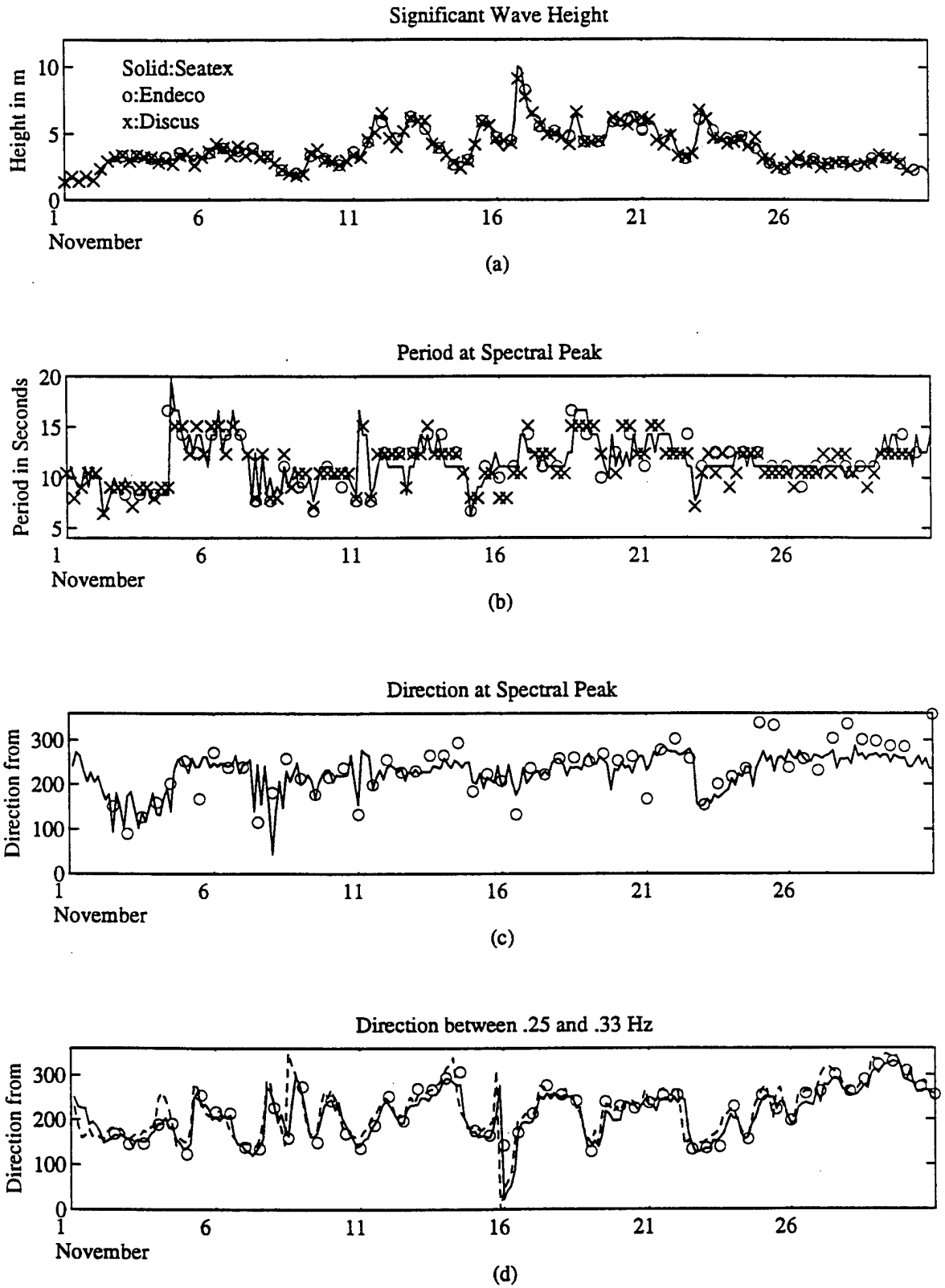

Figure 3.4.4: Wave parameters from three buoys. Solid: Seatex, o: Endeco, x: Discus. (a) Significant wave height in m. (b) Period of spectral peak in s. (c) Direction at spectral peak. (d) Direction of waves with 3-4 seconds period, dashed line is wind direction.

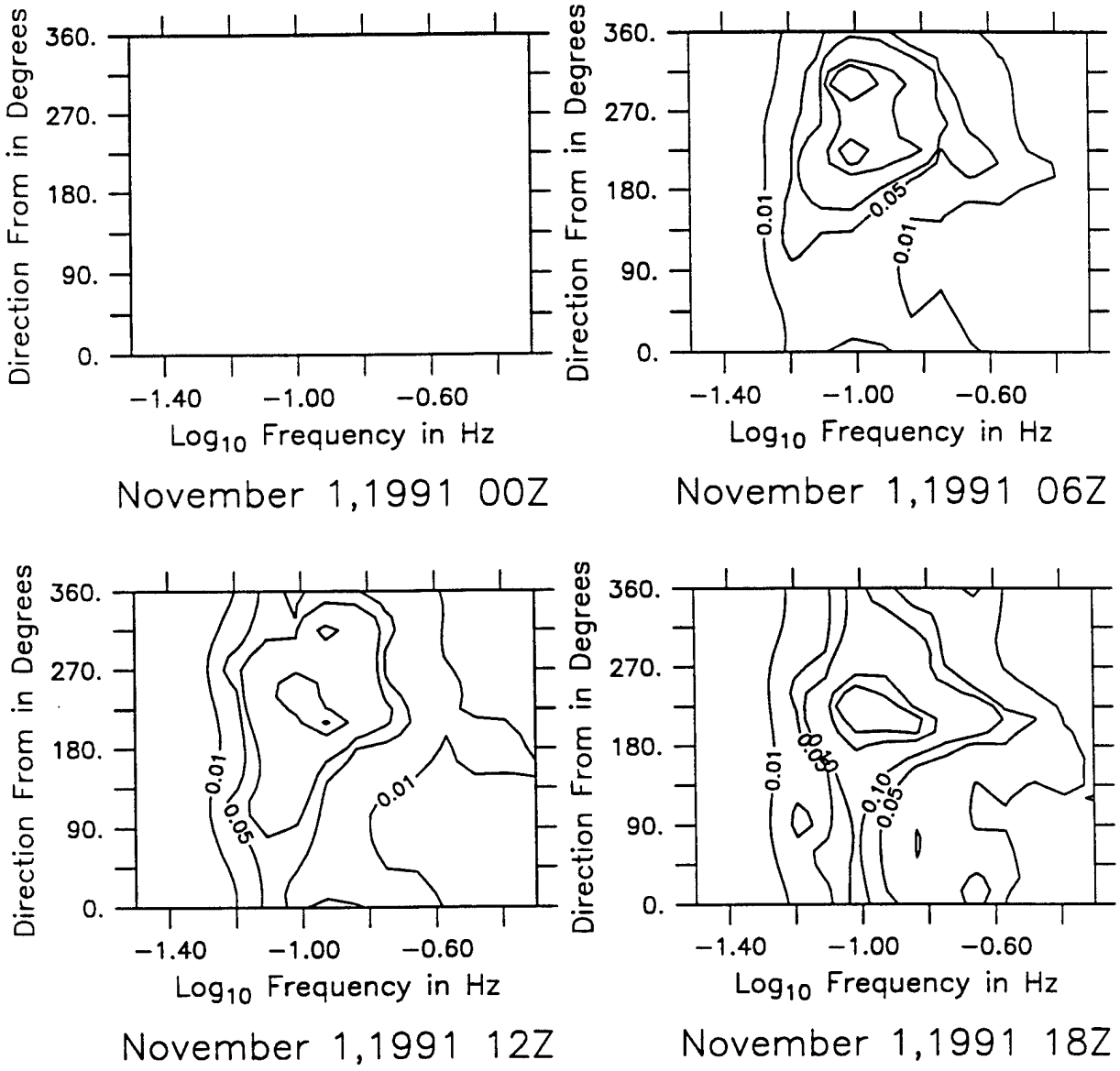

Figure 3.4.5: Directional wave spectra, Seatex buoy. Contours are 0.01, 0.05, 0.1, 0.5, 1, 5, 10, 50, 100, 500.

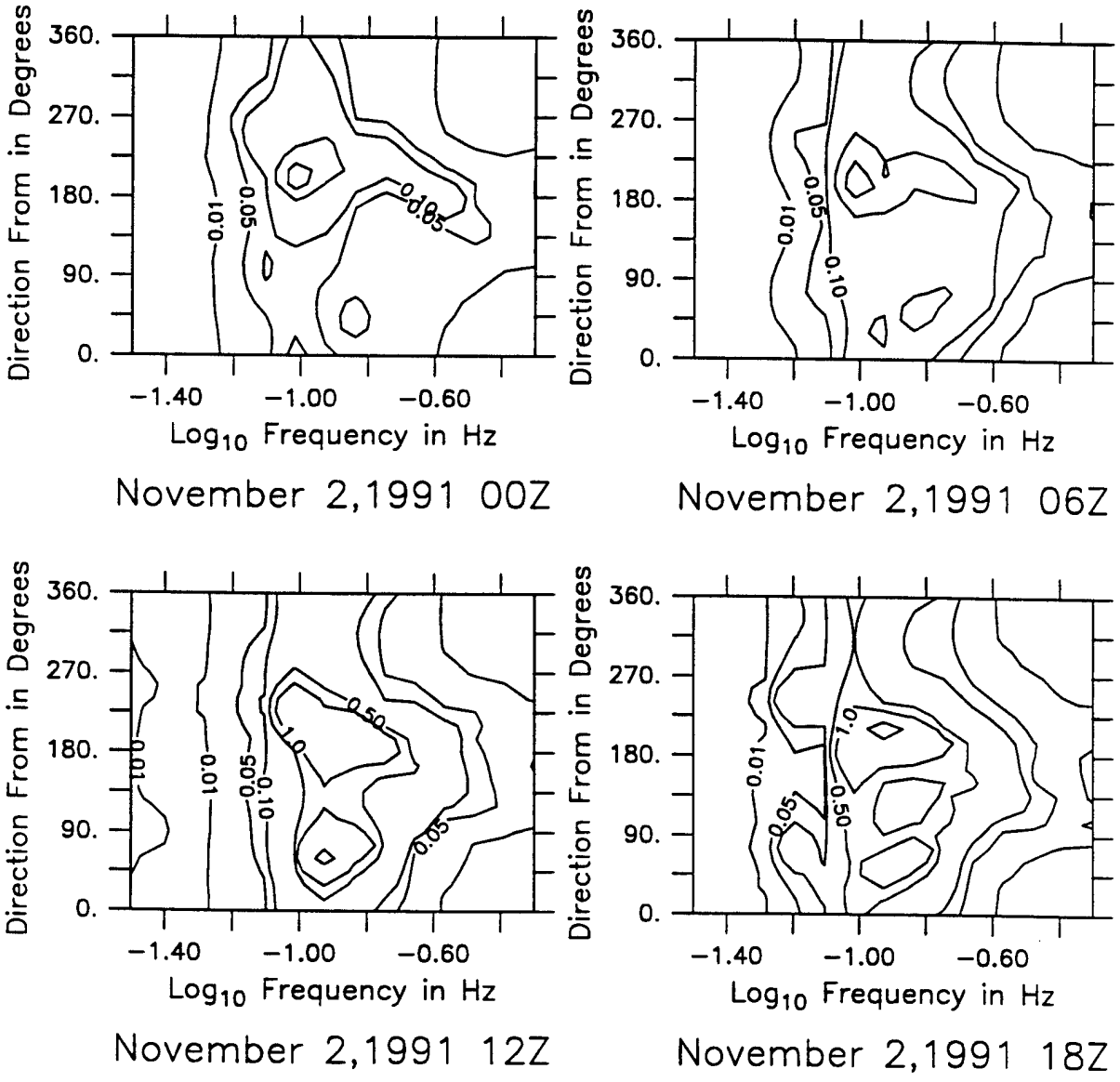

Figure 3.4.6: Directional wave spectra, Seatex buoy. Contours are 0.01, 0.05, 0.1, 0.5, 1, 5, 10, 50, 100, 500.

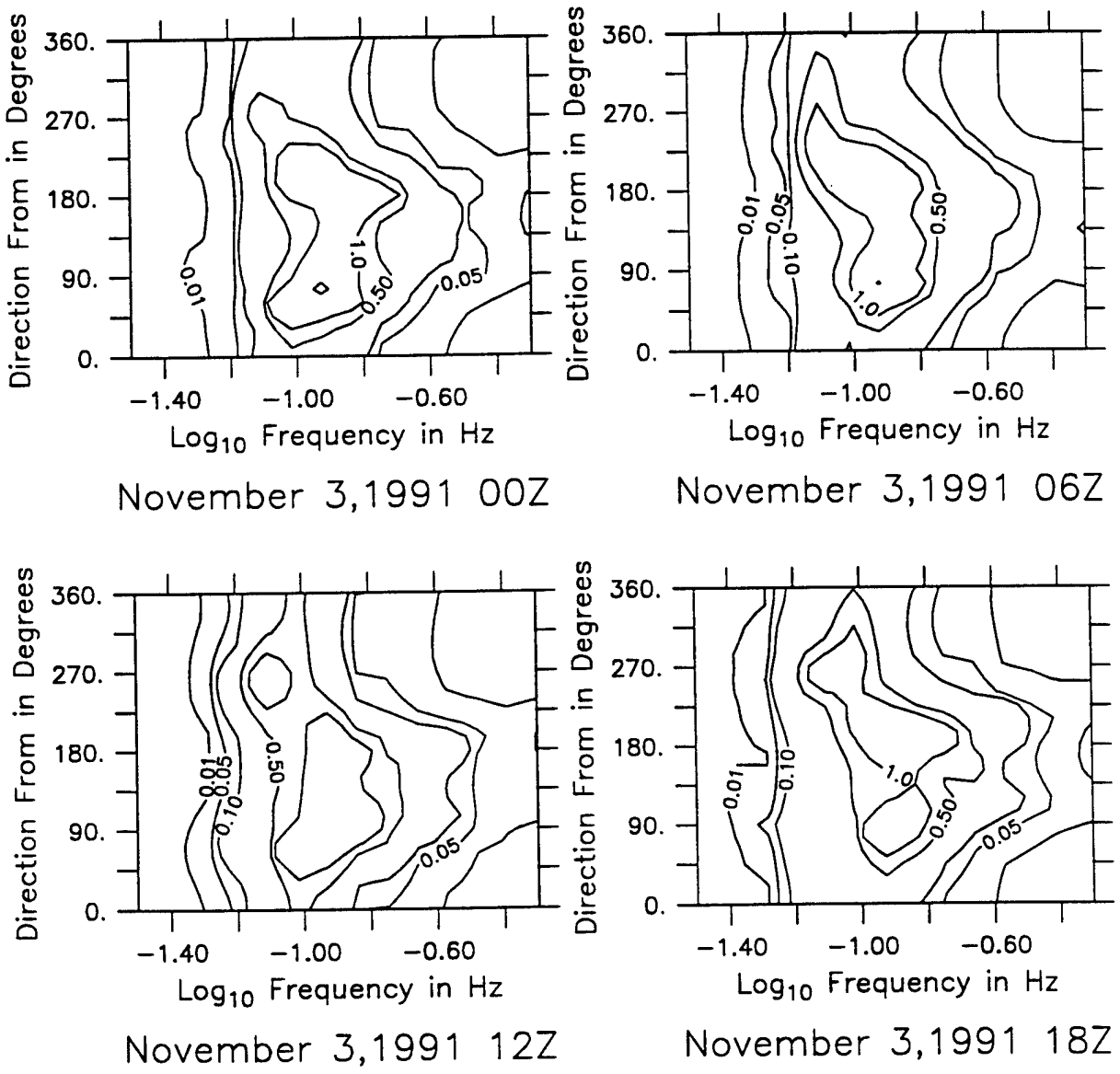

Figure 3.4.7: Directional wave spectra, Seatex buoy. Contours are 0.01, 0.05, 0.1, 0.5, 1, 5, 10, 50, 100, 500.

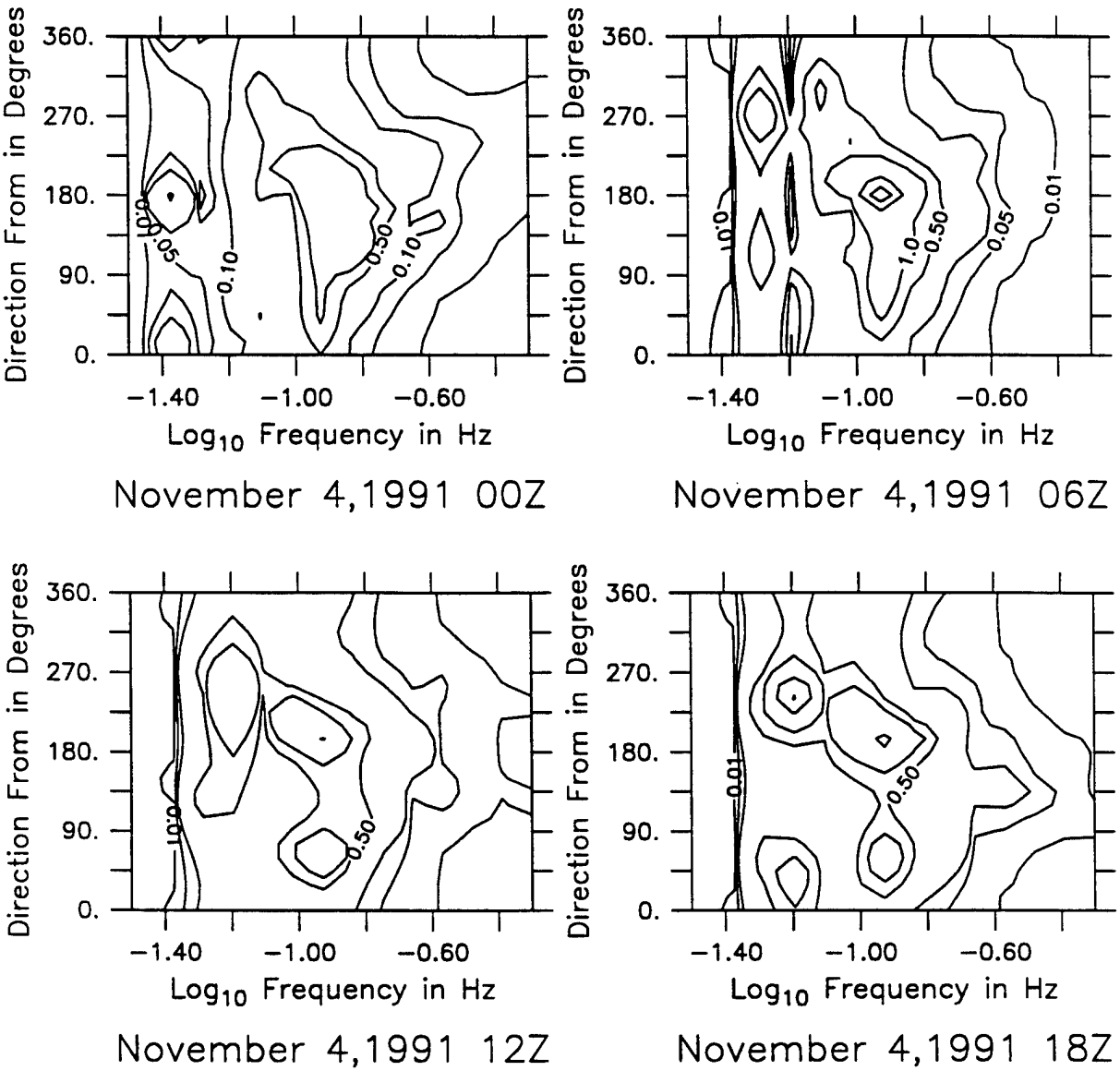

Figure 3.4.8: Directional wave spectra, Seatex buoy. Contours are 0.01, 0.05, 0.1, 0.5, 1, 5, 10, 50, 100, 500.

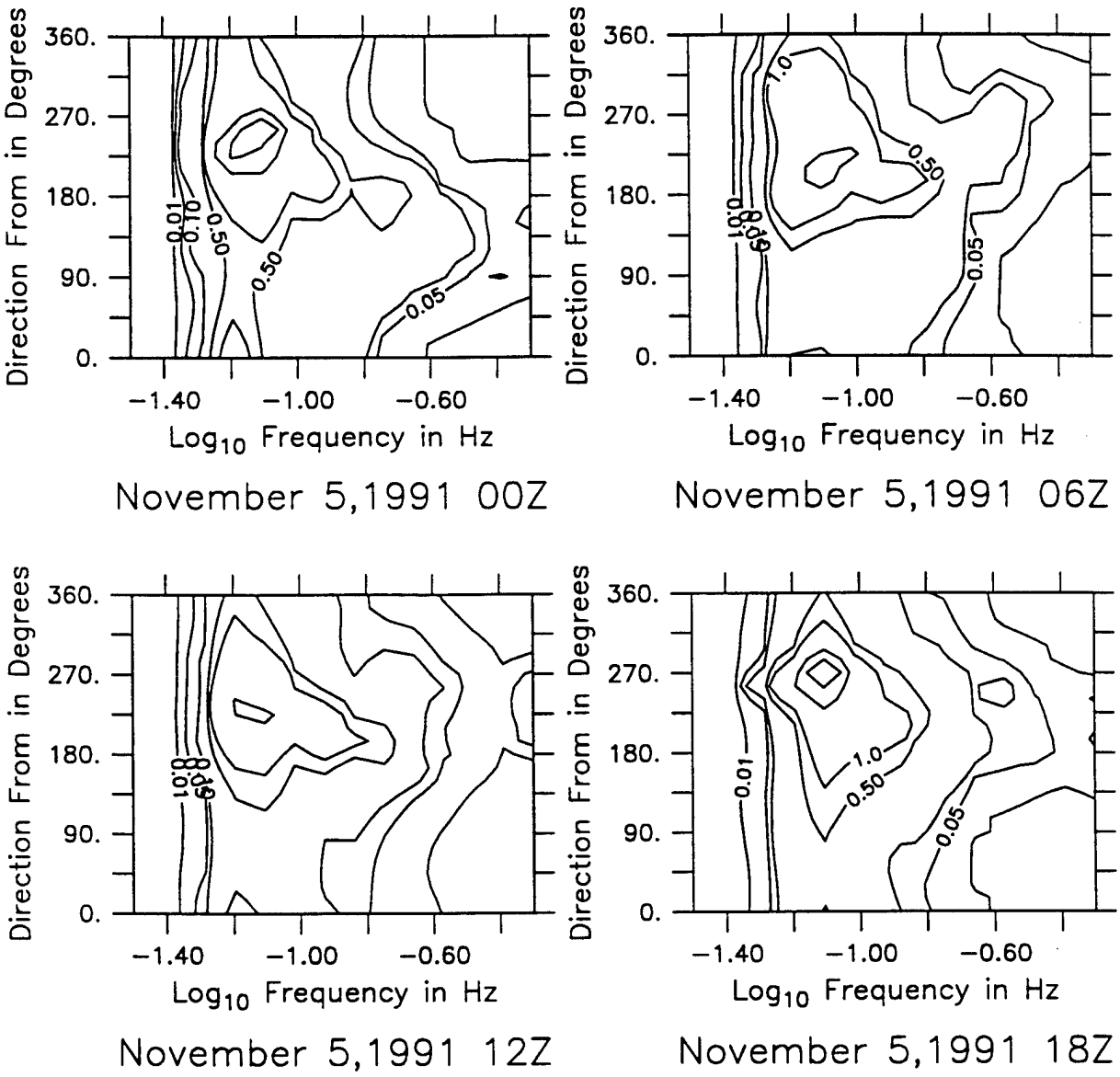

Figure 3.4.9: Directional wave spectra, Seatex buoy. Contours are 0.01, 0.05, 0.1, 0.5, 1, 5, 10, 50, 100, 500.

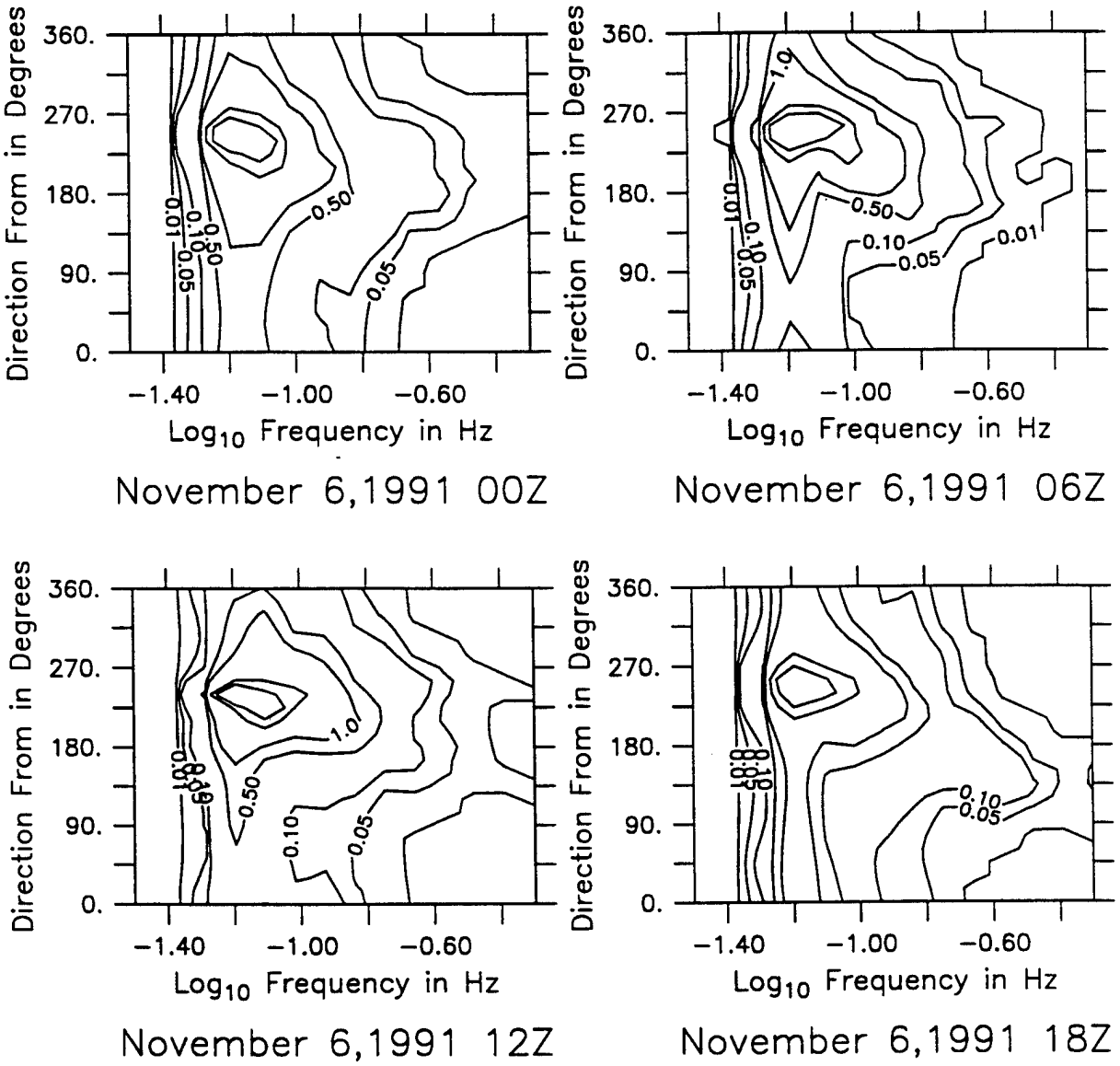

Figure 3.4.10: Directional wave spectra, Seatex buoy. Contours are 0.01, 0.05, 0.1, 0.5, 1, 5, 10, 50, 100, 500.

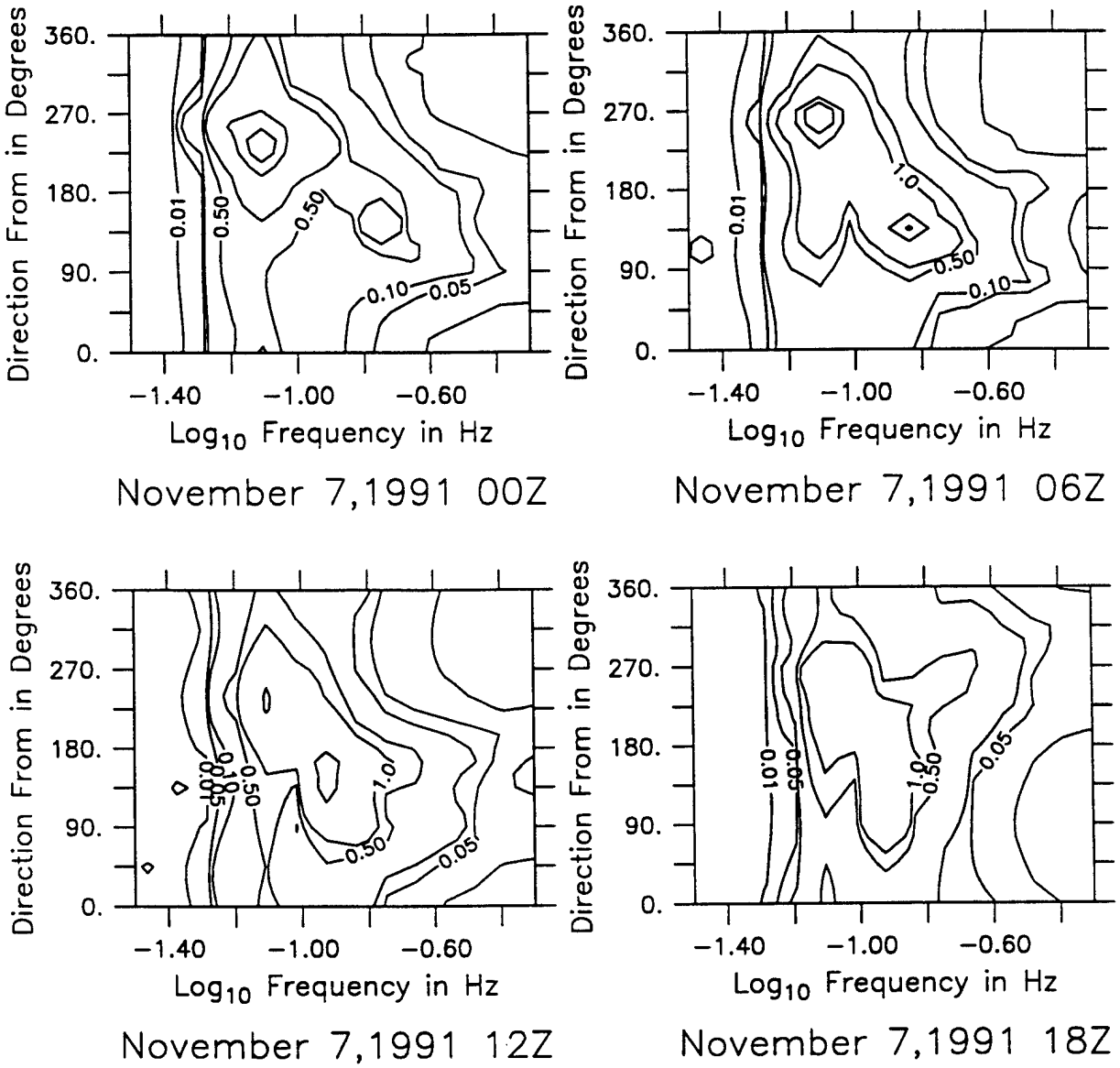

Figure 3.4.11: Directional wave spectra, Seatex buoy. Contours are 0.01, 0.05, 0.1, 0.5, 1, 5, 10, 50, 100, 500.

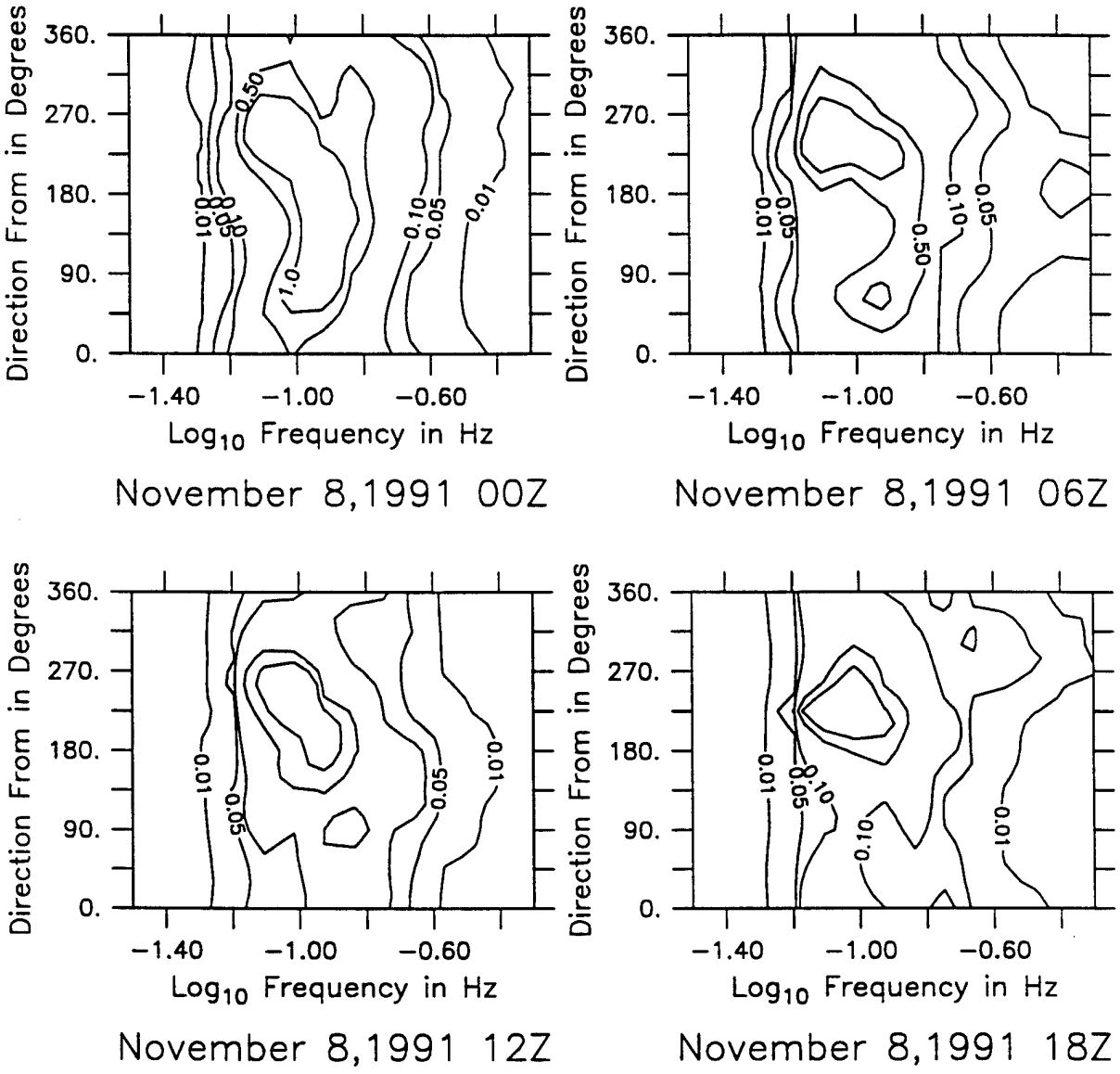

Figure 3.4.12: Directional wave spectra, Seatex buoy. Contours are 0.01, 0.05, 0.1, 0.5, 1, 5, 10, 50, 100, 500.

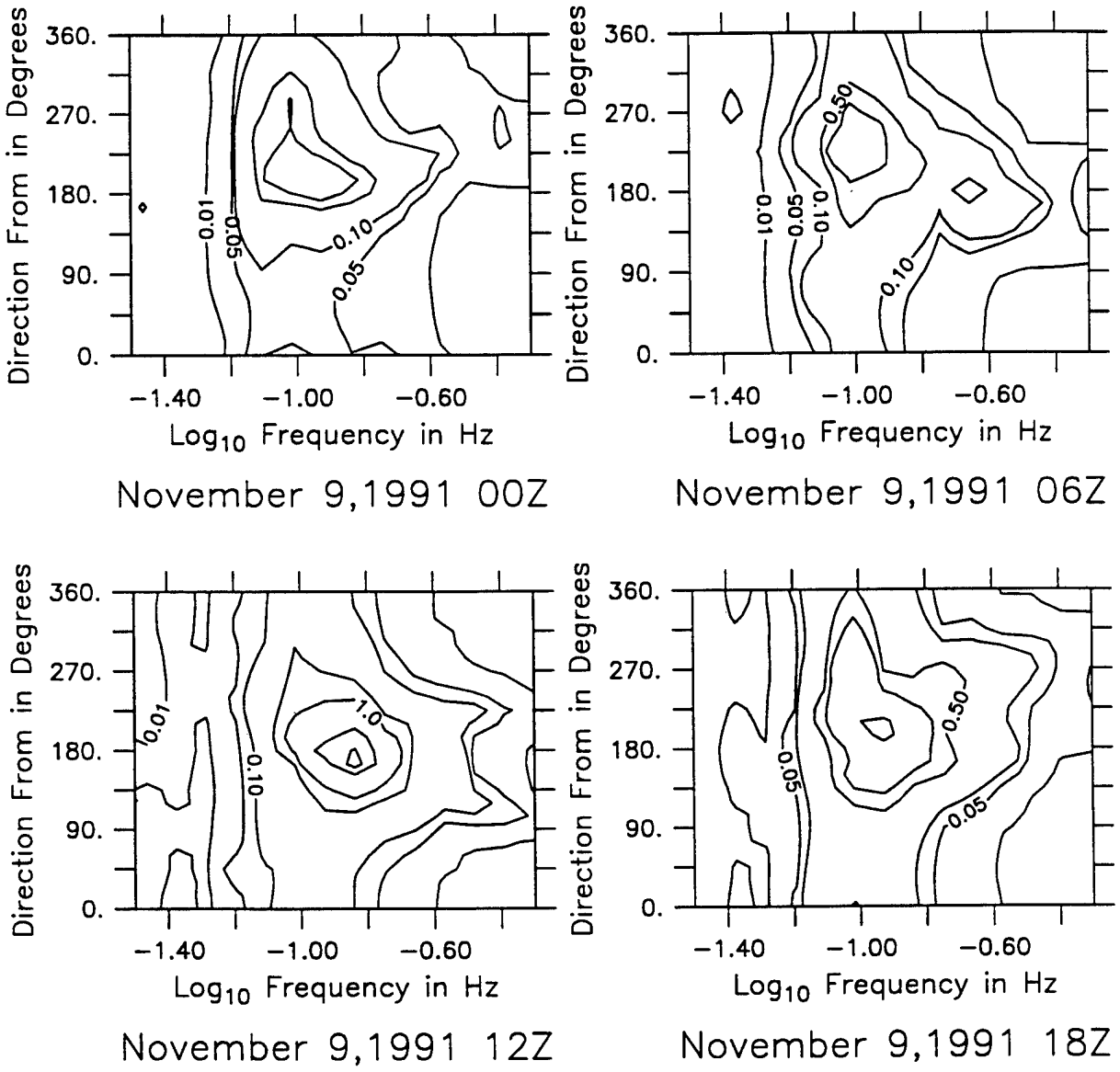

Figure 3.4.13: Directional wave spectra, Seatex buoy. Contours are 0.01, 0.05, 0.1, 0.5, 1, 5, 10, 50, 100, 500.

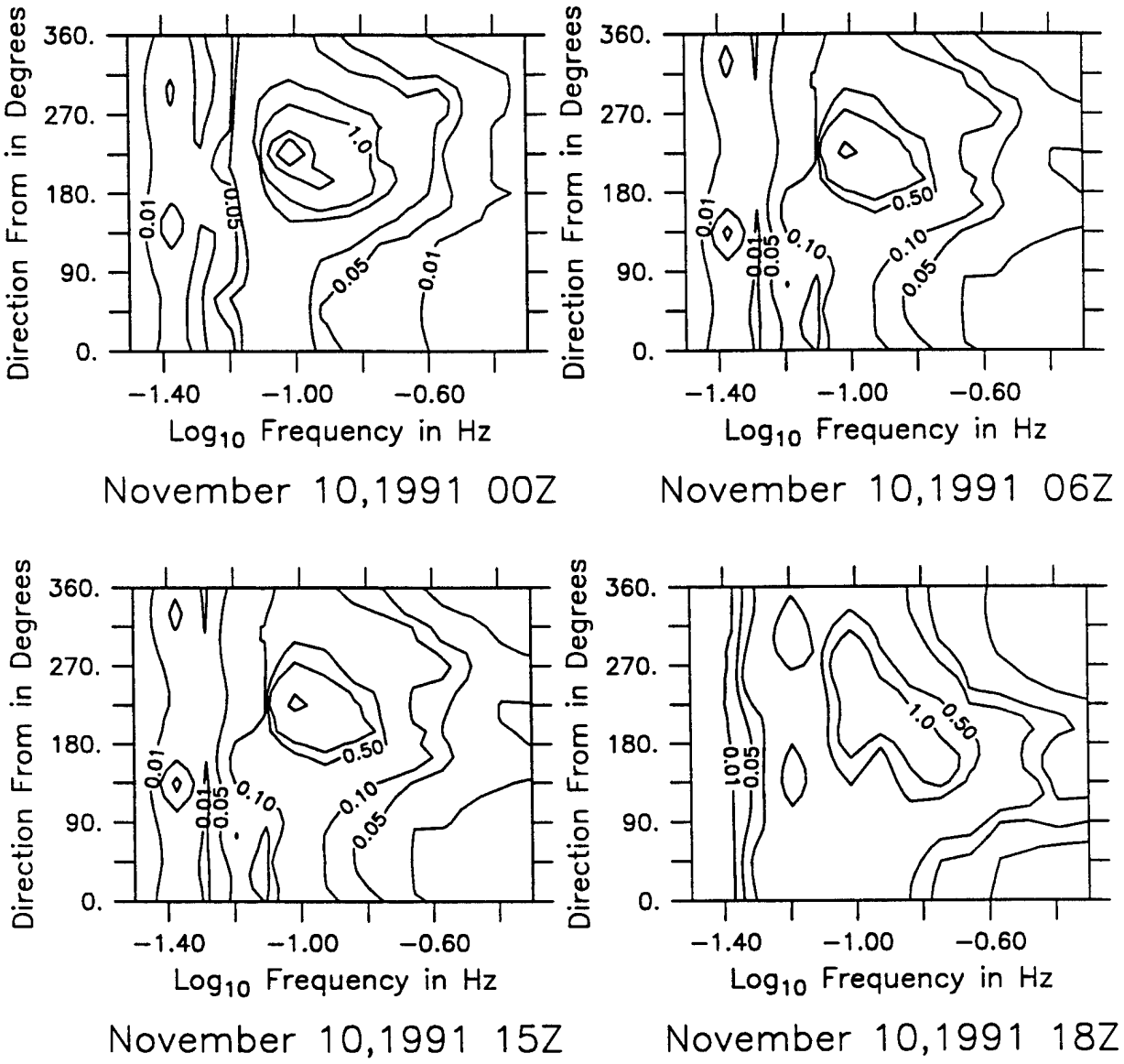

Figure 3.4.14: Directional wave spectra, Seatex buoy. Contours are 0.01, 0.05, 0.1, 0.5, 1, 5, 10, 50, 100, 500.

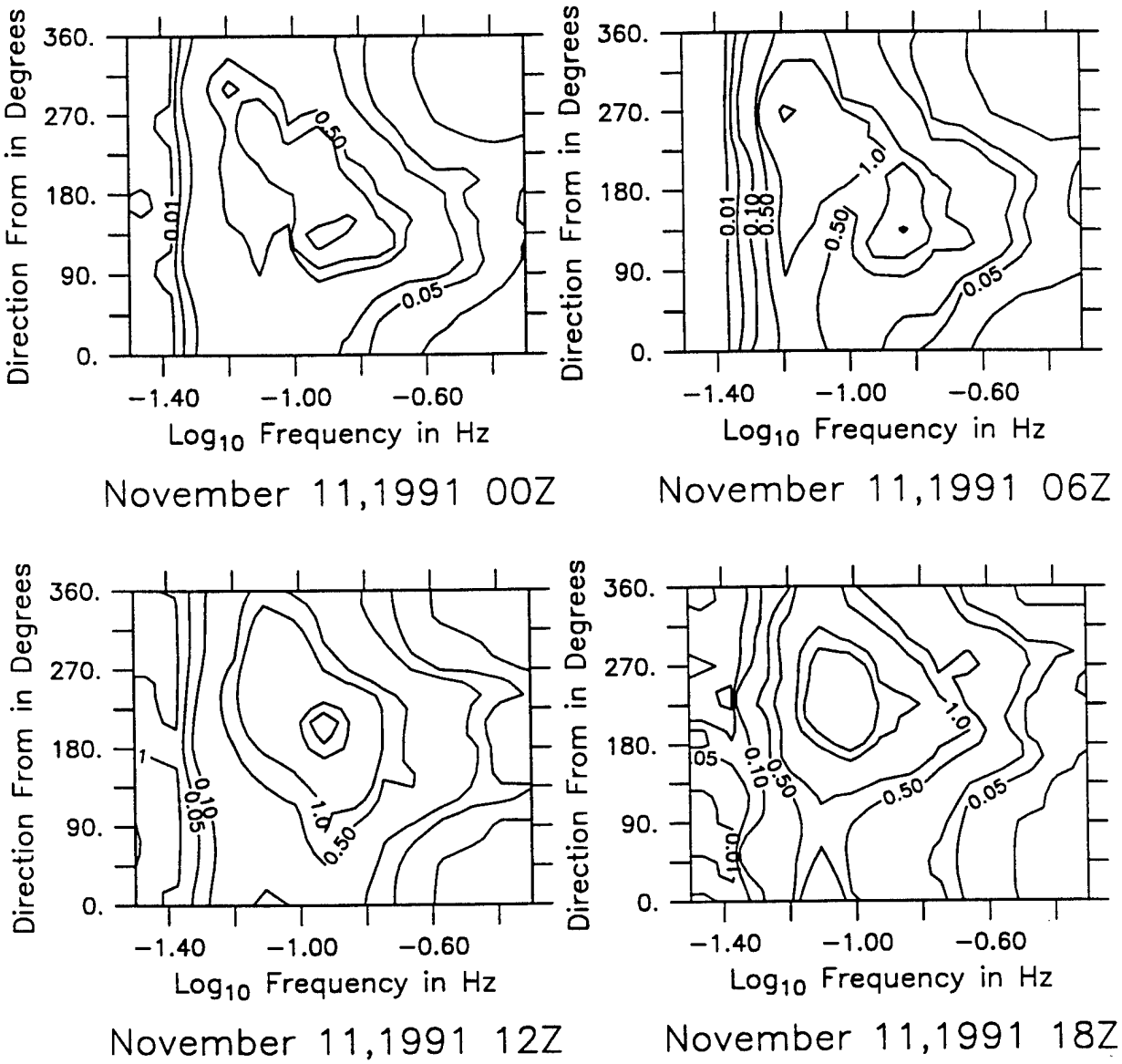

Figure 3.4.15: Directional wave spectra, Seatex buoy. Contours are 0.01, 0.05, 0.1, 0.5, 1, 5, 10, 50, 100, 500.

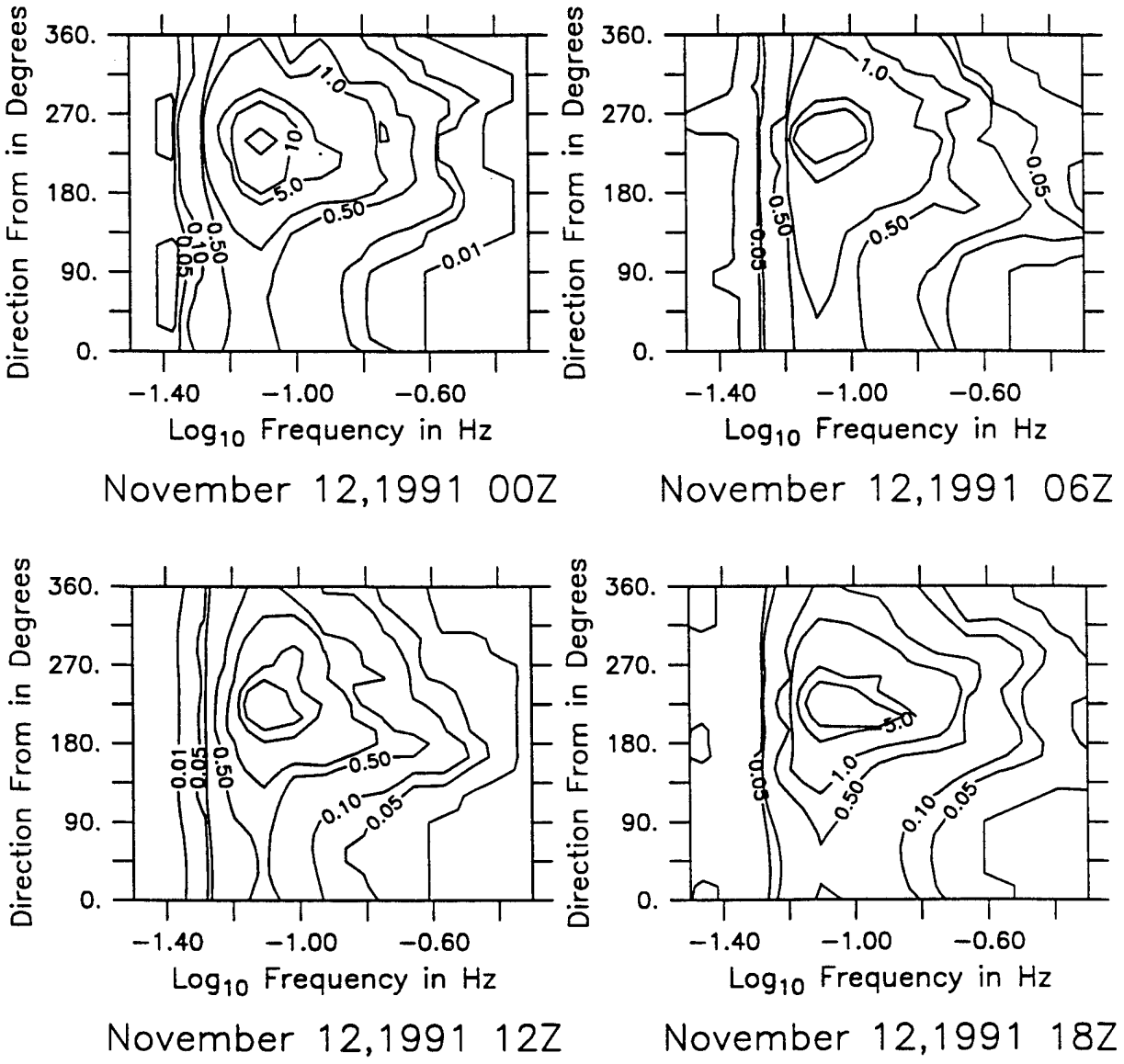

Figure 3.4.16: Directional wave spectra, Seatex buoy. Contours are 0.01, 0.05, 0.1, 0.5, 1, 5, 10, 50, 100, 500.

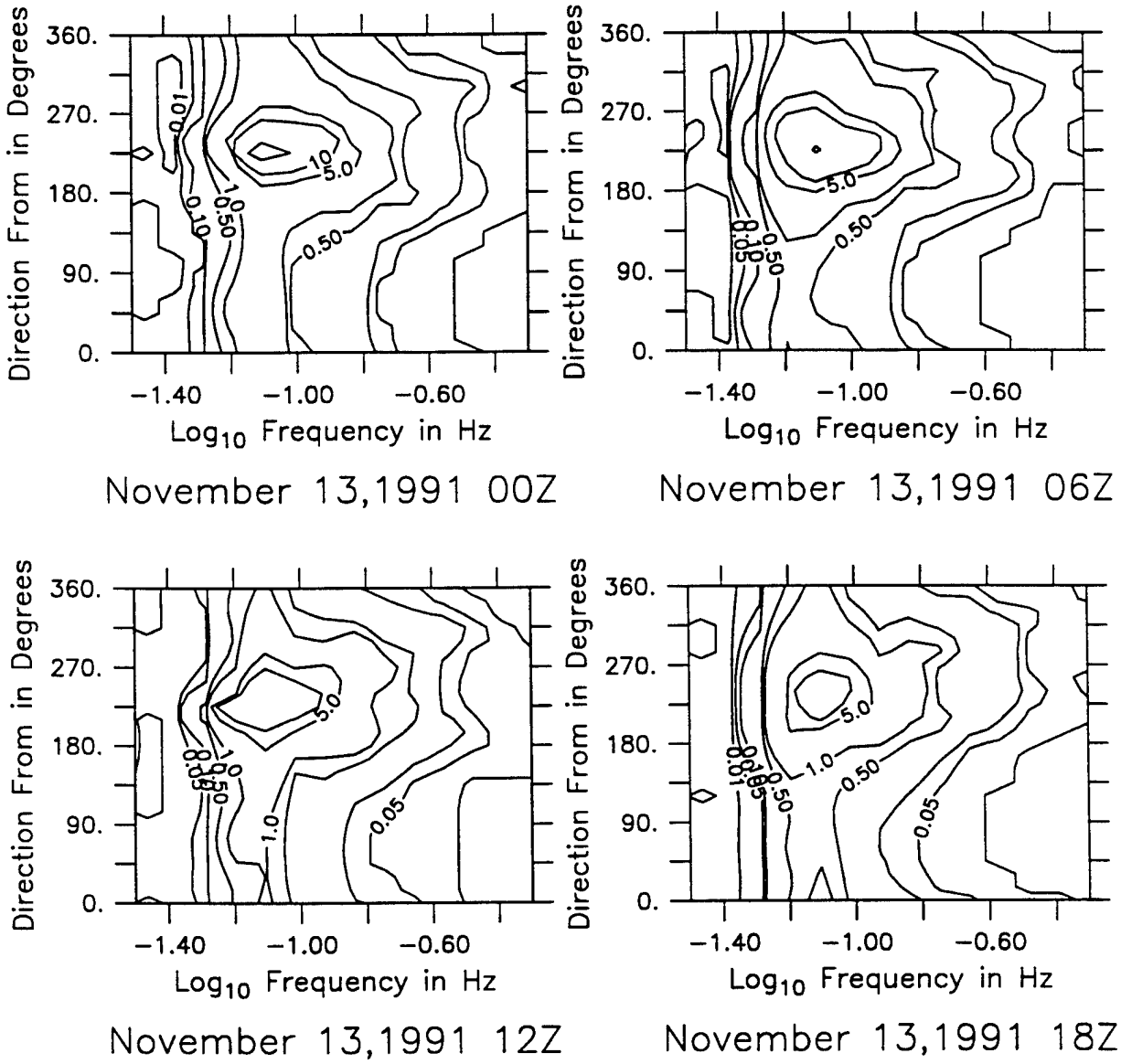

Figure 3.4.17: Directional wave spectra, Seatex buoy. Contours are 0.01, 0.05, 0.1, 0.5, 1, 5, 10, 50, 100, 500.

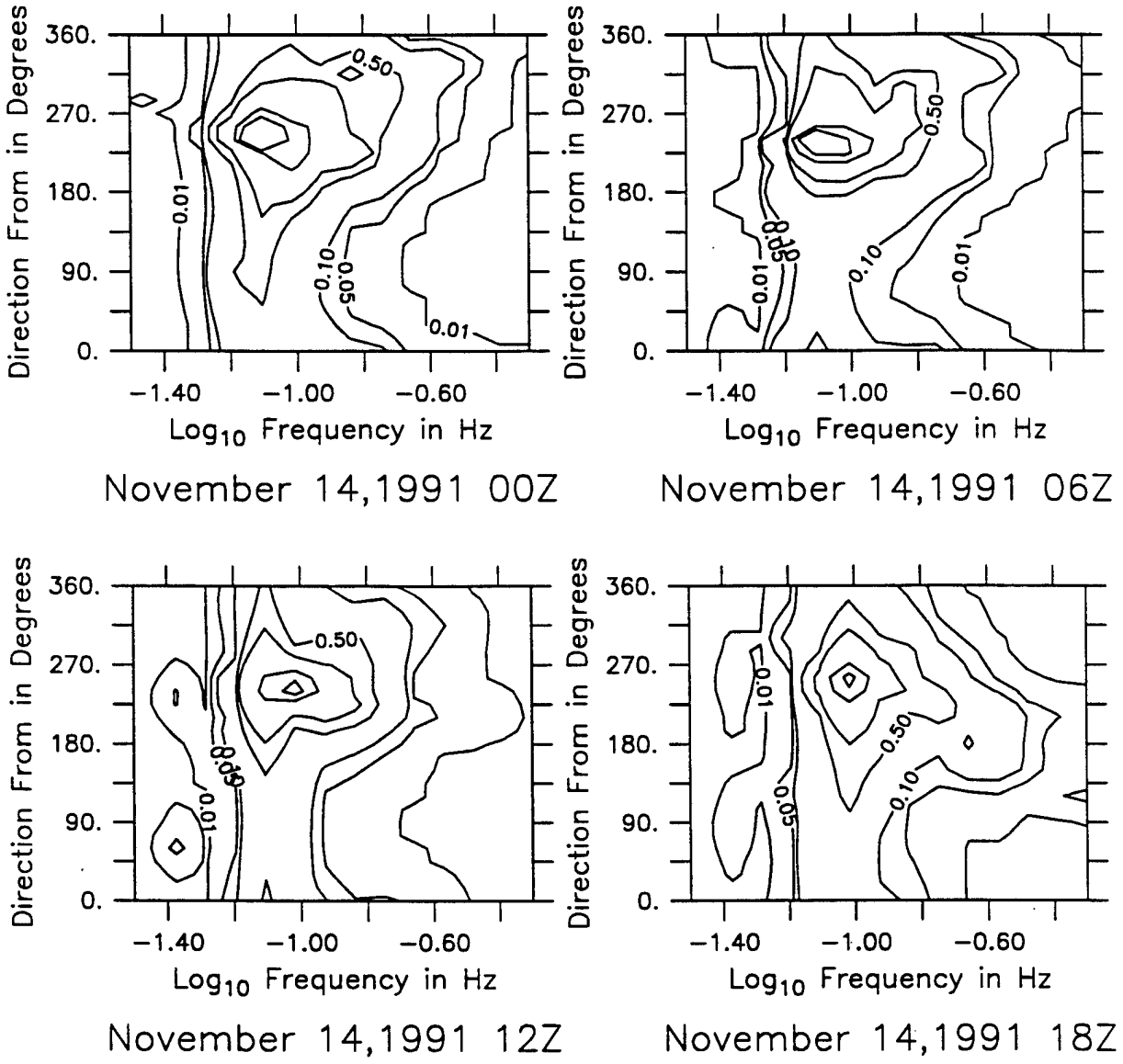

Figure 3.4.18: Directional wave spectra, Seatex buoy. Contours are 0.01, 0.05, 0.1, 0.5, 1, 5, 10, 50, 100, 500.

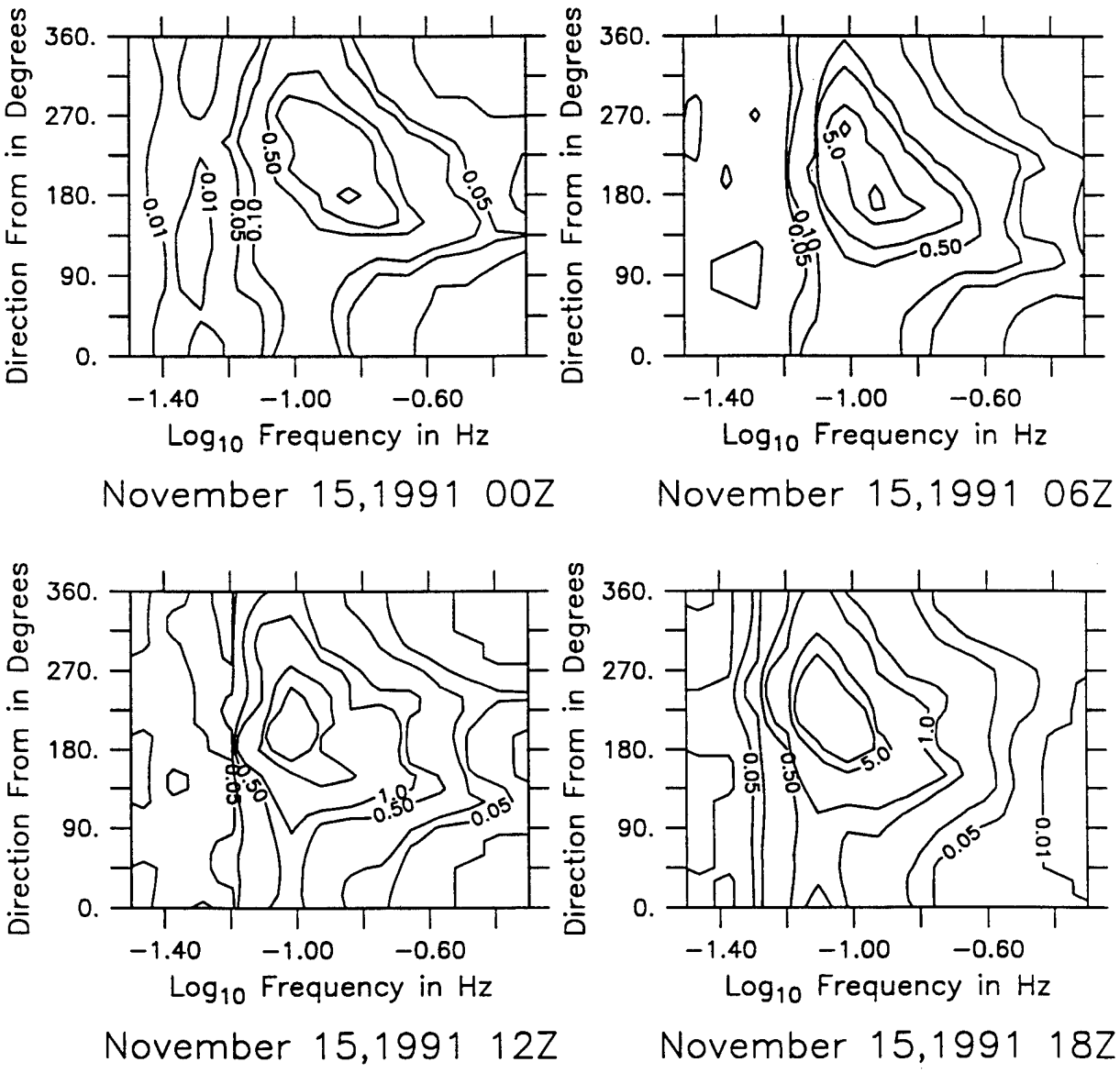

Figure 3.4.19: Directional wave spectra, Seatex buoy. Contours are 0.01, 0.05, 0.1, 0.5, 1, 5, 10, 50, 100, 500.

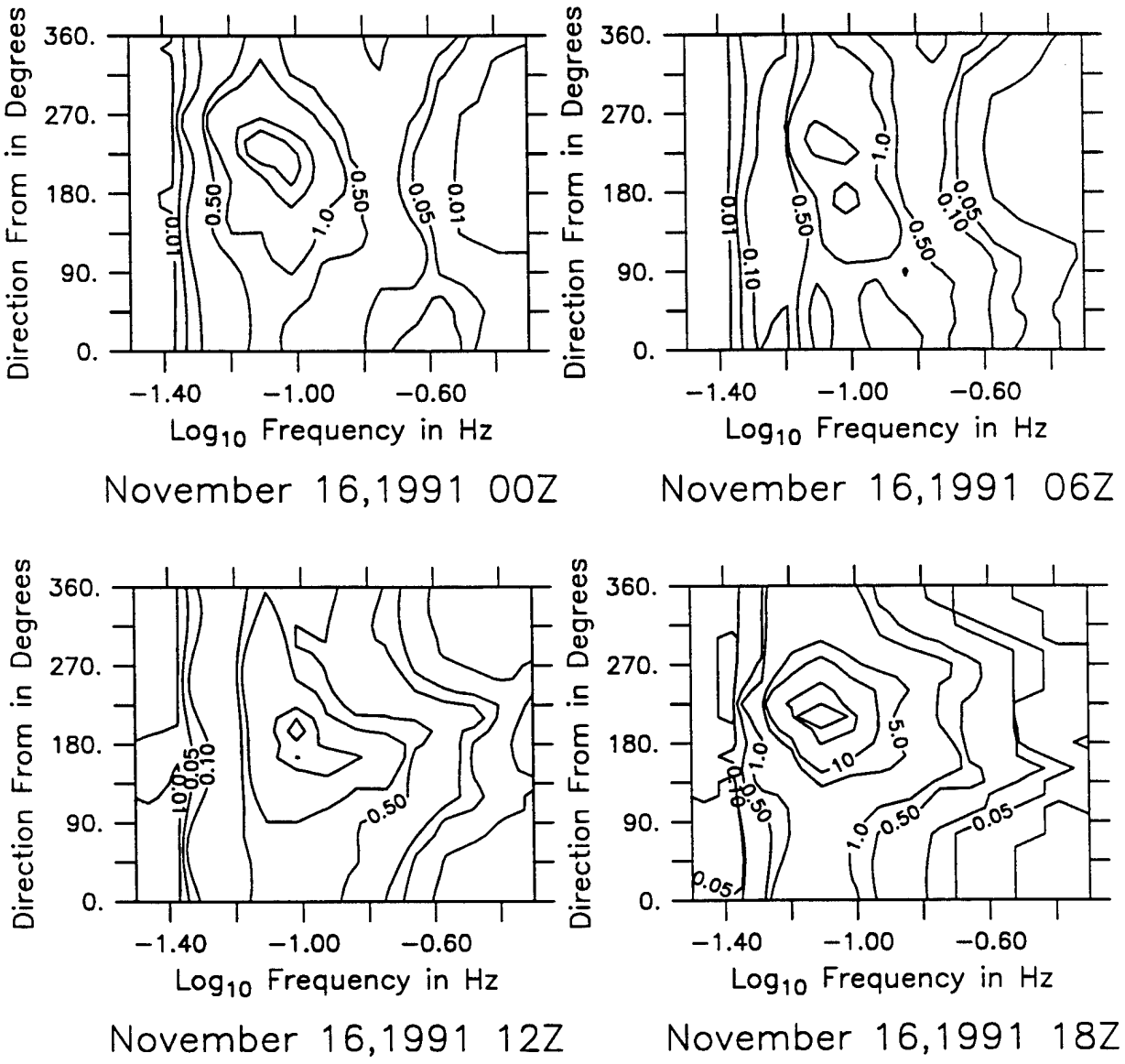

Figure 3.4.20: Directional wave spectra, Seatex buoy. Contours are 0.01, 0.05, 0.1, 0.5, 1, 5, 10, 50, 100, 500.

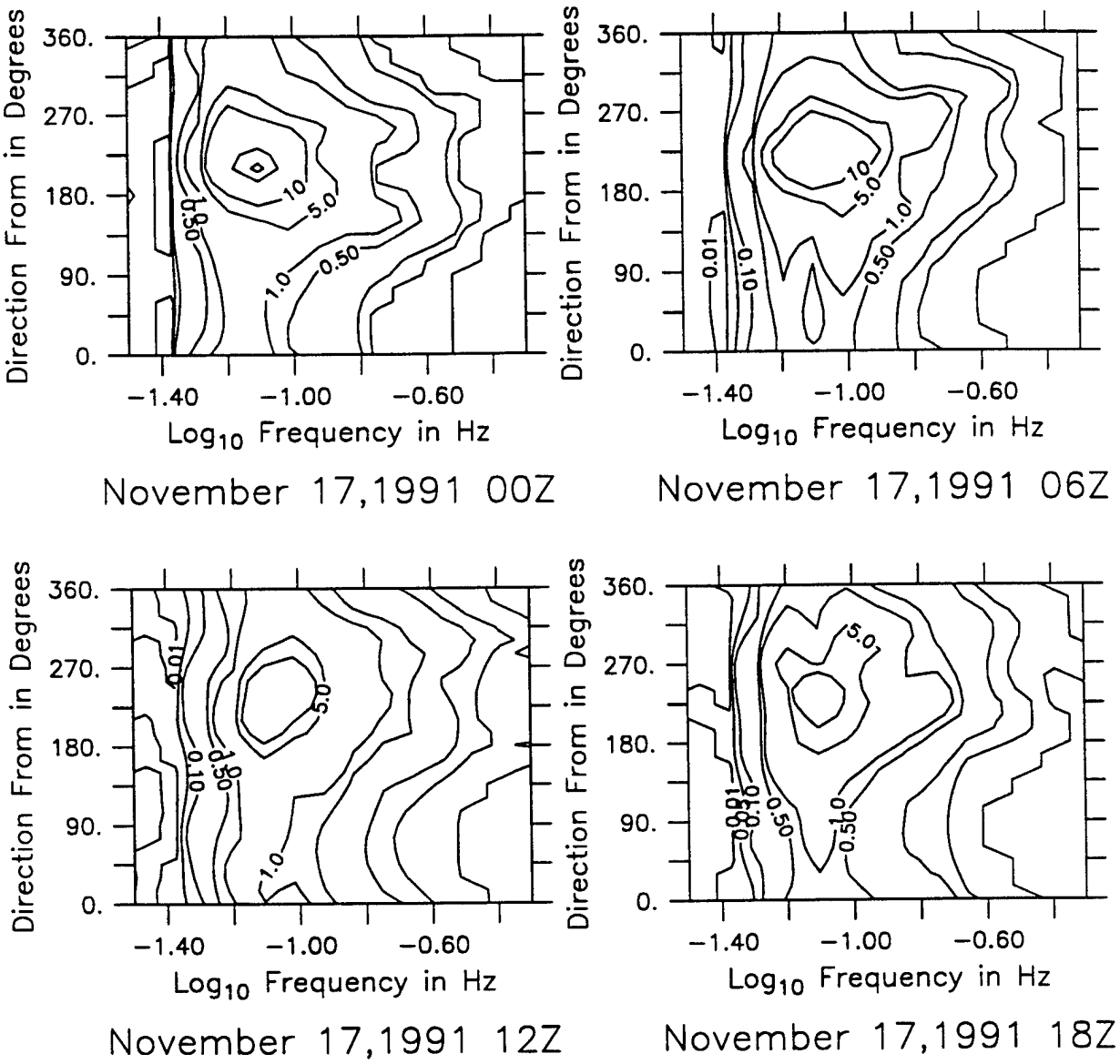

Figure 3.4.21: Directional wave spectra, Seatex buoy. Contours are 0.01, 0.05, 0.1, 0.5, 1, 5, 10, 50, 100, 500.

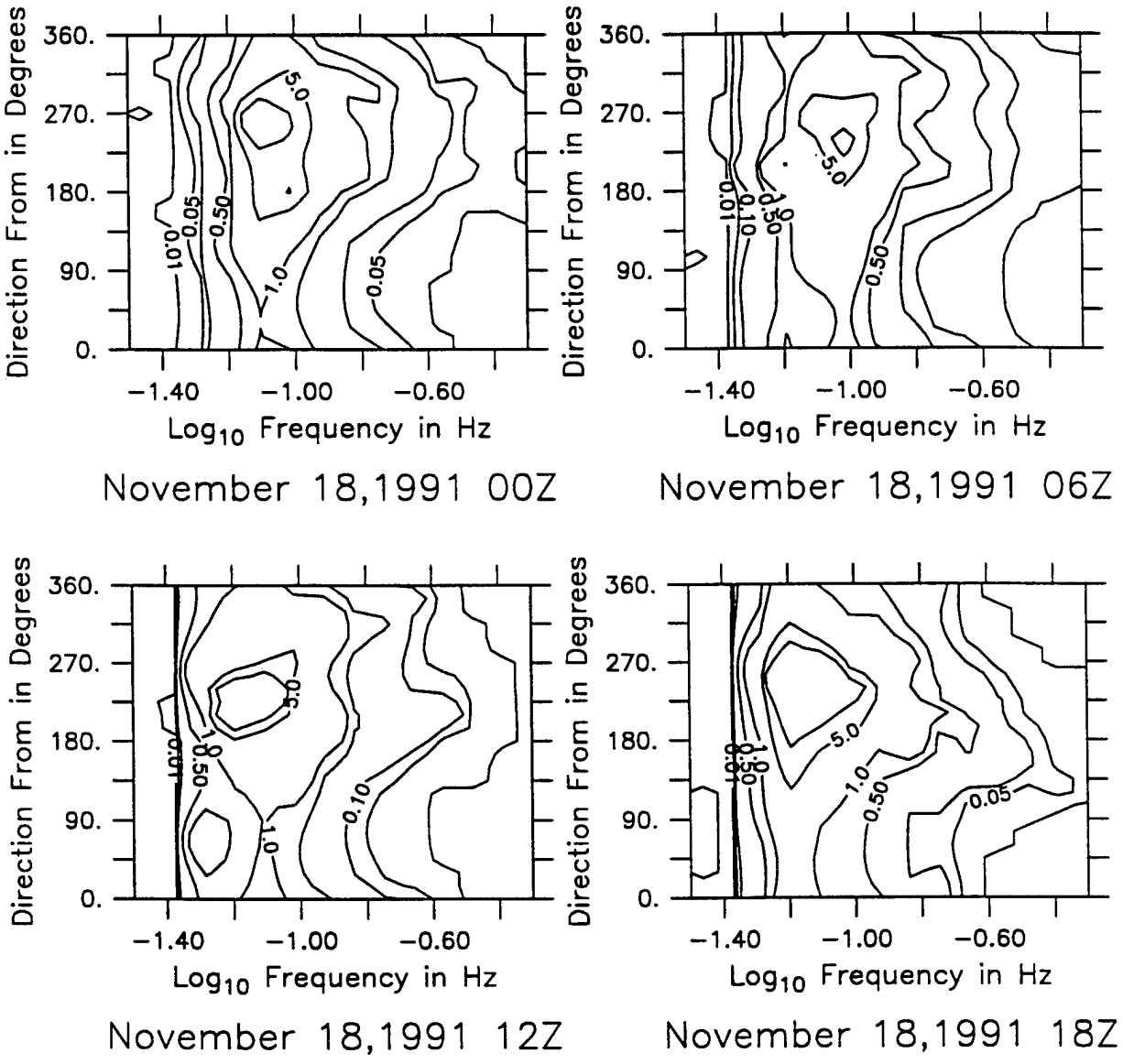

Figure 3.4.22: Directional wave spectra, Seatex buoy. Contours are 0.01, 0.05, 0.1, 0.5, 1, 5, 10, 50, 100, 500.

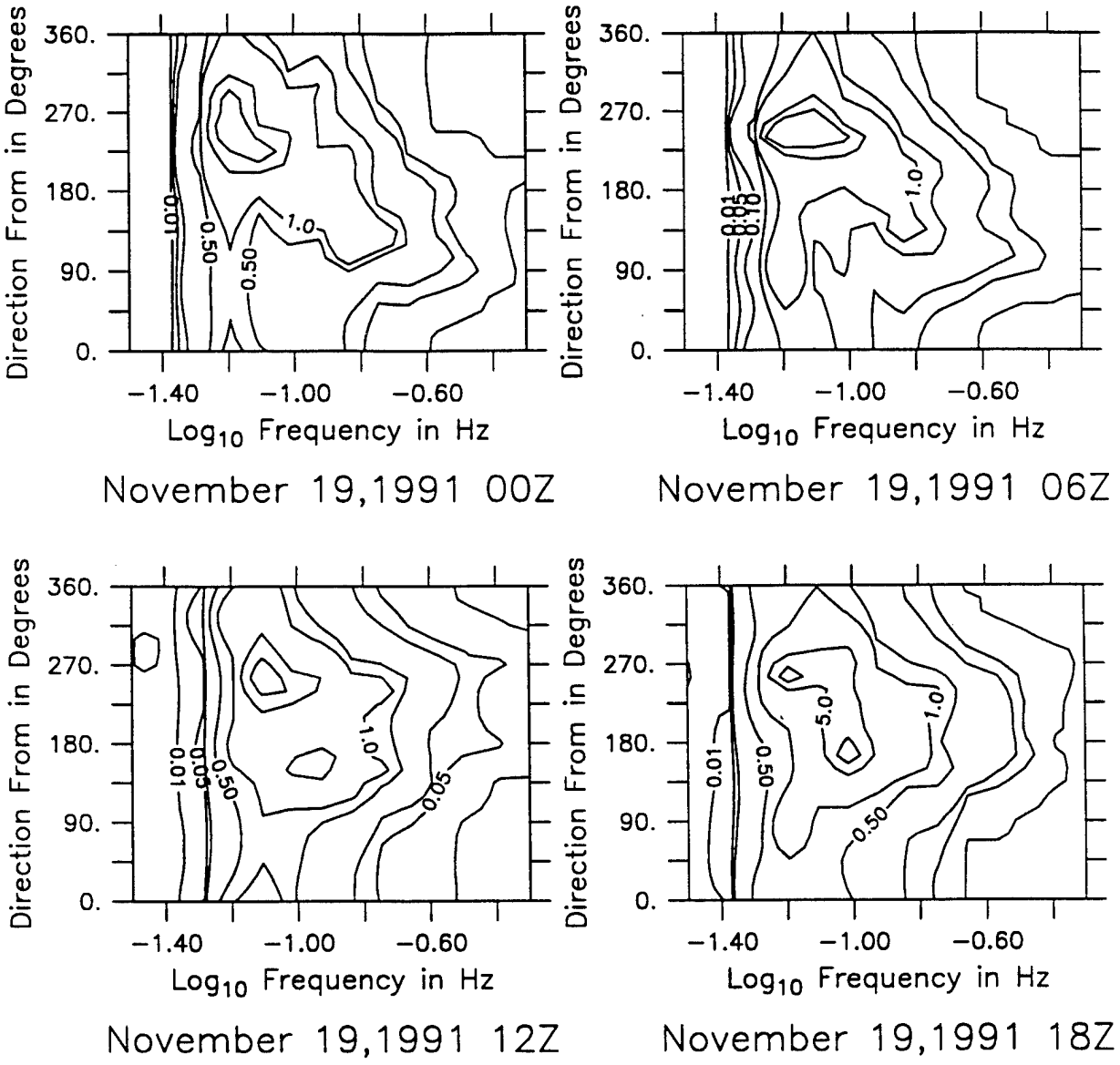

Figure 3.4.23: Directional wave spectra, Seatex buoy. Contours are 0.01, 0.05, 0.1, 0.5, 1, 5, 10, 50, 100, 500.

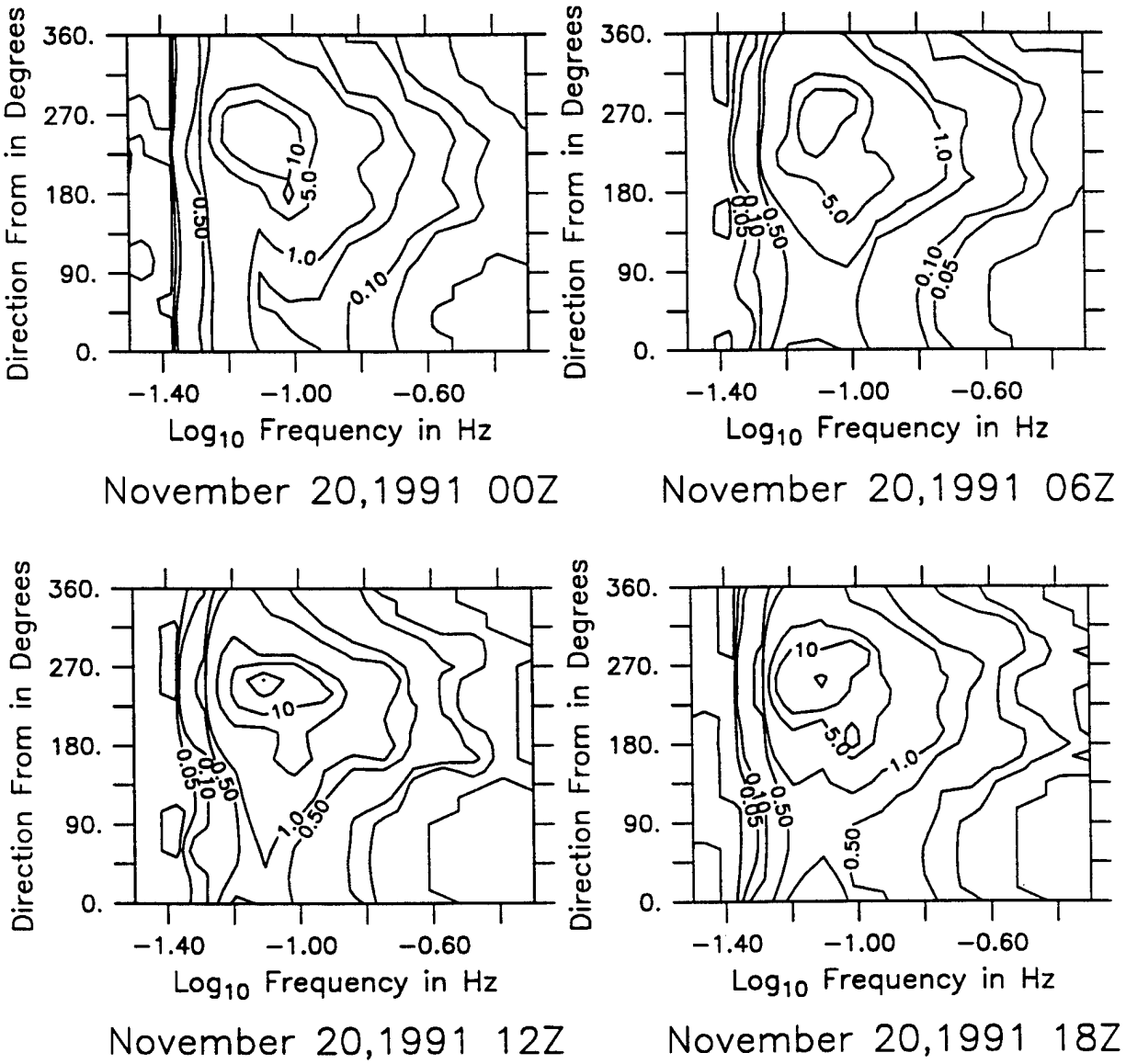

Figure 3.4.24: Directional wave spectra, Seatex buoy. Contours are 0.01, 0.05, 0.1, 0.5, 1, 5, 10, 50, 100, 500.

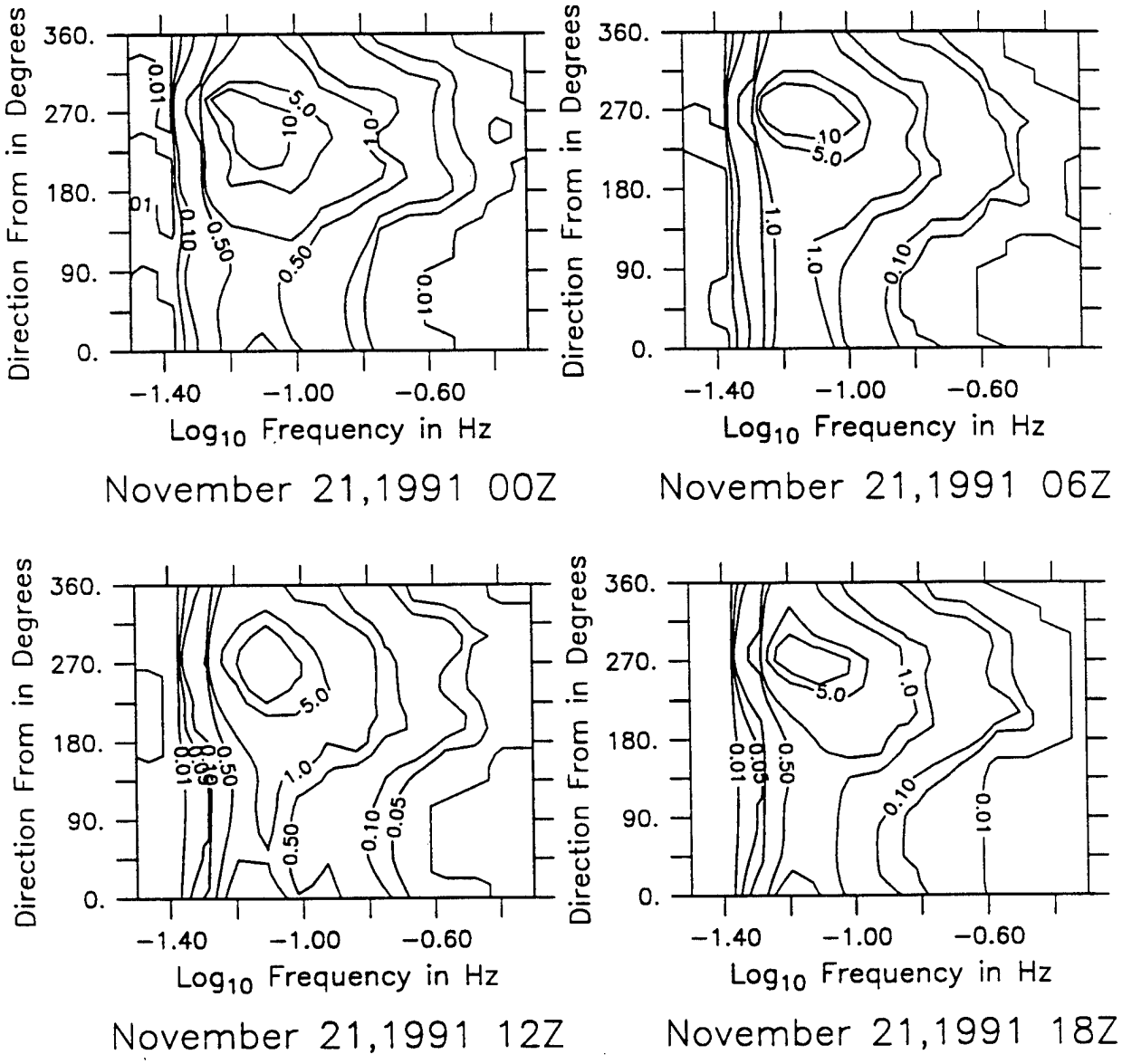

Figure 3.4.25: Directional wave spectra, Seatex buoy. Contours are 0.01, 0.05, 0.1, 0.5, 1, 5, 10, 50, 100, 500.

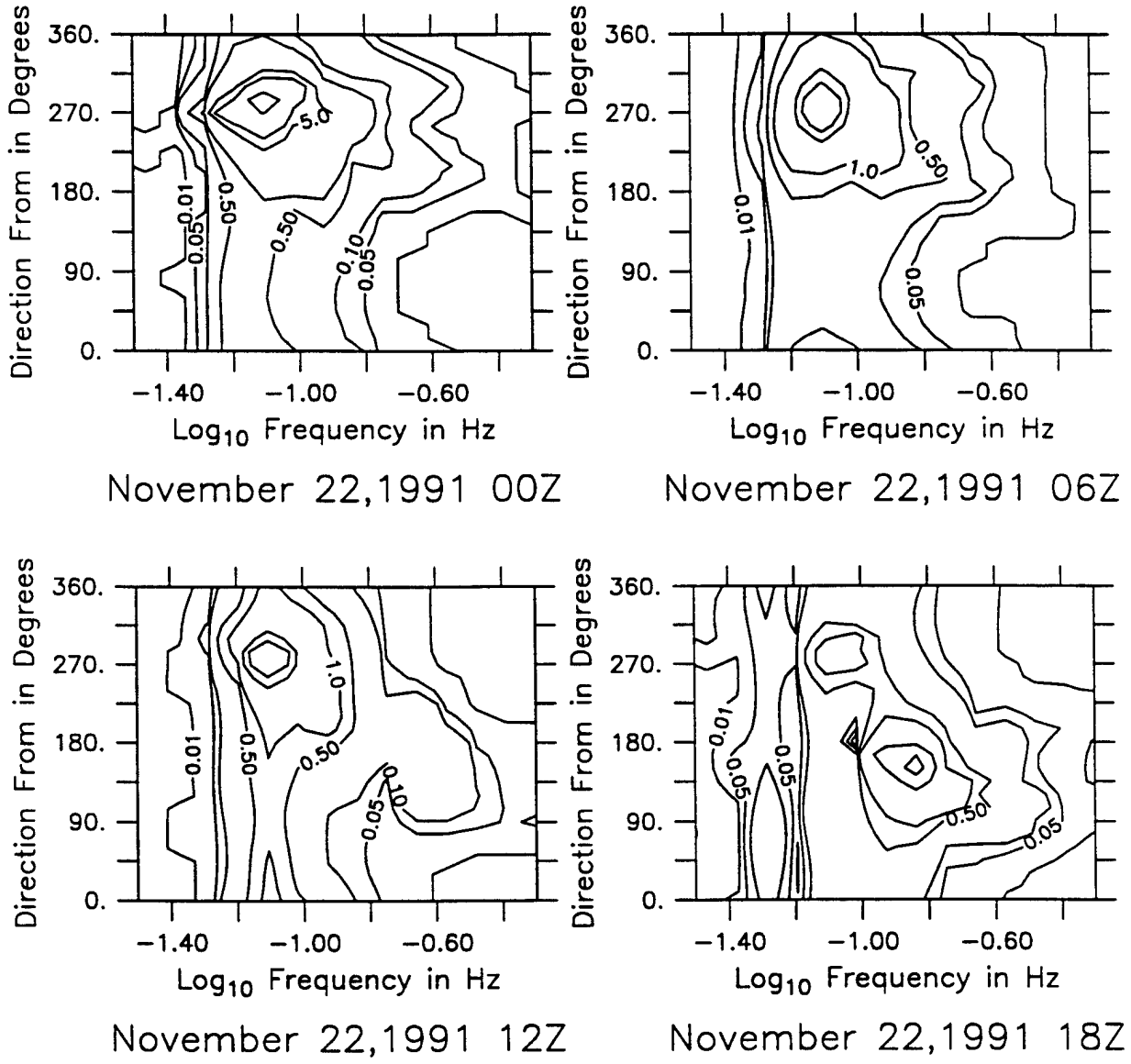

Figure 3.4.26: Directional wave spectra, Seatex buoy. Contours are 0.01, 0.05, 0.1, 0.5, 1, 5, 10, 50, 100, 500.

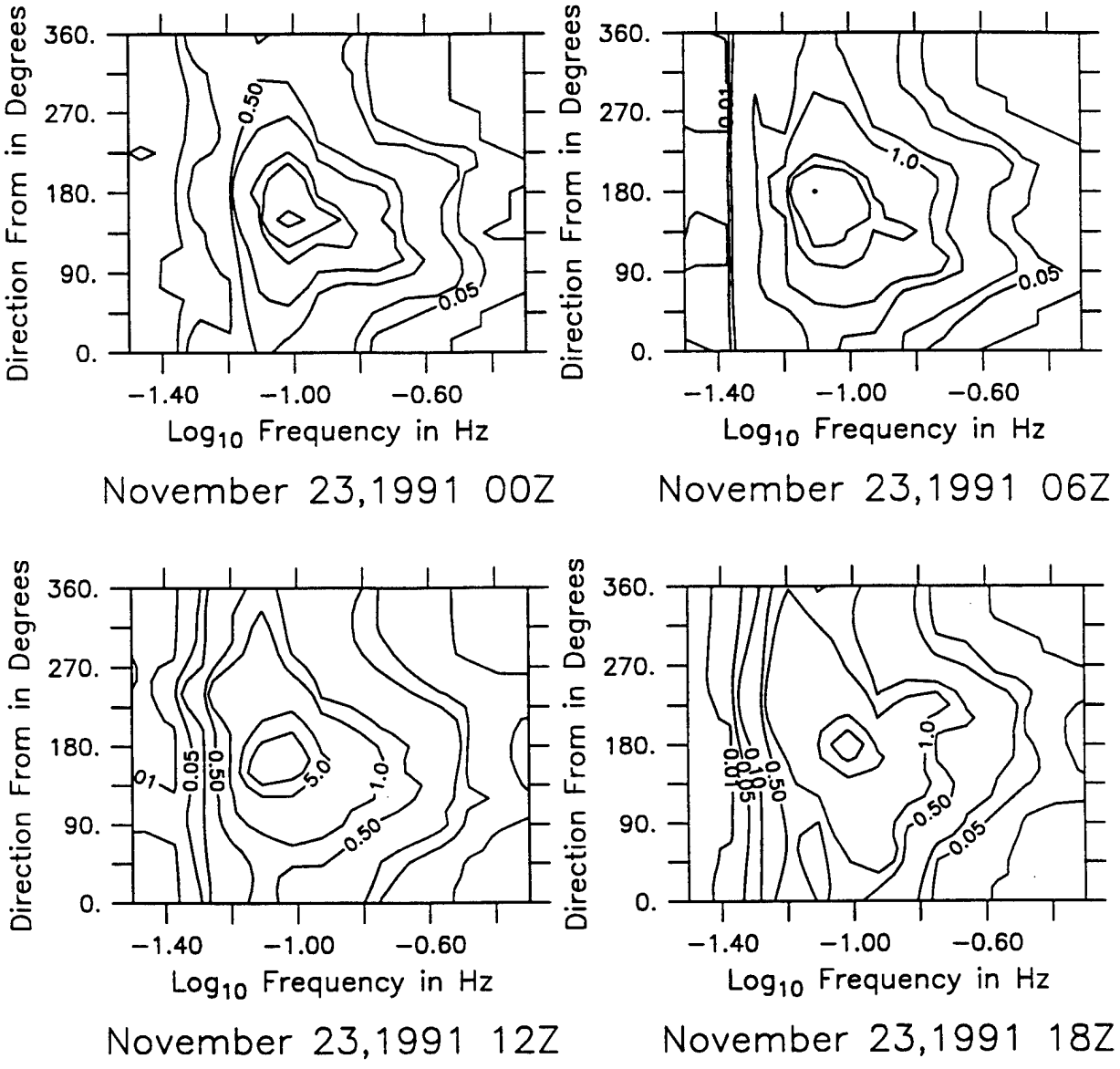

Figure 3.4.27: Directional wave spectra, Seatex buoy. Contours are 0.01, 0.05, 0.1, 0.5, 1, 5, 10, 50, 100, 500.

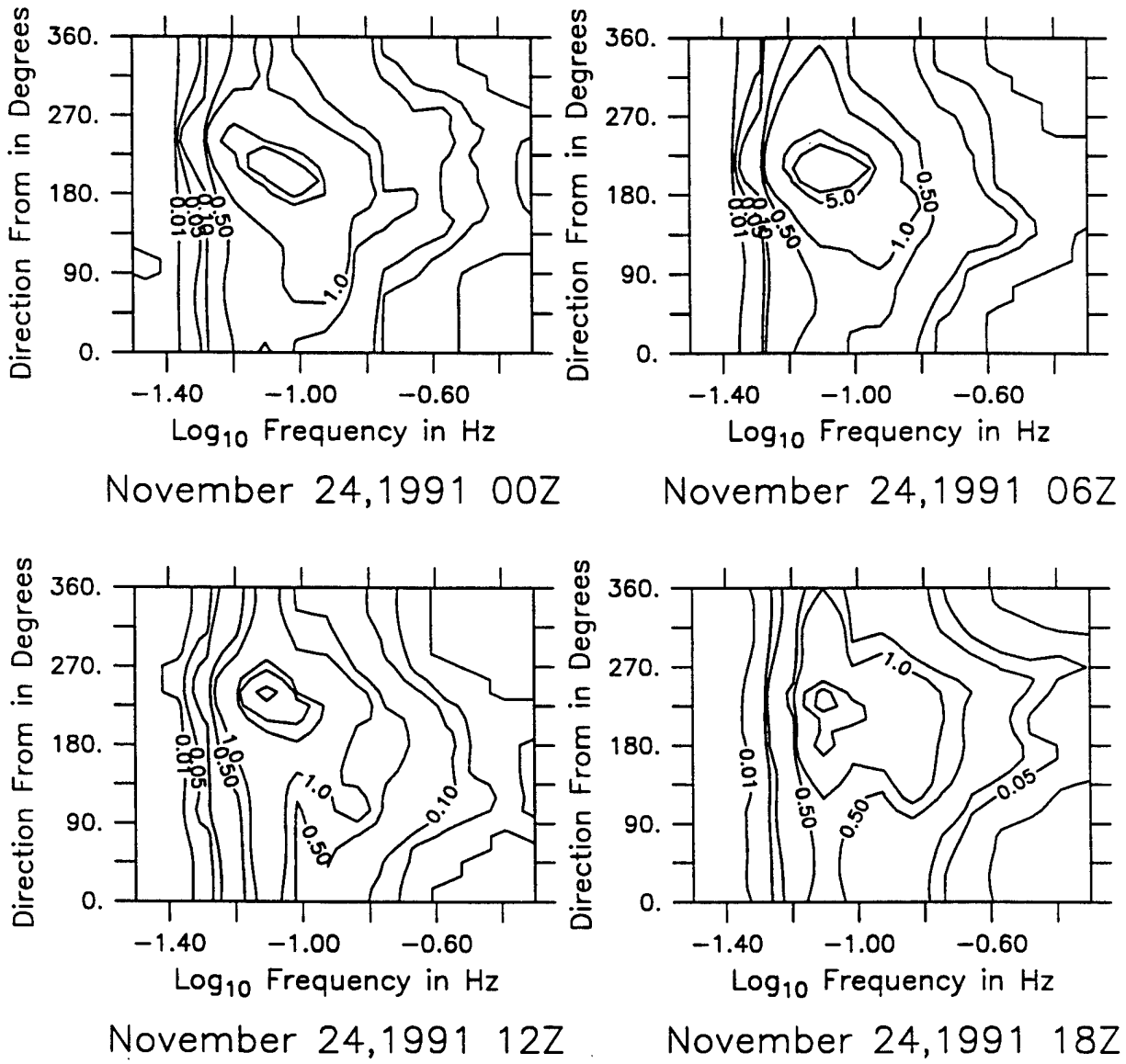

Figure 3.4.28: Directional wave spectra, Seatex buoy. Contours are 0.01, 0.05, 0.1, 0.5, 1, 5, 10, 50, 100, 500.

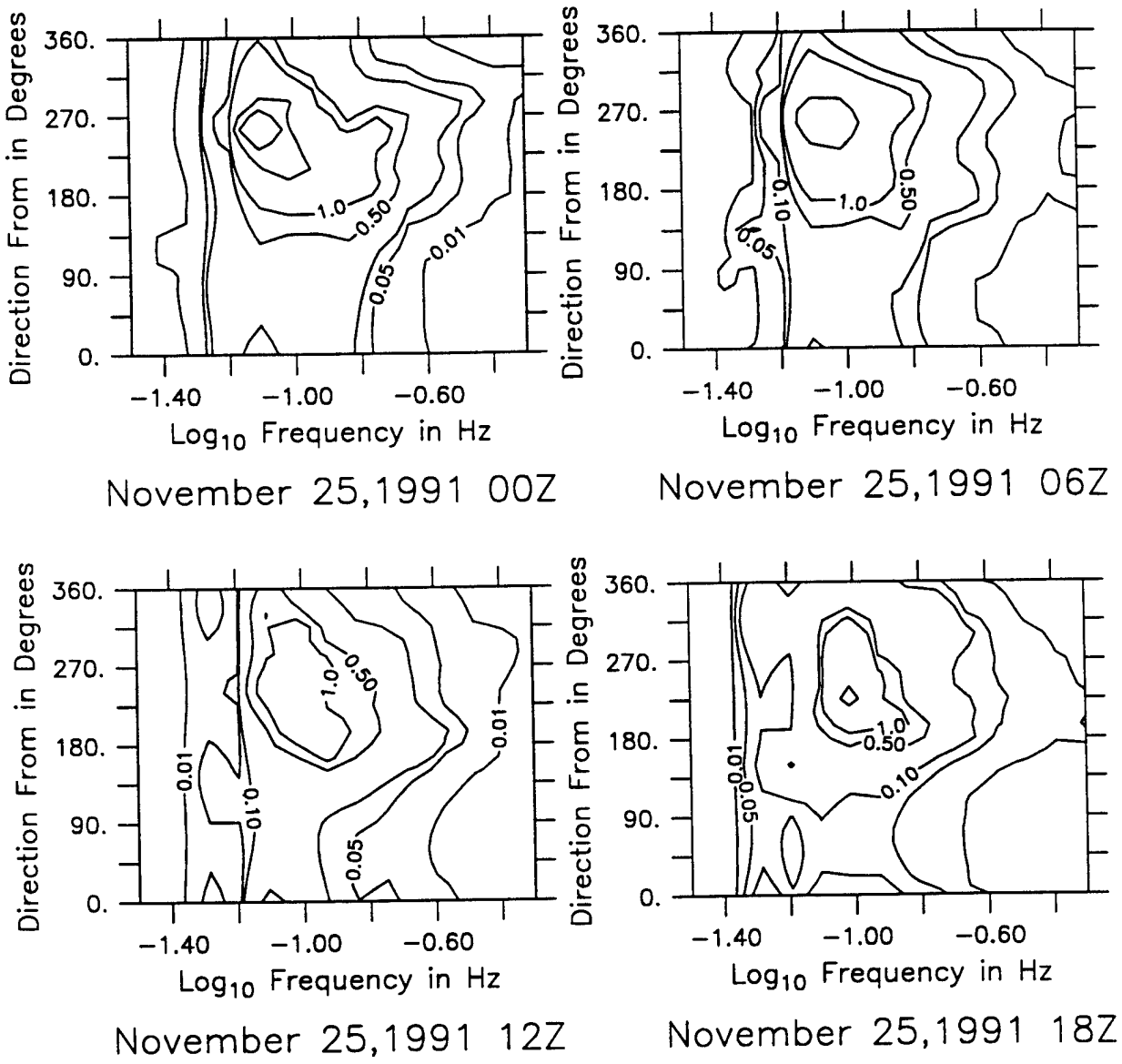

Figure 3.4.29: Directional wave spectra, Seatex buoy. Contours are 0.01, 0.05, 0.1, 0.5, 1, 5, 10, 50, 100, 500.

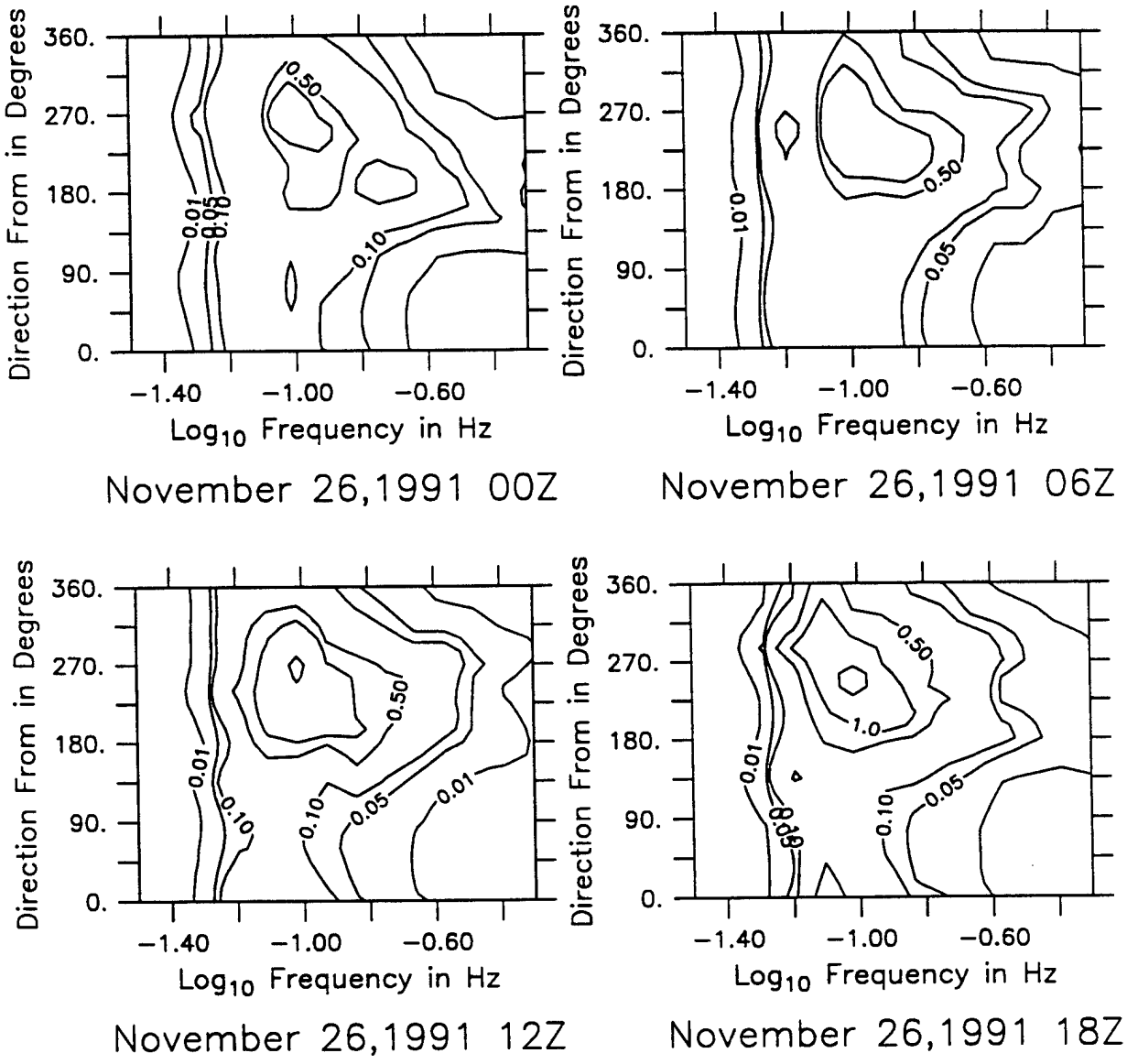

Figure 3.4.30: Directional wave spectra, Seatex buoy. Contours are 0.01, 0.05, 0.1, 0.5, 1, 5, 10, 50, 100, 500.

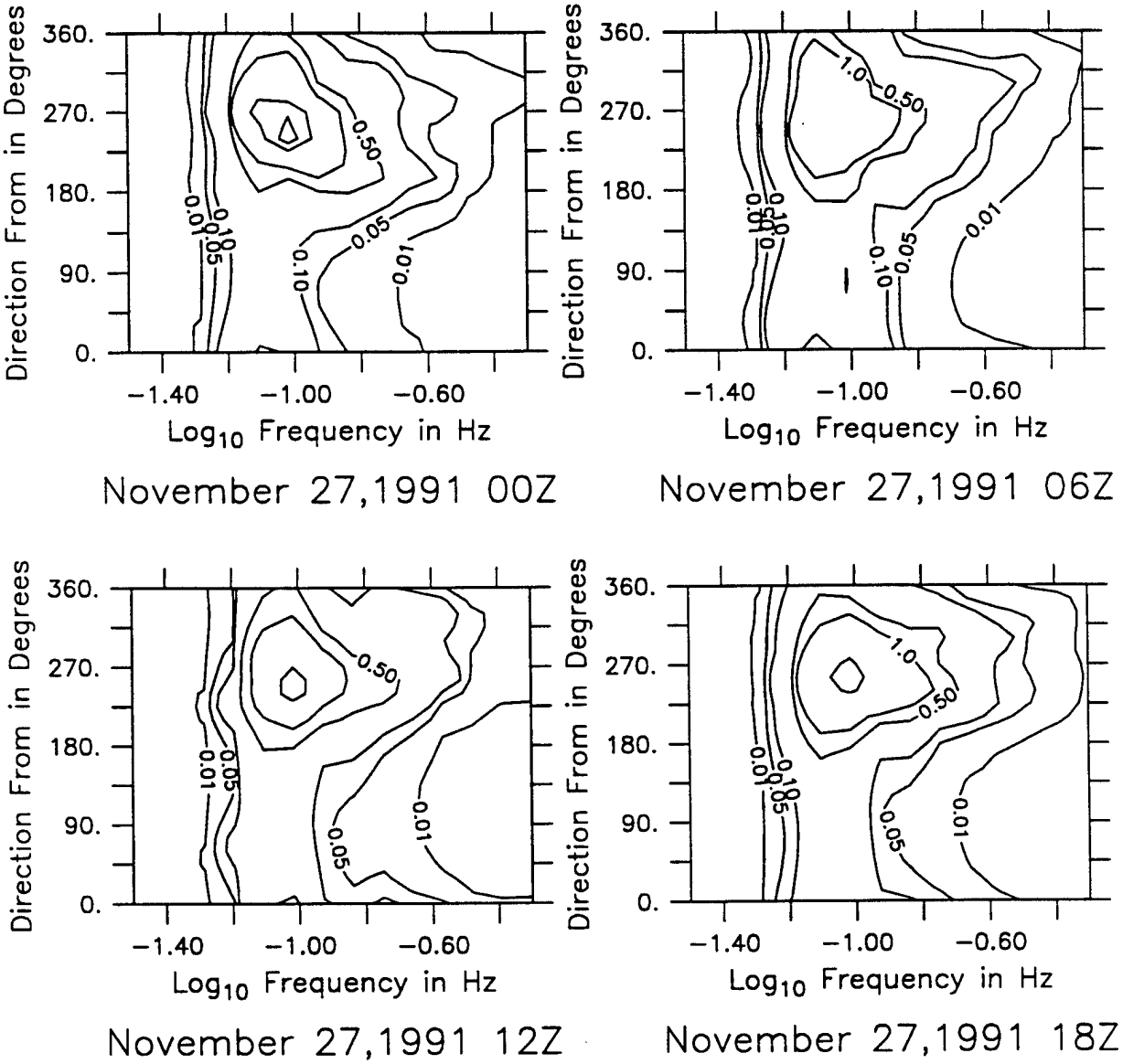

Figure 3.4.31: Directional wave spectra, Seatex buoy. Contours are 0.01, 0.05, 0.1, 0.5, 1, 5, 10, 50, 100, 500.

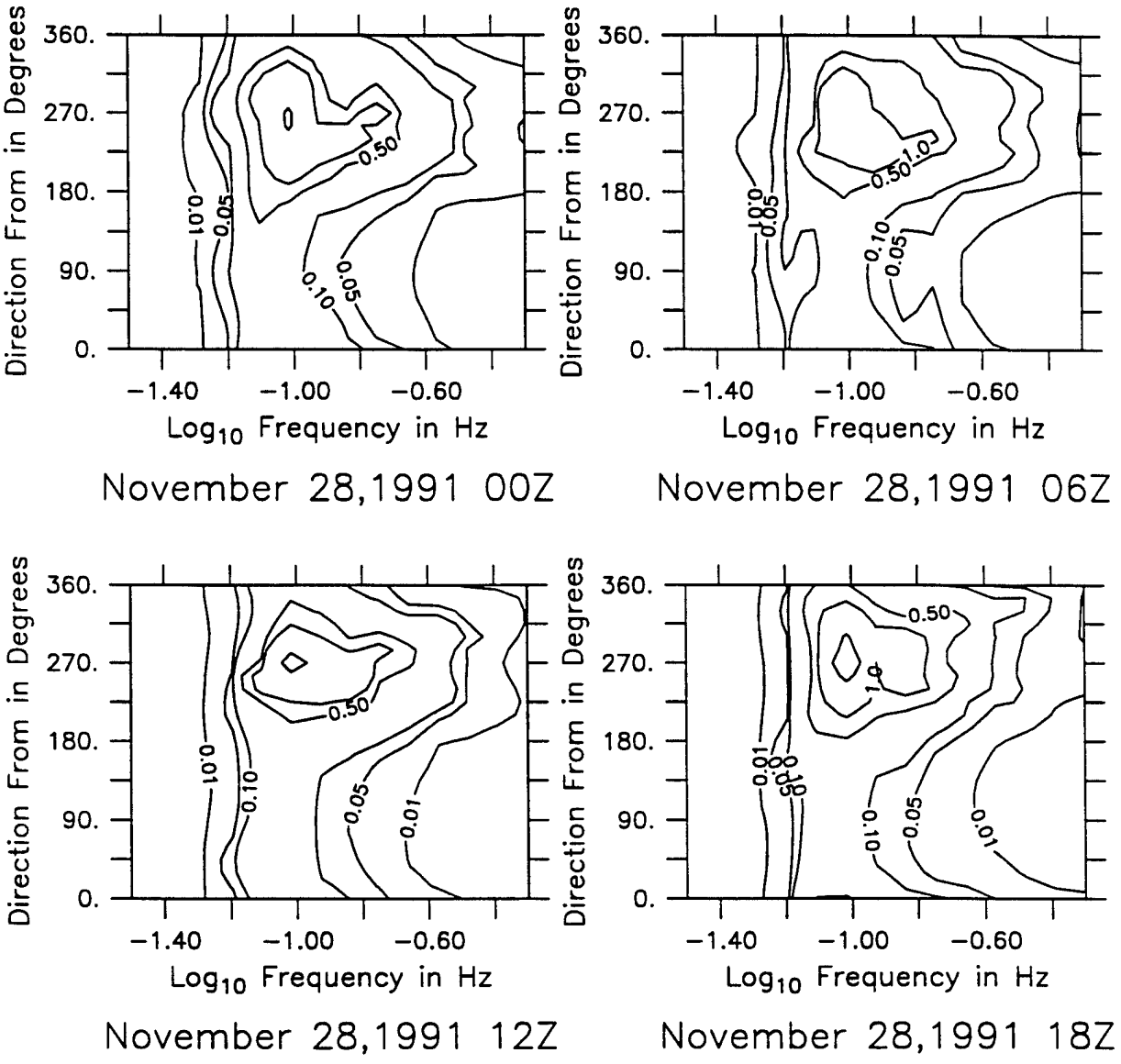

Figure 3.4.32: Directional wave spectra, Seatex buoy. Contours are 0.01, 0.05, 0.1, 0.5, 1, 5, 10, 50, 100, 500.

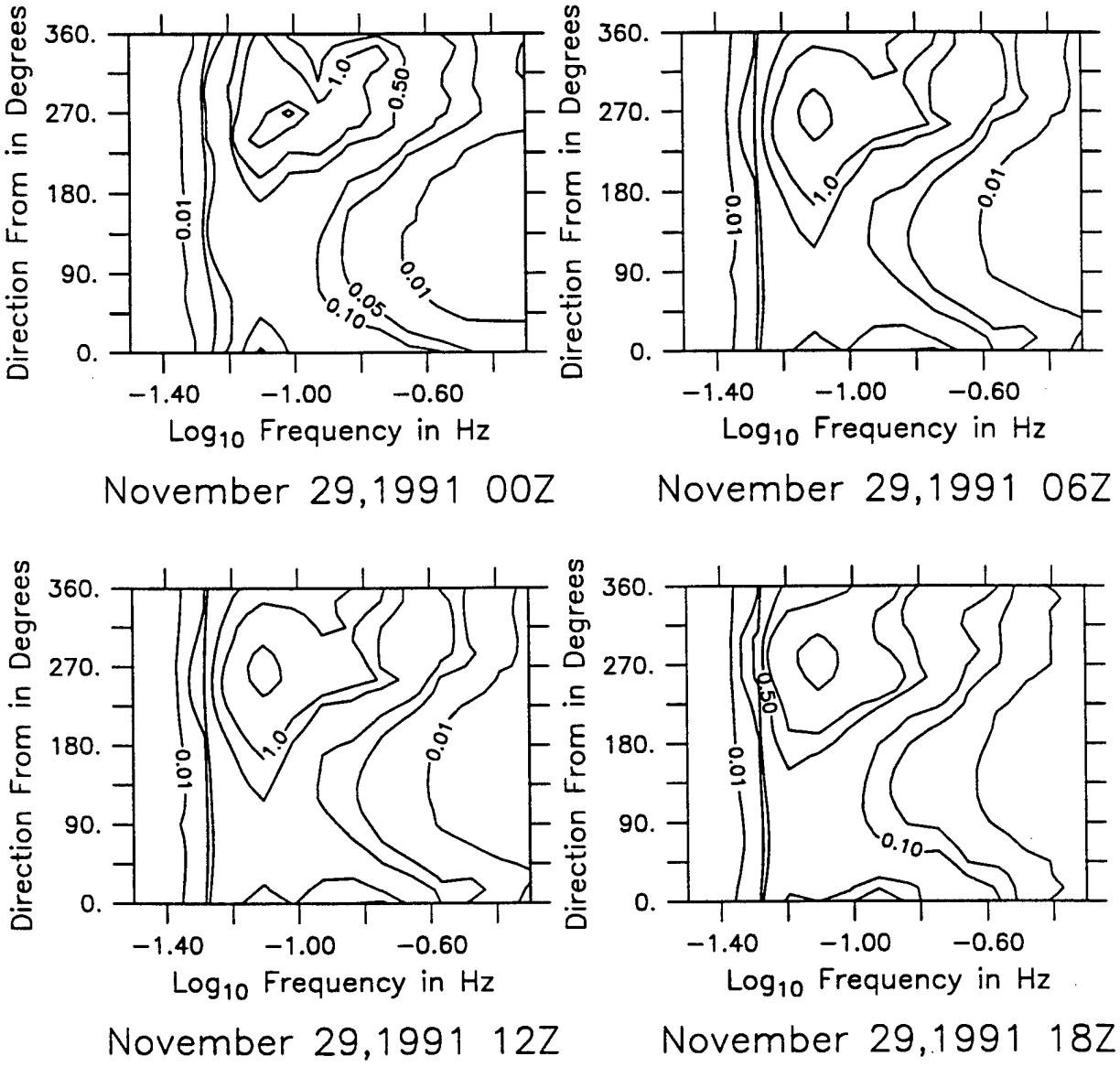

Figure 3.4.33: Directional wave spectra, Seatex buoy. Contours are 0.01, 0.05, 0.1, 0.5, 1, 5, 10, 50, 100, 500.

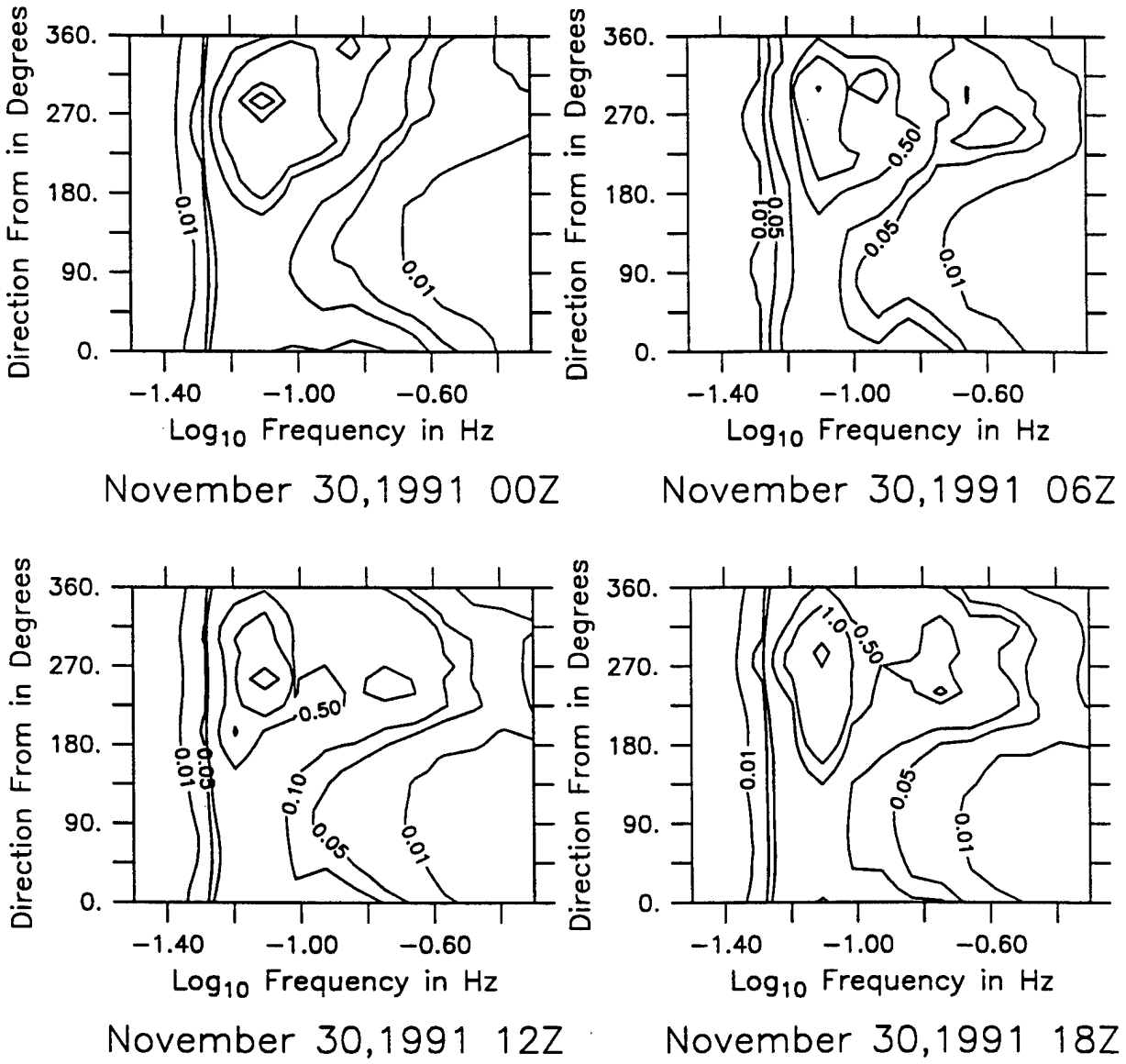

Figure 3.4.34: Directional wave spectra, Seatex buoy. Contours are 0.01, 0.05, 0.1, 0.5, 1, 5, 10, 50, 100, 500.

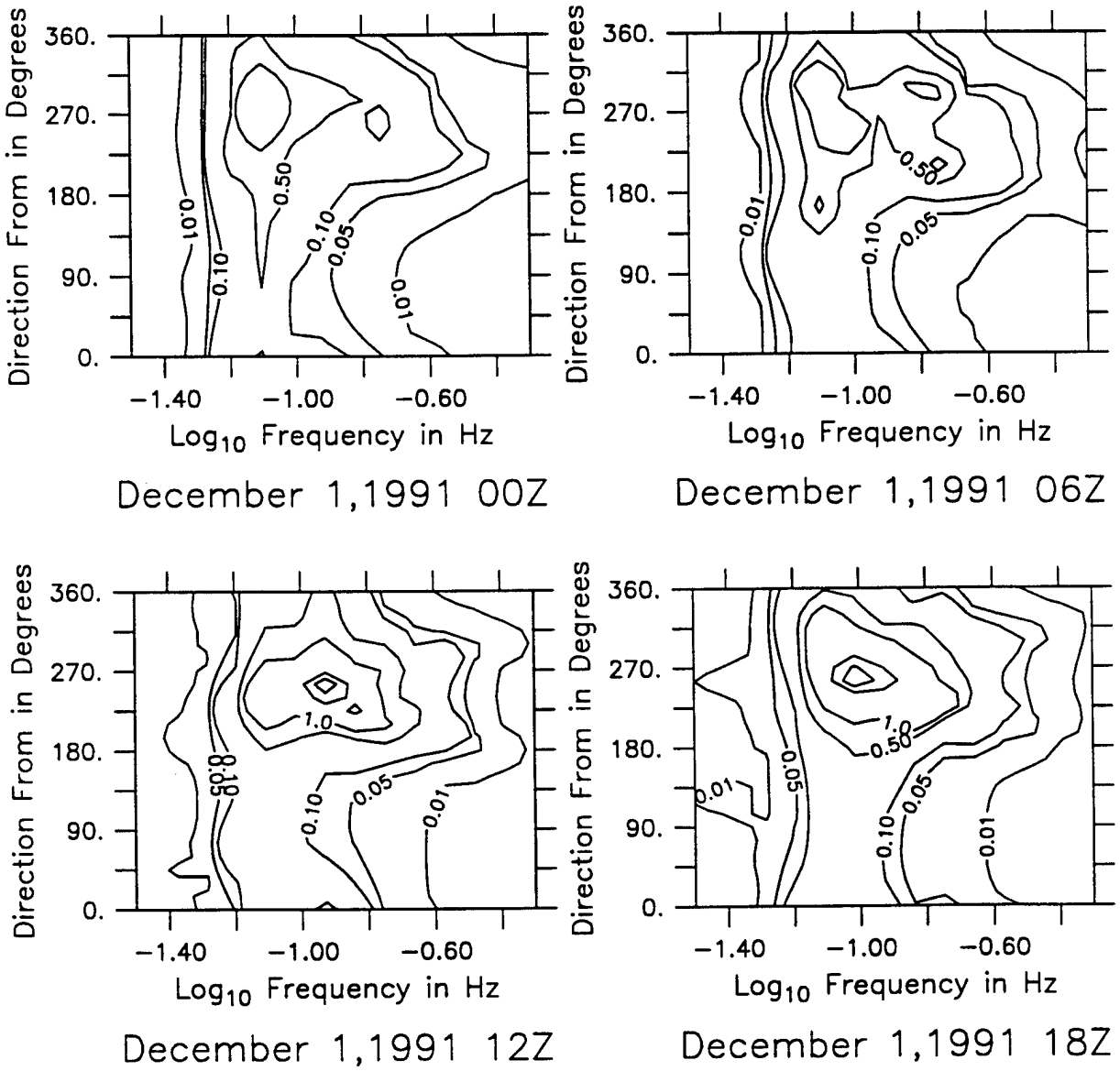

Figure 3.4.35: Directional wave spectra, Seatex buoy. Contours are 0.01, 0.05, 0.1, 0.5, 1, 5, 10, 50, 100, 500.

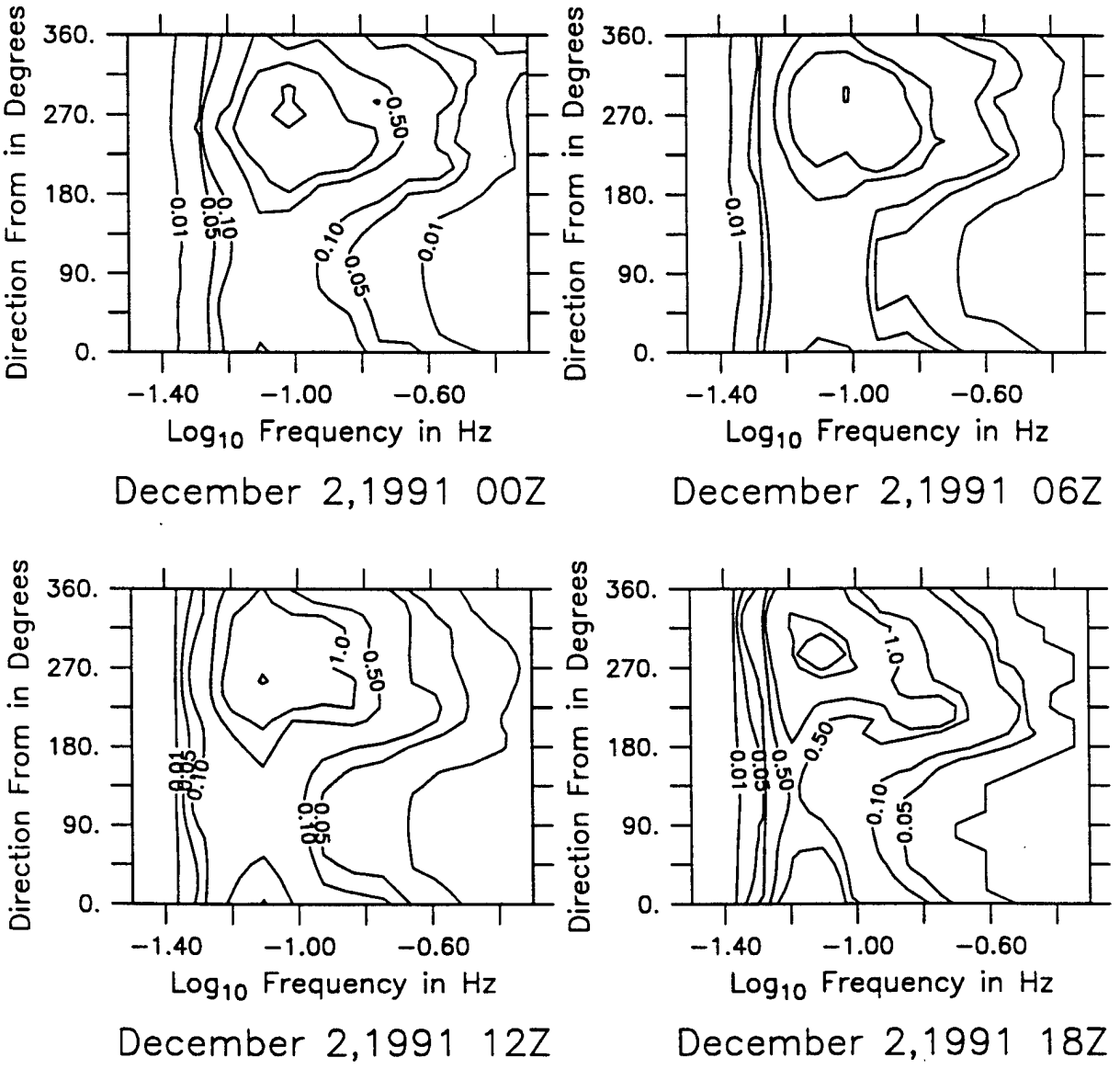

Figure 3.4.36: Directional wave spectra, Seatex buoy. Contours are 0.01, 0.05, 0.1, 0.5, 1, 5, 10, 50, 100, 500.

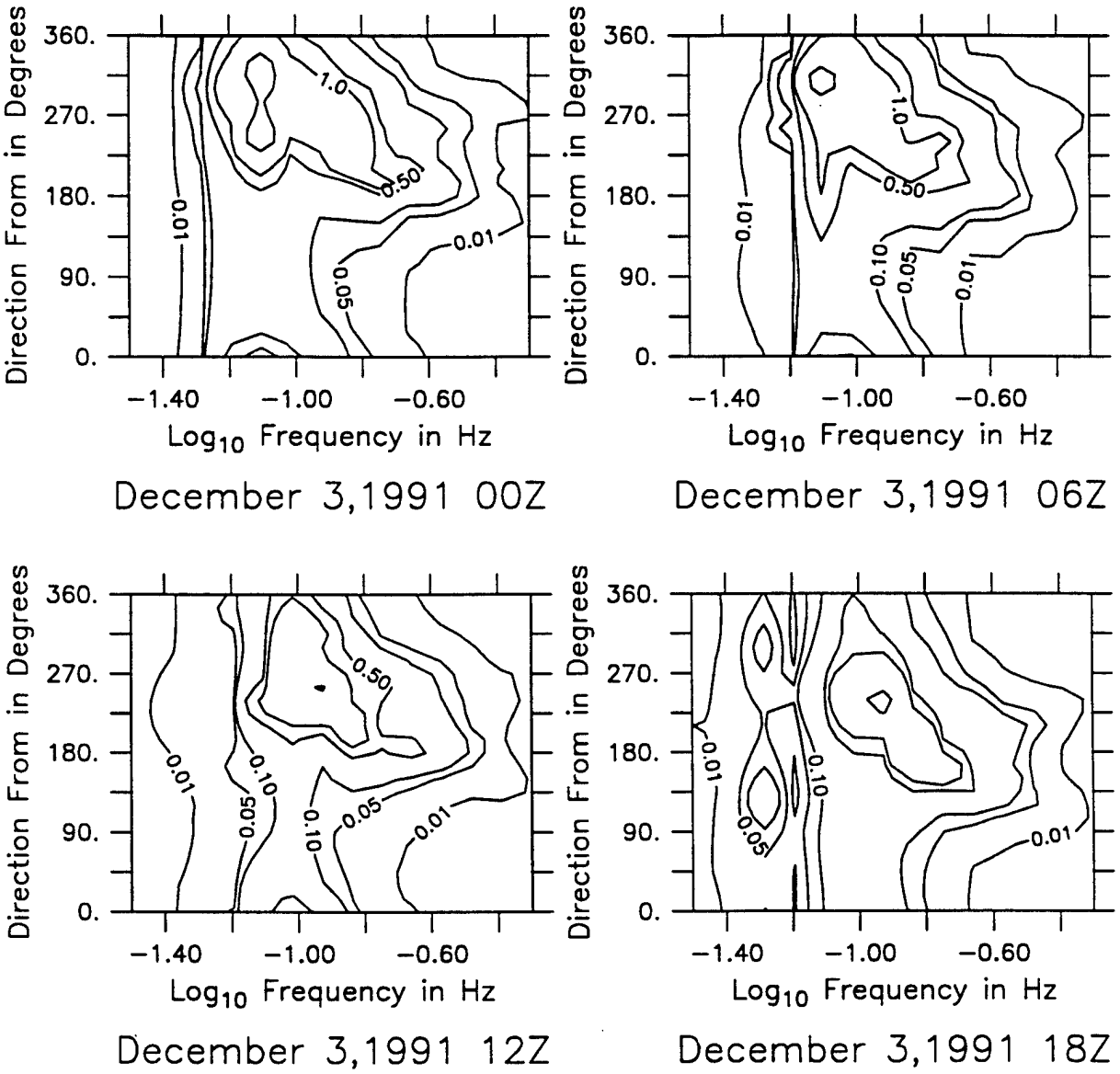

Figure 3.4.37: Directional wave spectra, Seatex buoy. Contours are 0.01, 0.05, 0.1, 0.5, 1, 5, 10, 50, 100, 500.

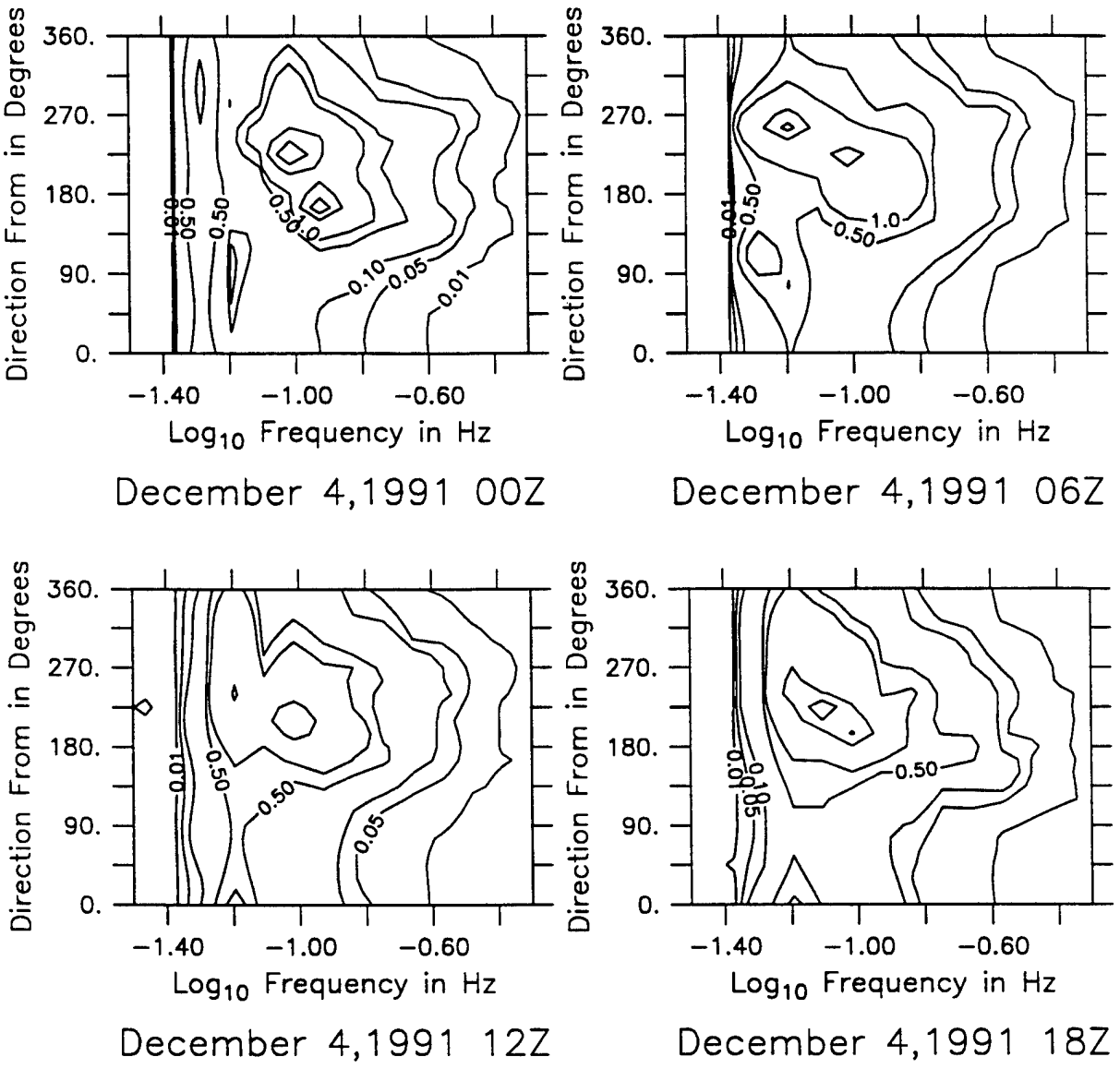

Figure 3.4.38: Directional wave spectra, Seatex buoy. Contours are 0.01, 0.05, 0.1, 0.5, 1, 5, 10, 50, 100, 500.

Acknowledgments

The Endeco/YSI corporation donated an 1156 Wave Buoy for use in this experiment. The Seatex and discus moorings were designed by George Tupper, and the Endeco mooring was designed by Sean Kerry. The moorings were fabricated in the WHOI rigging shop by David Simoneau. John Kemp of the Ocean Acoustics Laboratory supervised the mooring deployment and recovery, which was carried out with expert help from Captain Clampitt and the crew of the Research Vessel *Thomas Thompson.* Commander Frank Scherber and the crew of the *H.M.C.S. Huron* recovered the Seatex Buoy. Melora Park-Samelson of the UOP Group undertook the primary processing and calibration tasks for the VAWR, VMCM, and TPOD data. Dick Payne and Bill Horn performed the pre and post-cruise calibrations of the IMET, VAWR , and temperature sensors. Mary Ann Lucas assisted with the final compilation of the manuscript.We would like to acknowledge assistance from Endeco/YSI and Seatex A/S during the course of the data analysis. This work was supported by the Ocean Acoustics Program (Code 324OA) of the Office of Naval Research under contract N00014–91–J-1891.

References

Barstow, S.E., G. Ueland, H.E. Krogstad, and B.A. Fossum, (1991) The WAVESCAN Second Generation Wave Buoy, *IEEE J. Ocean. Eng.*, **16**:254-266.

Clark, N.E., L. Eber, R.M. Laurs, J. A. Renner, and J.F.T. Saur, (1974) Heat exchange between ocean and atmosphere in the eastern North Pacific for 1961-1971. NOAA Technical Report, NMFS SSRF–682, U.S. Department of Commerce, Washington, D.C.

Gnanadesikan A., and E.A. Terray, (1994), A comparison of three wave-measuring buoys, in Magoon, O.T., and J. M. Helmsley, eds., *Ocean Wave measurement and Analysis*, ASCE, New York.

Krogstad, H.E., (1992), Calibration of the WAVESCAN Directional Wave Buoy, SINTEF Report available from Seatex A/S, Trondheim, Norway.

Large, W.G. and S. Pond, (1981) Open ocean momentum flux measurements in moderate to strong winds. *J. Phys. Ocean.*, **11**: 324–336.

Large, W.G. and S. Pond, (1982) Sensible and latent heat flux measurements over the ocean. J. Phys. Ocean., **12**:464-482.

List, R.J., (1984), *Smithsonian Meteorological Tables*, Smithsonian Institution Press, Washington, D.C., 572 pp.

Lygre A. and H.E. Krogstad (1986), Maximum Entropy Estimation of the Directional Distribution in Ocean Wave Spectra, *J. Phys. Ocean.*, **16**:2052-2060.

Appendix 1: Cruise Participants

a. Deployment Cruise

Raymond Burge	NOARL	
John Cartmill	NOARL	
Harry Deferrari	U.Miami	(Chief Scientist)
Paul Bouchard	W.H.O.I.	
John Boutheilette	W.H.O.I.	
Anand Gnanadesikan	W.H.O.I.	
John Kemp	W.H.O.I.	
Eric Lamarre	M.I.T.	
Neil McPhee	W.H.O.I.	
Ken Melville	M.I.T.	
Michael Rebozo	U.Miami	
Jacob Roginsky	U.Miami	
Anatole Rozenberg	M.I.T.	
Joseph Steele	U.Conn.	
Ming Su	NOARL	
George Tupper	W.H.O.I.	
Bryan Way	W.H.O.I.	
Neil Williams	U.Miami	
Martin Wilson	U.Conn.	

b. Recovery Cruise

John Boutheilette	W.H.O.I.	
Raymond Burge	NOARL	
John Cartmill	NOARL	
Harry Deferrari	U.Miami	(Chief Scientist)
Carlton Grant	W.H.O.I.	
Anand Gnanadesikan	W.H.O.I.	
John Kemp	W.H.O.I.	
Ken Melville	M.I.T.	
Michael Rebozo	U.Miami	
Ming Su	NOARL	
George Tupper	W.H.O.I.	
Neil Williams	U.Miami	

Appendix 2: Chronology of Events

All times noted are UTC

Deployment Cruise: R/V Thomas Thompson Cruise No. TT004.

Date	Time	
29 Oct 91	0121	Underway on Cruise TT004 from Seattle
30 Oct 91	0858	Arrive at mooring area
	0948	Commence bottom survey using hydrosweep.
	1450-1803	Release Testing on wire.
	1840	Commence launch of Miami Acoustics Mooring.
	2319	Anchor over for Miami Acoustics Mooring
31 Oct 91	0015-0130	Anchor Position Survey
	0220	Launching sonabuoy, listening to Acoustics mooring.
	0315-0415	Release testing on wire.
	0457-0523	CTD Cast.
	0537	Deploy Acoustic spar buoy (W.K. Melville). Tethered to ship.
	0550-0649	Release Testing on wire.
	0705	Recover Acoustic spar buoy.
	1535	Commence launching Discus mooring. (WHOI mooring #920).
	2109	Anchor over, Discus mooring.
	2200-2300	Meteorological observations to compare ship readings with buoy.
	2305	Begin Anchor Position Survey.
1 Nov 91	0045	Finish anchor position survey.

	0222	Commence launching Seatex mooring. (WHOI mooring #921)
	0520	Anchor over, Seatex mooring.
	0643	Commence CTD cast.
	0709	Deploy Acoustic spar buoy (Time back not recorded).
	0712	CTD Aboard
	1752	Begin anchor position survey.
	1906	Finish anchor position survey.
	2145-2350	Release testing on wire.
2 Nov 91	0130	Commence launching Endeco mooring (WHOI mooring #923).
	0450	Anchor over, Endeco mooring.
	0512	Anchor on bottom, Endeco mooring.
	0535	Begin anchor position survey.
	0807	Finish anchor position survey.
	1600	Small boat launch to remove two temporary floats from Endeco buoy.
	1609	Small boat aboard, floats successfully removed.
	1740	Bubble population spar buoy (M. Su) deployed, tethered to ship.
	2040	Bubble population spar buoy recovered.
	2040	Breaking wave tripod buoy (E Monahan, UConn) deployed, tethered to ship.
	2204	Breaking wave tripod buoy recovered.
	2240	Acoustic spar buoy deployed, tethered to ship.
3 Nov 91	0210	Acoustic spar buoy recovered.

	0225	Bubble population spar buoy deployed, tethered to ship.
	0547	Bubble population spar buoy recovered.
	0626-0636	CTD Cast.
	1638	Acoustic spar buoy deployed, tethered to ship.
	2017	Acoustic spar buoy recovered.
	2025	Bubble population spar buoy deployed, tethered to ship.
4 Nov 91	0200	Bubble population spar buoy recovered.
	0203-0223	CTD cast.
	0525	Set course for Seattle.
5 Nov 91	1700	Arrive Seattle.

Moorings at Sea Recording Data.

1 Dec 91	1340	Seatex adrift.
3 Dec 91	1900	G. Tupper contacts Commander Johnson, (Royal Canadian Navy) at Esquimault, B.C. for possible recovery assistance.
4 Dec 91	1949	Seatex buoy recovered by HMCS Huron.
	2100	Commitment made to divert HMCS Huron, 170 miles from buoy, to attempt recovery.
5 Dec 91	0000	IMET data collection shut down due to insufficient sun.
2 Jan 92	0700-0800	Sometime during this hour the met tower on the Endeco buoy broke. Later examination revealed a faulty weld.

Recovery Cruise: R/V: Thomas Thompson Cruise No. TT005

5 Jan 92	0452	Underway on Cruise TT005 from Seattle.

6 Jan 92	1622	Release fired, Miami Acoustics Mooring.
	2201	Miami Acoustics Mooring recovered.
7 Jan 92	0238-0311	CTD cast near Discus Mooring.
	1418	Release fired. Discus Mooring.
	1846	Discus Mooring recovery completed.
	2052	Bubble population spar buoy deployed, tethered to ship.
	2222	Bubble population spar buoy recovered.
	2311	Release fired, remaining part of Seatex mooring.
8 Jan 92	0121	Remaining Seatex subsurface mooring recovery completed.
	1804	Release fired, Endeco mooring.
	2106	Endeco mooring recovery completed.
	2148	Bubble population spar buoy deployed, tethered to ship.
9 Jan 92	0100	Bubble population spar buoy recovered.
	0200	Underway to Seattle.
	0745	Arrive Seattle.

Appendix 3: CTD Cast Information

1. Pre-deployment Casts R/V Thomas G. Thompson Cruise TT004 Leg 1

Station TT004001 Thu Oct 31 04:58:05 1991
Latitude N49 12.2409 to N49 12.3439
Longitude W131 43.8676 to W131 43.5234

Station TT004002 Fri Nov 01 06:49:11 1991
Latitude N49 11.8471 to N49 11.8288
Longitude W131 54.6433 to W131 54.4354

Station TT004003 Sat Nov 02 05:38:10 1991
Latitude N49 08.4530 to N49 08.6263
Longitude W131 45.5396 to W131 45.4347

Station TT004004 Sun Nov 03 06:12:54 1991
Latitude N49 25.1633 to N49 25.4107
Longitude W131 42.0551 to W131 41.9707

Station TT004005 Mon Nov 04 02:09:29 1991
Latitude N49 16.0861 to N49 16.0843
Longitude W131 33.9778 to W131 33.7746

2. Post-deployment Casts R/V Thomas G. Thompson Cruise TT005 Leg 1

Station TT005001 Tue Jan 7 03:14:46 1992
Latitude N49 15.3600
Longitude W131 51.9404

Station TT005002 Wed Jan 8 04:47:53 1992
Latitude N49 08.9403
Longitude W131 46.7333

Appendix 4: The Seatex Mooring Failure

The Seatex buoy was set on 1 November at 0520Z. On 1 December, information from system Argos made it clear that the Seatex buoy was adrift. The buoy was recovered by the HMCS Huron at 1949Z on 4 December. The Canadian Navy then transported the buoy to the marine facility at the University of Washington, Seattle.

A schematic of the surface expression of the mooring is shown below in Figure A.3.1. A nylon tether with attached floats came up to the surface and lay along the surface for about 70 meters. This tether was then attached to a stainless steel chain which was attached to a clamp on the buoy. The clamp was in turn attached to a stainless steel rod which ran through the buoy. The buoy hull consisted of two floatation elements, each of which was a half-toroid (sliced vertically) which were clamped around the central well with an outer steel band. rod ran in between the two halves of the floatation hull with the clamps keeping it in place.

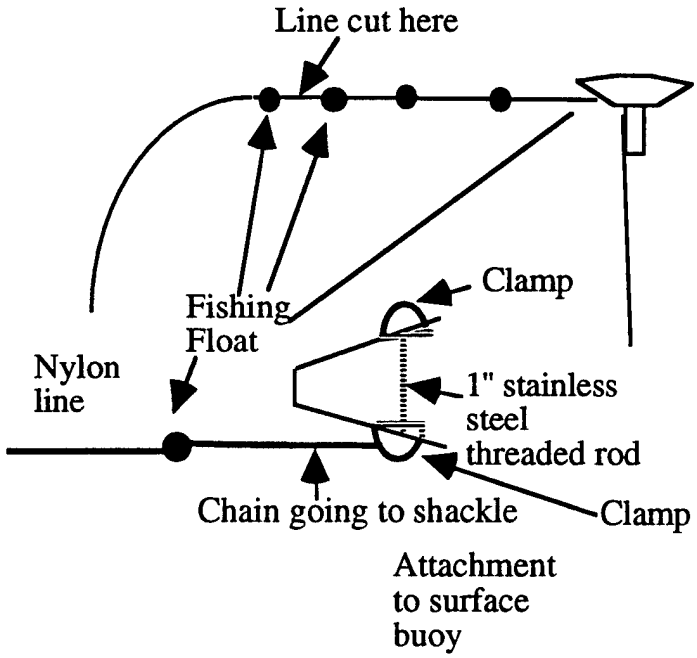

Figure A.4.1: Figure Schematic of the surface expression of the Seatex mooring and of the attachment of the mooring line to the buoy.

When the buoy was examined on the dock at Seattle, it became clear that something very unusual had occurred. The entire assemblage for attaching the mooring, including the stainless steel rod and both clamps, was missing, as was a similar rod and clamp assembly on the other side of the buoy *to which no lines had been attached.* The floatation elements are jacketed with very soft plastic which can be scratched with a blunt instrument. The hull showed no signs of the stainless steel threaded rod having worked free on either side.

Upon recovery, it was discovered that the surface line had been cut just above the last float. Analysis of the line end, carried out by Bryce Prindle at WHOI, revealed that the line had been cut by something which produced strong tensile and torsional forces. The cutting instrument was blunt, indicating the line was probably not cut with a knife or by fish teeth. Some yarns in the cut end retained their original structure and were fused together, indicating possible tensile failure. The yarns in the mooring line were tightly wrapped around a central mass of fibers, suggesting strong rotational motion was involved in the failure.

At this point the most likely hypothesis is that the surface line was cut by a propellor. Possibly in an effort to unfoul the boat which cut the line, or else as a calculated act of theft, the clamps and threaded rod assemblies on the buoy were then removed intentionally. This would explain the lack of damage to the floatation hull.

Appendix 5: MATLAB Code for Calculating Directional Wave Spectra from the Seatex Buoy

```
function [dth,sw,f]=mems1(x)
% mems1.m  Computes the five spectral coefficients from a Seatex wave record
%        using an fft with cosine tapering at the edges and then averaging
%        over nw points. The results are then inserted into a maximum
%        entropy routine of Lygre and Krogstad (JPO 16:2052-2060)
%        Input has form sampno, heave, pitch, roll.
%        Output has format [dth sw f] dth the directional wave
%        spectrum. sw the nondirectional spectrum and
%        f the array of frequencies.
%        Modified 8/21/92 to correct for directional changes
%        due to tilting.


nw=16;
heave=x(:,2);

fn=((0:1023)*.5)/1024;
Txyi=(.43.^2)./(.43^2-fn.^2+2*i*.1*fn);
Txy=1.0./Txyi;
ht=ones(1:1024);
it=34:1024;
ht(it)=(1.0-1.0./(30.8*fn(it)).^2-sqrt(2)*i*1.0./(30.8*fn(it))).* ..
       (1.0-1.0./(170*fn(it)));

thp=x(:,3)*pi/180.;
thr=x(:,4)*pi/180.;
thc=x(:,5)*pi/180.;

nx=tan(thp);
ny=sin(thr).*(cos(2*thp)./cos(thp))./sqrt(cos(thp).^2-sin(thr).^2);
nn=real((nx+i*ny).*exp(i*thc));
ne=imag((nx+i*ny).*exp(i*thc));

trif(1:128)=sin((0:127)*pi/256).^2;
trif(129:1920)=1.0*ones(129:1920);
trif(1921:2048)=trif(128:-1:1);
trif=trif';

ffh=fft(heave.*trif)/sqrt(2048);
ffn=fft(nn.*trif)/sqrt(2048);
ffe=fft(ne.*trif)/sqrt(2048);

f=zeros(1:1024/nw)';
c11=zeros(1:1024/nw)';
c22=zeros(1:1024/nw)';
c33=zeros(1:1024/nw)';
c23=zeros(1:1024/nw)';
q12=zeros(1:1024/nw)';
q13=zeros(1:1024/nw)';


for n=1:64
  for j=1:nw
   j1=(n-1)*nw+j;
   f(n)=f(n)+fn(j1)/nw;
   c11(n)=c11(n)+abs(ffh(j1)*ht(j1)).^2;
   c22(n)=c22(n)+abs(ffn(j1)*Txy(j1)).^2;
   c33(n)=c33(n)+abs(ffe(j1)*Txy(j1)).^2;
   q12(n)=q12(n)-imag(conj(ffh(j1)*ht(j1))*ffn(j1)*Txy(j1));
   q13(n)=q13(n)-imag(conj(ffh(j1)*ht(j1))*ffe(j1)*Txy(j1));
   c23(n)=c23(n)+real(conj(ffn(j1))*ffe(j1)*abs(Txy(j1)^2));
  end
end

d1=q12./sqrt(c11.*(c22+c33));
d2=q13./sqrt(c11.*(c22+c33));
```

DOCUMENT LIBRARY

Distribution List for Technical Report Exchange – May 5, 1994

University of California, San Diego
SIO Library 0175C (TRC)
9500 Gilman Drive
La Jolla, CA 92093-0175

Hancock Library of Biology & Oceanography
Alan Hancock Laboratory
University of Southern California
University Park
Los Angeles, CA 90089-0371

Gifts & Exchanges
Library
Bedford Institute of Oceanography
P.O. Box 1006
Dartmouth, NS, B2Y 4A2, CANADA

Commander
International Ice Patrol
1082 Shennecossett Road
Groton, CT 06340-6095

NOAA/EDIS Miami Library Center
4301 Rickenbacker Causeway
Miami, FL 33149

Library
Skidaway Institute of Oceanography
10 Ocean Science Circle
Savannah, GA 31411

Institute of Geophysics
University of Hawaii
Library Room 252
2525 Correa Road
Honolulu, HI 96822

Marine Resources Information Center
Building E38-320
MIT
Cambridge, MA 02139

Library
Lamont-Doherty Geological Observatory
Columbia University
Palisades, NY 10964

Library
Serials Department
Oregon State University
Corvallis, OR 97331

Pell Marine Science Library
University of Rhode Island
Narragansett Bay Campus
Narragansett, RI 02882

Working Collection
Texas A&M University
Dept. of Oceanography
College Station, TX 77843

Fisheries-Oceanography Library
151 Oceanography Teaching Bldg.
University of Washington
Seattle, WA 98195

Library
R.S.M.A.S.
University of Miami
4600 Rickenbacker Causeway
Miami, FL 33149

Maury Oceanographic Library
Naval Oceanographic Office
Building 1003 South
1002 Balch Blvd.
Stennis Space Center, MS 39522-5001

Library
Institute of Ocean Sciences
P.O. Box 6000
Sidney, B.C. V8L 4B2
CANADA

Library
Institute of Oceanographic Sciences
Deacon Laboratory
Wormley, Godalming
Surrey GU8 5UB
UNITED KINGDOM

The Librarian
CSIRO Marine Laboratories
G.P.O. Box 1538
Hobart, Tasmania
AUSTRALIA 7001

Library
Proudman Oceanographic Laboratory
Bidston Observatory
Birkenhead
Merseyside L43 7 RA
UNITED KINGDOM

IFREMER
Centre de Brest
Service Documentation - Publications
BP 70 29280 PLOUZANE
FRANCE

50272-101

REPORT DOCUMENTATION PAGE	1. REPORT NO. WHOI-94-18	2.	3. Recipient's Accession No.

4. Title and Subtitle
Meteorological and Oceanographic Data Collected during the ASREX 91 Field Experiment

5. Report Date
August 1994

6.

7. Author(s) Nancy R. Galbraith, Anand Gnanadesikan, George H. Tupper, Bryan S. Way, and Eugene A. Terray

8. Performing Organization Rept. No.
WHOI-94-18

9. Performing Organization Name and Address

Woods Hole Oceanographic Institution
Woods Hole, Massachusetts 02543

10. Project/Task/Work Unit No.

11. Contract(C) or Grant(G) No.
(C) N00014-91-J-1891
(G)

12. Sponsoring Organization Name and Address

Office of Naval Research

13. Type of Report & Period Covered
Technical Report

14.

15. Supplementary Notes
This report should be cited as: Woods Hole Oceanog. Inst. Tech. Rept., WHOI-94-18.

16. Abstract (Limit: 200 words)

The 1991 Acoustic Surface Reverberation Experiment (ASREX 91) took place in November and December off the coast of British Columbia. As part of this experiment, three moorings were deployed to characterize the environmental background. The moorings consisted of a meteorological/oceanographic mooring designed to measure surface meteorology, current and temperature in the upper 120 meters, and nondirectional wave parameters and two wave moorings which were instrumented with pitch-roll buoys to characterize the directional wave spectrum. This report presents results from these three moorings. The conditions seen during the experiment were extremely rough, with wind speeds at 3.4m above the water surface reaching a maximum of 22 m/s and wave heights reaching a maximum of over 10 meters. The air-sea flux of heat was strongly cooling, and the mixed layer deepened over the course of the experiment from approximately 40 to approximately 70 meters. Spectra of the temperature showed a strong semidiurnal tidal signal associated with temperature excursions of several degrees C. The velocity signal showed strong inertial oscillations with amplitudes of 30-50 cm/s. Weaker low-frequency and semidiurnal tidal signals were also seen. The waves were very strong with significant wave heights of 5-6 meters persisting for up to 2 weeks at a time. Waves were generally out of the south or the west.

17. Document Analysis a. Descriptors
Meteorology: North Pacific
Oceanography: North Pacific
Moored Instrument Measurements

b. Identifiers/Open-Ended Terms

c. COSATI Field/Group

18. Availability Statement	19. Security Class (This Report)	21. No. of Pages
Approved for public release; distribution unlimited.	UNCLASSIFIED	118
	20. Security Class (This Page)	22. Price

(See ANSI-Z39.18) *See Instructions on Reverse*

OPTIONAL FORM 272 (4-77)
(Formerly NTIS-35)
Department of Commerce